Supplementary Information for

Explosive volcanism as a key driver of the Late Paleozoic Ice Age

Gerilyn S. Soreghan, Michael J. Soreghan, and Nicholas G. Heavens

Corresponding Author Email: LSOREG@OU.EDU

The Supplementary Information includes:

Detailed Methods text
Fig. S1
Tables S1 and S2
References for citations used in the Supplementary Information

Methods.

Data Compilation of Glacial Deposits and Ages (Devonian-Triassic). We began with the Hambrey and Harland (1) compilation of glacial units reported from the late Paleozoic ice age (LPIA) interval. This compilation lists what at the time of publication (1981) were all known glacial units globally, and are the data that Frakes (2) used to plot the age-frequency histogram for the LPIA, which has been widely reproduced (3). In the data compilation, we follow the convention of these earlier compilations in listing glacial deposits per basin, so we do not report multiple deposits of the same age from the same basin. The justification for this is that the compilation becomes more qualitative if we assign more than one deposit for a given time in a given basin. Note, however, that many of the units previously reported in Hambrey and Harland (1) had only tenuous age dates, with many commonly restricted to period-level resolution (e.g. "Permian") or even lower resolution (e.g. "Permo-Carboniferous"). We updated these units with the most recent age dates (paleontologically or geochronological constrained) and provide references for these new age dates (Supplementary Table 1). In nearly all cases, these new age dates achieve stage-level resolution. Moreover, we searched the literature (using GeoRef) for all glacial units reported from Devonian through Triassic time globally, and found many additional units that have been documented since the publication of Hambrey and Harland (1), and report the most recent age dates (to stage resolution where possible) for all units (Supplementary Table 1) For the age-frequency plot (Figure 1), we show age resolution to stage level, because most units are dated with relative-age dating techniques, and have stage-level age designations. International stages of the Pennsylvanian and Permian are typically <10 My duration, and most (>60%) are <5 My duration, so we consider stage-level resolution most scientifically defensible and reproducible given that resolution on radiometric dates for this interval published prior to a few years ago commonly reported errors of 1-5 My. Some stages of the Mississippian and Devonian exceed 10 My duration; accordingly, for these stages we attempt to show sub-stage divisions (informally: early, middle, late), as these are commonly expressed in the literature even given relative-age dating techniques. To construct the plot (Fig. 1), we assigned one unit to a glacial deposit that represents a given stage in a given basin. Rarely, especially for deposits from Antarctica, no stage-level dating exists, and the age is constrained only to "Permo-Carboniferous." In these cases, we assigned 0.25 units per stage, as a means to illustrate the uncertainty in the age designation.

This new compilation includes primary data mined from 77 papers published since the much-reproduced histogram of Frakes (2), and from an additional 40 papers published since the compilation presented by Fielding et al. (3). This new compilation indicates highs and lows in the (frequency of) glacial deposits, but does not support the existence of nonglacial intervals (at the dating resolution currently available). The newest age data from Metcalfe et al. (4) explicitly calls into question the Fielding et al. (3, 5) dates on glacial intervals. For these reasons, we began with a re-assessment of the record of glaciation during the LPIA, drawing upon the primary literature. At stage-level resolution, the hypothesis (3, 5) that the LPIA consists of a series of discrete glacial episodes separated by non-glacial intervals is not supported. Furthermore, deposits were not coded as recording "alpine" or "continental" glaciation, as this designation is nearly always an interpretation, and thus would compound potential error.

References for glacial units data sources are 1-85**.**

Data Compilation of Volcanic Unit Ages (Devonian-Triassic). We compiled data on radiometrically dated volcanic rocks (lava and pyroclastic units) of felsic to intermediate composition (rhyolite, dacite, andesite, and trachyte). Units described as ash, tephra, tonstein, bentonite, ignimbrite, and tuff were all coded as "pyroclastic," and any unit identified as an ignimbrite was coded as such. We focused on felsic to intermediate compositions because these types of eruptions are most energetic, and thus most capable of injecting aerosols into the stratosphere. We selected the base Devonian (~420 Ma) and end Triassic (~200 Ma) as the bounds of the volcanic units data compilation in order to fully envelope the icehouse interval of the LPIA with greenhouse intervals and avoid any "edge" effects in the dataset. This data compilation was intended to assess whether the felsic-intermediate volcanism of the LPIA exceeded baseline felsic-intermediate volcanism of the greenhouse intervals bounding it.

We searched the literature for data on volcanic units of Triassic through Devonian age using GeoRef, the most comprehensive geoscience database available, cataloguing >140 journals, in addition to theses, dissertations, conference proceedings, maps, geological survey publications, etc. Search terms included the geologic period (Devonian, Mississippian, Pennsylvanian, Carboniferous, Permian, Triassic), + volc* OR tuff + zircon, and also searched using geographic designators (country names). We included material published in all languages (most are in English, but many appear in Chinese, German, and Spanish, as well as other languages). Most sources were published within the last <<20 years, owing to the recent escalation in availability of high-precision radiometric dating capabilities, and most are based on the U-Pb system using zircons. All metadata regarding dating techniques are included in our compilation. Only dates with associated errors were included; 99% of dates included have associated errors <<10 My, and 91% have associated errors <<5 My. Latitude and longitude data were assigned to each date according to information provided in the original source, and to within <1° (commonly 0.1° resolution where possible), to enable paleolocation reconstructions, using the open-source software GPlates (86).

Some units have been re-dated in the literature. For those, if we could be certain that it was the same unit (same bed), we used the newest (most accurate) date, and disregarded older dates reported. For example, several of the dates on tuffs from glacial basins of South America (especially in the Paraná Basin) previously reported in de Matos (87), Guerra Sommer (87-90), Mori (91), and Cagliari et al. (92) were re-dated and reported in Griffis et al. (93). Similar issues arose from basins of eastern Australia. Metcalfe et al. (4) noted that many of the dates previously reported for volcanics of eastern Australia used a heterogeneous standard (SL-13), such that the resultant dates are imprecise. Metcalfe et al. (4) re-dated 8 units that had been previously reported (94) using SHRIMP on the SL13 standard, thus, we used only the more recent dates (4). Additionally, dates from Australia (95) are corrected for the new (TEMORA 1) standard for U-Pb SHRIMP dating (96), and ages previously reported on duplicate units were deleted. Similarly, owing to the interest in the Permo-Triassic boundary and extinction, sections containing the P-T boundary have garnered a disproportionately large amount of attention with regard to age dates. This is particularly true for South Africa and China. Dates on ashes from the Karoo Supergroup (Karoo Basin and sub-basins therein) appear in multiple publications (97-101), but many problems occur with out-of-sequence age dates (101) (complicated by e.g. zircon recycling). We chose to use only the ID-TIMS

ages from the Central Basin (100) as these have minimal errors and fall in sequence. Dates on ashes from the P-T boundary sections in China (102-104) include repeat dates on the same beds, especially for the Meishan section. For individual beds that have been multiply dated, only the most recent date is used.

References for volcanic units data sources are 86-472.

Estimating the Intensity of Past Volcanism Relative to the Present Day. The intensity of past volcanism (I_{past}) relative to the present day ($I_{present}$) as a function of time, t, was estimated from this formula:

$$\hat{I}(t) = \frac{I_{past}(t)}{I_{present}} = \frac{N_{past}(t)}{\tilde{N}_{present}} \quad (1)$$

where N_{past} is the frequency (or number in a defined time window) of past volcanic events and $\tilde{N}_{present}$ is the frequency of volcanic events that would be expected to occur over the recent past if sampled like a compilation of volcanic events in the deep past. $\tilde{N}_{present}$ can be defined more explicitly in terms of the size-frequency distribution of recent events and the properties of the deep past compilation, such that:

$$\tilde{N}_{present} = \frac{\int_{M_1}^{M_2} \frac{f_{bib}\left[X_{dispersion}(M),t\right]}{f_{land}} n(M)_{present}(M)\,dM}{\Delta T_{present}} \quad (2)$$

f_{bib} is the fraction of the Earth's surface that the database samples at a characteristic scale, $X_{dispersion}$, equal to the typical scale at which volcanic material is dispersed and can be recognized in the sedimentary record, and $\Delta T_{present}$ is the length of the recent past record used to estimate $\tilde{N}_{present}$. The probability distribution $n(M)_{present}$ in this context is the number of events within an infinitesimal magnitude range dM in the recent past record. In practice, magnitude is typically reported at a resolution of 0.1 units.

Equations 1 and 2 were then evaluated on the assumption that the relative activity of silicic explosive volcanism can be inferred from the relative activity of ignimbrite-producing eruptions. The data for dM and the parameter $\Delta T_{present}$ were derived from the Quaternary record (0-2.5 Ma) of silicic volcanic events of M≥6.5 (that is, presumptive ignimbrite-producing events (473)), as recorded in the LaMEVE database (474, 475). Two different models for $n(M)_{present}$ were considered. In one model (EVE), $n(M)_{present}$ is simply the total number of events at a given eruptive magnitude. In the other model (MAX), $n(M)_{present}$ is calculated from the maximum magnitude of eruption of individual volcanoes, on the principle that multiple events at the same volcano in our compilation usually would not be chronostratigraphically resolved on a 2.5 Myr timescale.

The bibliographic sampling function f_{bib} [$X_{dispersion}$, t] was evaluated by dividing the Earth into uniform longitude-latitude bins at resolutions of 0.1°, 0.2°, 0.5°, 1°, 2°, 4°, 10°, 30°, and 45°, determining whether those bins overlapped with the paleo-locations of all points in the volcanic database at time t as determined using the GPlates web service and the reconstruction of Matthews (476), and then evaluating the fraction of the Earth

covered by the sampled bins (Supplementary Figure 1a). In some cases, the paleo-locations of volcanic deposits in the database could not be reconstructed (Supplementary Figure 1b). This analysis suggests that sampling is relatively constant with scale over time and that the inability to reconstruct paleo-locations is relatively unimportant.

The bibliographic sampling function relies on the assumption that the literature search is a complete accounting of volcanic deposits over the period studied in all areas where volcanic deposits have been reported and dated according to the filters used in the database. On one hand, the sampling is wider than this, because areas that may have never had volcanic activity during the period studied are also sampled. On the other hand, the sampling is narrower than this, because some areas may have been non-depositional during some time intervals, have not been investigated, or were not investigated according to the filters used in the database.

Two models were used to estimate $\boldsymbol{X}_{dispersion}$ for ignimbrites as a function of magnitude. In both cases, the deposits are modeled as circular in shape as the least biased assumption. (Some deposits may be more extensive in one direction than another (477)). In the first model (EMP), ignimbrite dispersion radius is assumed to be 0 km at M6.5, be 35 km for M7.0 (the radius of deposition for the 1815 Tambora eruption (477)), be 120 km for M8.0 (the radius of deposition for the 1 Ma Kidnappers ignimbrite of the Taupo Volcanic Zone), and be 85 km for the M8.8 74 ka Younger Toba (477). In the SAT model, radius of deposition saturates at 85 km at M≥8.0, on the principle that ignimbrites as dispersed as the Kidnappers are relatively rare, even in similar geological settings. For instance, the dispersion radius of the M8.2 25 ka Taupo eruption was only 85 km. Finally, $\boldsymbol{X}_{dispersion}$ was estimated by interpolating these functions with M, multiplying by 2, and dividing by one equatorial degree (111 km).

The parameter f_{land} was approximated as a constant 0.29 and is used on the principle that the volcanic database primarily samples continental crustal areas, because most oceanic crust older than 200 Ma has been subducted.

The underreporting of eruptions in the recent past, especially at smaller magnitudes in LaMEVE (475), and reduced preservation in our deep past compilation underlines the appropriateness of the MAX and SAT models and/or will shift the starting magnitude of integration in Equation 2 toward higher magnitude, making $\tilde{N}_{present}$ calculated with MAX and EMP an upper estimate under most circumstances.

Estimating Radiative Forcing. The radiative forcing of sulfate aerosols was estimated estimated to be:

$$RF_{sulfate} = \left[\hat{I}(t)\left(SAOD_{quat,volc}\right) + \left(SAOD_{quat,bkgrnd}\right)\right]\frac{dRF}{dSAOD}\frac{S_0(t)}{S_0(0)} \qquad 3)$$

The parameter $SAOD_{quat,\ volc}$ is mean stratospheric aerosol optical depth (SAOD) due to explosive volcanism during the Quaternary, which was estimated from the database of Toohey and Sigl (478) for the period 500 BCE-1900 CE (0.010), with the contribution of eruptions by the Icelandic volcano, Laki, over that period removed in proportion to its estimated S emission (~2.5% of all volcanic S emission from 500 BCE-1900 CE). Laki is an unusual basaltic system whose interactions with glaciers may enable it to generate

significant stratospheric S injection, but the height of its eruptive plumes and their climate impact remain controversial (479-484). Moreover, such systems would be excluded from our survey.

The parameter $SAOD_{quat,\,bkgrnd}$ accounts for "background" S transport to the stratosphere from the troposphere from sources other than large volcanic eruptions, such as effusive volcanism, biological activity etc. We assume it to be equal to 0.004. The parameter $\frac{dRF}{dSAOD}$, the radiative forcing per unit change in SAOD, is estimated to be -23.7 W m^{-2}, which is based on modeling the atmospheric response to satellite estimates of volcanic S emissions between 1979-2015 with a latest generation, stratosphere-resolving climate model (485).

The parameter S_0 is the solar constant, which is assumed to vary with time in line with the equation of Gough (486) assuming a solar age of 4.49 Ga (487). It is assumed to have a present day value of 1367 Wm^{-2}. We neglect potential enhancement in stratospheric S injection because of a lower tropopause during colder climates (490) or the possibility that volcanic activity during the last 2400 years has been affected by glacial rebound, because these effects are most strongly concentrated within 3000 yrs of glacial termination (491, 492).

The radiative forcing due to a change in CO_2 is calculated from the third equation in Table 6.2 of the IPCC Third Assessment Report (after WMO 493). This expression is based on global average meteorological data in present day climate and thus is somewhat uncertain for application to deep time on account of variability in atmospheric thermal structure and clouds. However, it is in good agreement with line-by-line calculations to at least 50000 ppmv of CO_2 (494).

The radiative forcing due to the combined effect of CO_2 and sulfate is calculated by interpolating the radiative forcing due to sulfate at 0.5 Ma resolution, doing likewise with the most recent (495) pCO_2 reconstruction, and calculating the CO_2 value such that a change in pCO_2 from this (495) value to the new value would result in the same radiative forcing as the sulfate radiative forcing.

References for estimating the intensity of past volcanism are predominantly 474-495.

Data Availability

Primary data used for this manuscript can be found in Supplementary Tables S1 and S2, with primary sources cited therein, and provided in the references in the Supplementary Information.

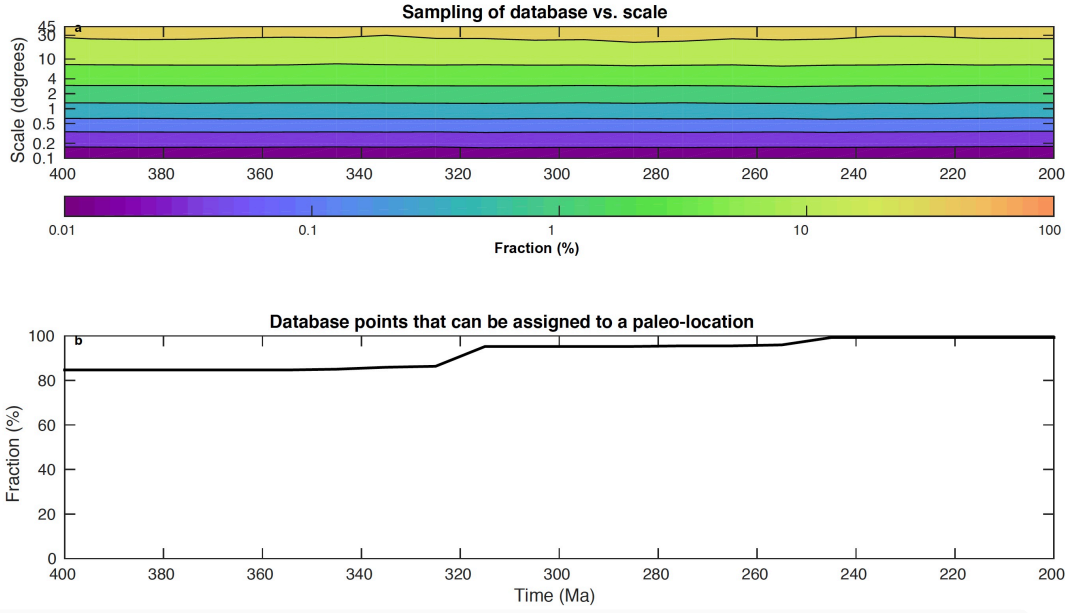

Figure S1.
Approximate sampling by the literature search: (a) Fraction of the Earth's land area sampled (%) as a function of time and scale of sampling; (B) Fraction of points that can be assigned to a paleo-location at the specified time using the paleogeographic reconstruction employed by this study.

Table S1. Compilation of Glacial Deposits (Devonian-Triassic).

Data table for all glacial units and associated ages for Devonian-Triassic (available in supplementary materials).

Table S2. Compilation of Volcanic Units (Devonian-Triassic).

Data table for all volcanic units ages for Devonian-Triassic (available in supplementary materials).

Supplementary References Cited in Methods

Timescale accessed from stratigraphy.org Feb 6, 2017.

References— Glacial Deposits

1. Hambrey MJ, Harland WB (1981) *Earth's Pre-Pleistocene Glacial Record* (Cambridge University Press, Cambridge).
2. Frakes LA (1992) in *Climate Modes of the Phanerozoic* (Cambridge University Press, Cambridge), chap. 5.
3. Fielding CR, Frank TD, Isbell JL (2008) in *Resolving the Late Paleozoic Ice Age in Time and Space*, Fielding, CR, Frank, TD, Isbell, JL, Eds. (Geological Society of America, Boulder, Colorado) 441:343– 354. doi: 10.1130/2008.2441(24).
4. Metcalfe I, Crowley JL, Nicoll RS, Schmitz M (2015) High-precision U-Pb CA-TIMS calibration of Middle Permian to Lower Triassic sequences, mass extinction and extreme climate change in eastern Australian Gondwana. *Gondwana Res*. 28:61-81.
5. Fielding CR, Frank TD, Birgenheier LP, Rygel MC, Jones AT, Roberts J (2008) Stratigraphic imprint of the Late Palaeozoic Ice Age in eastern Australia: a record of alternating glacial and nonglacial climate regime. *J. Geol. Soc. London* 165:129-140.
6. Modie BN, Hérissé ALe (2009) Late Palaeozoic palynomorph assemblages from the Karoo Supergroup and their potential for biostratigraphic correlation, Kalahari Karoo Basin, Botswana. *Bull. Geosci.,* 84:337-358.
7. Singh KJ, Chandra A, Chandra S (2005) Evaluation of earliest Permian flora of India and its equivalents in other Gondwana continents. *Palaeobotanist* 54:107-113.
8. d'Engelbronner ER (1996) Palynological data from Karoo sediments, Mana Pools Basin, northern Zimbabwe. *J. Afr. Earth Sci*. 23:17-30.
9. Falcon RMS (1975) Palynostratigraphy of the Lower Karroo Sequence in the central Sebungwe District, Mid-Zambezi Basin, Rhodesia. *Palaeontologica Afr*. 18:1-29.
10. Stollhofen H, Werner M, Stainstreet IG, Armstrong RA (2008) Single-zircon U-Pb dating of Carboniferous-Permian tuffs, Namibia, and the intercontinental deglaciation cycle framework, in *Resolving the Late Paleozoic Ice Age in Time and Space*, C. R. Fielding, T. D. Frank, J. L. Isbell, Eds. *Geol. Soc. Am. Spec. Pap*. 441:83-96.
11. Isbell JL, Cole DI, Catuneanu O (2008) Carb-Permian glaciation in the main Karoo Basin, South Africa: Stratigraphy, depositional controls, and glacial dynamics. *Geol. Soc. Am. Spec. Paper* 44:71-82.
12. Nyambe IA, Utting J (1997) Stratigraphy and palynostratigraphy, Karoo Supergroup (Permian and Triassic), mid-Zambezi Valley, southern Zambia. *J. Afr. Earth Sci*. 24:563-583.
13. Wopfner H, Jin XC (2009) Pangea megasequences of Tethyan Gondwana-margin reflect global changes of climate and tectonism in Late Palaeozoic and Early Triassic times— A review. *Palaeoworld* 18:169-192.

14. Lang PJ, Yahaya DM, El Hamet MO, Besombes NJC, Cazoulat M (1991 Depots glaciaires du Carbonifere inferieur a l'ouest d l'Air (Niger). *Geol. Rundsch.* 80 :611-622.
15. Wopfner H (2002) Tectonic and climatic events controlling deposition in Tanzanian Karoo basins. *J. Afr. Earth Sci.* 34:167-177.
16. Weiss RH, Wopfner H (1997) Palynology and palaeoecology of Late Palaeozoic glacigene Idusi Formation of southern Tanzania. *Sonderveroffentlichungen*, 114:535-559.
17. Censier C, Lang J (1992) La Formation glaciaire de la Mambere (Republic Centralafricaine): reconstruction paleogeographique et implications a l'echelle du Paleozoique Africain. *Geol. Rundsch.* 81 :769-789.
18. Isaacson PE, Diaz-Martinez E, Grader GW, Kalvoda J, Babek O et al. (2008) Late Devonian-earliest Mississipian glaciation in Gondwananland and its biogeographic consequences. *Palaeogeogr. Palaeoclimatol.* 268:126-142.
19. Bussert R (2014) Depositional environments during the Late Palaeozoic ice age (LPIA) in northern Ethiopia, NE Africa. *J. Afr. Earth Sci.* 9:386-407.
20. Klitzsch E (1983) Paleozoic formations and a Carboniferous glaciation from the Gilf Kebir-Abu Ras Area in southwestern Egypt. *J. Afr. Earth Sci.*, 1:17-19.
21. Wycisk P, Klitzsch E, Jas C, Reynolds O (1990) Intracratonal sequence development and structural control of Phanerozoic strata in Sudan. *Berliner Geowiss. Abh.,* 120: 45-86.
22. Le Heron DP, Craig J, Etienne JL (2009) Ancient glaciations and hydrocarbon accumulations in North Africa and the Middle East. *Earth-Sci. Rev.* 93:47-76.
23. Stephenson MH, Jan IU, Kader SZ, Al-Mashaikie (2013) Palynology and correlation of Carboniferous-Permian glacigene rocks in Oman, Yemen, and Pakistan. *Gondwana Res.* 24:203-211.
24. Heward AP, Penney RA (2014)Al Klata glacial deposits in the Oman Mountains and their implications, in *Tectonic evolution of the Oman Mountains*: H. R. Rollinson, et al., Eds. (Geol. Soc. London, Spec. Publ.) 392:279-301.
25. Melvin J, Norton JK (2013) Advances in Arabian stratigraphy: Comparative studies of the glaciogenic Juwayl and lower Unayzah strata (Carboniferous and Permian) of Saudi Arabia. *GeoArabia* 18:97-134.
26. Lakin JA, Marshall JEA, Troth I, Harding IC (2016) Greenhouse to icehouse: a biostratigraphic review of latest Devonian-Mississippian glaciations and their global effects, in *Devonian Climate, Sea Level, and Evolutionary Events*, Becker, R.T., et al., Eds. (Geol. Soc. London, Spec. Publ.) 423:439-464.
27. Isbell JL, Koch ZJ, Szablewski GM, Lenaker PA (2008) Permian glacigenic deposits in the Transantarctic Mountains, Antarctica, in *Resolving the Late Paleozoic Ice Age in Time and Space*, C. R. Fielding et al., Eds. (Boulder, Geol. Soc. Am.) Spec. Pap. 441:59-71.
28. Isbell JL (2010) Environmental and paleogeographic implications of glaciotectonic deformation of glaciomarine deposits within Permian strata of the Metschel Tillite,

southern Victoria Land, Antarctica, in *Late Paleozoic Glacial Events and Postglacial Transgressions in Gondwana,* O. R. López-Gamundí, L. A. Buatois (Boulder, Geol. Soc. Am.) Spec. Pap. 468:81–100. doi: 10.1130/2010.2468(03)

29. Cornamusini G, Talarico FM, Cirilli S, Spina A, Olivetti V, Woo J (2017) Upper Paleozoic glacigenic deposits of Gondwana: Stratigraphy and paleoenvironmental significance of a tillite succession in Northern Victoria Land (Antarctica). *Sediment. Geol*. 358:51-69.
30. Matsch CL, Ojakangas RW (1992) Stratigraphy and sedimentology of the Whiteout Conglomerate; an upper Paleozoic glacigenic unit, Ellsworth Mountains, West Antarctica, in *Geology and Paleontology of the Ellsworth Mountains, West Antarctica,* G. F. Webers et al., Eds. (Boulder, Geol. Soc. Am.) Memoir 170. doi 10.1130/MEM170-p37
31. Shah A, Haneef M, Hanif M, Jan IU (2010) Lithofacies and palaeoenvironmental analysis of Carboniferous-Permian Nilawahan Group, Salt Range, Pakistan. *Pakistan J. Hydrocarb. Res*. 20:49-52.
32. Jan IU, Shah A, Stephenson MH, Iqbal S, Hanif M, Wagreich M, Hussain HS (2016) The sedimentology of the Lower Permian Dandot Formation: A component of the Gondwana deglaciation sequence of the Salt Range, Pakistan. *Revista Ital. Paleont. Strat*. 122:75-90.
33. Garzanti E, Nicora A, Tintori A, Sciunnach D, Angiolini L (1994) Late Paleozoic stratigraphy and petrography of the Thini Chu Gropu (Manag, central Nepal); sedimentary record of Gondwana glaciation and rifting of Neotethys. *Revista Ital. Paleont. Strat*. 100:155-194.
34. Gaetani M, Garzanti E (1991) Multicyclic history of the northern India continental margin (NW Himalaya). *Am. Assoc. Pet. Geol. Bull*. 75:1427-1446.
35. Srivastava S, Bhattacharyya AP (1994) Palynology in stratigraphy of Lesser Himalayan sedimentary sequences from Arunachal Pradesh, India. *The Palaeobotanist* 49:371-383.
36. Garzanti E, Sciunnach D (1997) Early Carboniferous onset of Gondwanian glaciation and Neo-Tethyan rifting in south Tibet. *Earth Planet. Sci. Lett*. 148:359-365.
37. Sinha AK, Misra DK, Paul SK (1997) Geology and tectonic features of Kulu and Spiti-- Lahaul Sector of NW Himalaya. *Himalayan Geol*. 18:1-15.
38. Shi GR (1997) Early Permian brachiopods from the Singa Formation of Langkawi Island, northwestern peninsular Malaysia; biostratigraphical and biogeographical implications: *Newslett. Geol. Soc. Malaysia*, 23:243-244.
39. Meor HH, Lee CP (2005) The Devonian-Lower Carboniferous succession in northwest peninsular Malaysia. *J. Asian Earth Sci*. 24:719-738.
40. Shi GR, Raksakulwong L, Campbell HJ (2002) Early Permian brachiopods from central and northern Peninsular Thailand. *Can. Soc. Petrol. Geol. Mem*. 19:596-608.
41. Ampaiwan T, Hisada KI, Charusiri P (2015) Lower Permian glacially influenced deposits in Phuket and adjacent islands, peninsular Thailand. *Island Arc* 18:52-68.

42. Zhang Y (2010) Discoveries of Permian fusuline fauna from the Shuanghu area, central Tibet and its implications for the climatic change and tectonic evolution of the Qiangtang Block. *Geol. Soc. Am. Abst. Prog.* 42.5:621.

43. Hu J, Li Q, Fang N, Yang J, Ge D (2015) Geochemistry characteristics of the Low Permian sedimentary rocks from central uplift zone, Qiangtang Basin, Tibet; insights into source-area weathering, provenance, recycling, and tectonic setting. *Arab. J. Geosci.* 8.8:5373-5388.

44. Xiaochi J (2002) Permo-Carboniferous sequences of Gondwana affinity in southwest China and their paleogeographic implications. *J. Asian Earth Sci.* 20:633-646.

45. Shi Y, Jin X (2008) Permian fusulinids from the Tengchong Block, western Yunnan, *China. J. Paleont.* 82:118-127.

46. Hassan MHA, Aung A-K, Becker RT, Rahman NAA, Ng TF, Ghani AA, Shuib MK (2014) Stratigraphy and palaeoenvironmental evolution of the mid- to upper Palaeozoic succession in Northwest Peninsular Malaysia. *J. Asian Earth Sci.* 83:60-79.

47. Lakin JA, Marshall JEA, Trot I, Hardin IC (2016), Greenhouse to icehouse: a biostratigraphic review of latest Devonican-Mississippian glaciations and their global effects, in *Devonian Climate, Sea Level, and Evolutionary Events*, R. T. Becker, P. Konigshof, C. E. Brett, Eds. (Geol. Soc. London), Spec. Pub. 423:439-464.

48. Eyles N, Mory AJ, Backhouse J (2002) Carboniferous-Permian palynostratigrapy of west Australian marine rift basins: resolving tectonic and eustatic controls during Gondwanan glaciation. *Palaeogeogr. Palaeoclimatol.* 184:305-319.

49. http://www.ga.gov.au/data-pubs/data-standards/reference-databases/stratigraphic-units

50. Cesar Taboada A, Mory AJ, Shin G-R, Haig DW, Pinilla MK (2015) An Early Permian brachiopod-gastrood fauna from the Calytrix Formation, Barbwire Terrace, Canning Bain, Western Australia. *Alcheringa* 39:207-223.

51. Eyles CH, Mory AJ, Eyles N (2003) Carboniferous-Permian facies and tectono-stratigraphic successions of the glacially influenced and rifted Carnarvon Basin, Western Australia. *Sed. Geology* 155:63-86.

52. Eyles N, Mory AJ, Eyles CH (2006) 50-million-year-long record of glacial to post-glacial marine environments preserved in a Carboniferous-Lower Permian graben, northern Perth Basin, western Australia. *J. Sed. Res.* 76: 618-632.

53. Jones AT, Fielding CR (2008) Sedimentary facies of a glacially influenced continental succession in the Pennsylvanian Jericho Formation, Galilee Basin, Australia. *Sedimentology* 55:531-556.

54. Palmieri V (1998) Foraminifera zonation in the Permian stratigraphy of the Denison Trough (Bowen Basin), central Queensland. *Proceed. Royal Soc. Victoria* 110:173-195.

55. Birgenheier LP (2007) *A Sedimentologic, Stratigraphic, and Geochemical Study of the Late Paleozoic Ice Age, Eastern Australia*. PhD, Univ. Nebraska.

56. Webb JA (2008) Glaciomarine Early Permian strata at Bacchus Marsh, central Victoria; the final phase of late Palaeozoic glaciation in southern Australia. *Proceed. Roy. Soc. Victoria*, 120:373-388.

57. Henry LC (2013) *Late Paleozoic glaciation and ice sheet collapse over western and eastern Gondwana: sedimentology and stratigraphy of glacial to post-glacial strata in western Argentina and Tasmania, Australia*. PhD, Univ. Wisconsin Milwaukee.

58. Cagliari J, Lavina ELC, Philipp RP, Tognoli FMW, Stipp Basei MA, et al. (2014) New Sakmarian ages for the Rio Bonito Formation (Parana Basin, southern Brazil) based on LA-ICP-MS U/Pb radiometric dating of zircon crystals. *J. South Am. Earth Sci*. 56:265-277.

59. Neves JP, Anelli LE, Simoes MG (2014) Early Permian post-glacial bivalve faunas of the Itarare Group, Parana Basin, Brazil; paleoecology and biocorrelations with South American intraplate basins. *J. So. Am. Earth Sci*. 52:203-233.

60. Rocha-Campos AC, dos Santos PR, Canuto JR (2008) Late Paleozoic glacial deposits of Brazil: Paraná Basin, Fielding CR, Frank TD, Isbell JL, Eds., *Resolving the Late Paleozoic Ice Age in Time and Space* (Geol. Soc. Am., Boulder) Spec. Pap. 441:97-114.

61. Crisafulli A, Herbst R, Stortti LM (2009) Maderas gimnospermicas de la Formacion Tres Islas (Permico Inferior) de Uruguay. *J. Geosci*. 5:1-14.

62. Beri A, Martinez-Blanco X, Mourelle D (2010) A synthesis of palynological data from the Lower Permian Cerro Pelado Formation (Parana Basin, Uruguay): A record of warmer climate stages during Gondwana glaciations. *Geologica Acta* 8:419-429.

63. Campos JE, Dardenne MA (1994) A glaciacao Neopaleozoica na porcao meridional da bacia sanfranciscana. *Revista Brasil. Geocie*. 24:65-76.

64. Anderson H (2011) *Sedimentology and lithostratigraphy of the Carboniferous Tarija-Chaco Basin, southern Bolivia; geodynamic and paleoclimatic evolution* (University of Idaho, Moscow) pp 496.

65. di Pasquo M, Anderson H, Isaacson P (2017), Record of a Pennsylvanian-Cisuralian marine transgression, southern Bolivia: A short-lived event in western Gondwana?: *Palaeogeogr. Palaeoclimatol*. 485:30-45.

66. Gulbranson EL, Montanez IP, Schmitz MD, Limarino CO, Isbell JL, Marenssi SA, Crowley JL (2010) High-precision U-Pb calibration of Carboniferous glaciation and climate history, Paganzo Group, NW Argentina. *Geol. Soc. Am. Bull*. 122:1480–1498. http://doi.org/10.1130/B30025.1

67. Limarino CO, Alonso-Murauaga PJ, Ciccioli PL, Perez Loinaze VS, Césari SN (2014) Stratigraphy and palynology of a late Paleozoic glacial paleovalley in the Andean Precordillera, Argentina: *Palaeogeogr. Palaeoclimatol*. 412:223-240.

68. Cesári SN, Limarino CO, Gulbranson EL (2011) An Upper Paleozoic bio-chronostratigraphic scheme for the western margin of Gondwana. *Earth-Sci. Rev*. 106:149-160.

69. Valdeze Buso V, di Pasquo M, Milana JP, Gomes Paim PS (2017) Integrated U-Pb zircon and palynological/palaeofloristic age determinations of a Bashkirian

palaeofjord fill, Quebrada Grande (Western Argentina). *J. So. Am. Earth Sci*. 73:202-222.

70. Gutierrez PR, Cexari SN (2000) Palynology of the Bajo de Veliz Formation (Lower Permian), San Luis, Argentina: Systematic revision and biostratigraphic considerations. *Ameghiniana* 37:439-462.
71. di Pasquo M, Grader GW, Isaacson P, Souza PA, Iannuzzi R, Diaz-Martinez E (2015) Global biostratigraphic comparison and correlation of an early Cisuralian palynoflora from Bolivia. *Historical Biol*. 27:868-897.
72. Toboada AC (2010) Mississippian-Early Permian brachiopods from western Argentina: Tools for middle- to high-latitude correlation, paleobiogeographic and paleoclimatic reconstruction *Palaeogeogr. Palaeoclimatol*. 298:152-173.
73. Henry LC, Isbell JL, Limarino CO (2014) The late Paleozoic El Imperial Formation, western Argentina: Glacial to post-glacial transition and stratigraphic correlations with arc-related basins in southwestern Gondwana. *Gondwana Res*. 25:1380-1395.
74. di Pasquo M, Martinez MA, Freije H (2008) Primer registro palinologico de la Formacion Sauce Grande (Pennsylvaniano-Cisuraliano) en las Sierras Australes, provincia de Buenos Aires, Argentina. *Ameghiniana* 45 (3).
75. Lopez-Gamundi O, Fildani A Weislogel E, Rossello E (2013) The age of the Tunas Formation in the Sauce Grande basin-Ventana foldbelt (Argentina): Implications for the Permian evolution of the southwestern margin of Gondwana. *J. So. Am. Earth Sci*. 45:250-258.
76. Cisterna G (1997) Spiriferida (brachiopoda) from Las Salinas Formation (late Carboniferous), Chubut Province, Argentina. *Ameghiniana* 34:155-161.
77. Isaacson PE, Hladil J, Shen JW, Kalvoda J, Grader G (1999) Late Devonian (Famennian) glaciation in South America and marine offlap on other continents. R. Feist, J. A. Talent, A. Daurer, A., Eds. (North Gondwana: Mid-Paleozoic Terranes, Stratigraphy and Biota, Wien, 1999) *Abh. Geol. Bund*. 54:239–257.
78. Góes AMO, Feijó FJ (1994) Bacia do Parnaíba. *Boletim de Geociências da Petrobras* 8:57–67.
79. Caputo MV, Melo JHG, Streel M, Isbell JL (2008) Late Devonian and Early Carboniferous glacial records of South America. Fielding CR, Frank TD, Isbell JL, Eds., *Resolving the Late Paleozoic Ice Age in Time and Space* (Geol. Soc. Am., Boulder) Spec. Pap. 441.
80. Melo JHG, Barrilari IMR, Quadros LP, Loboziak S, Matsuda NS, et al. (2000) Miospore-based correlations of the Late Devonian Curua Group, Amazon Basin, Brazil: *International Geol. Congress* 31.
81. di Pasquo M, Iannuzzi R (2015) New palynological information from the Poti Formation (upper Visean) at the Rondacor creek, Paranaiba Basin, northeastern Brazil: *Boletin Geologico y Minero* 125 (4).
82. Streel M, Caputo MV, Loboziak S, Melo JHG, Thorez J (2000) Palynology and sedimentology of laminites and tillites from the latest Famennian of the Parnaiba Basin, Brazil. *Geologica Belgica* 3:87-96.

83. Streel M, Caputo MV, Loboziak S, Melo JHG (2000) Late Frasnian-Famennian climates based on palynomorph analyses and the question of the Late Devonian glaciations. *Earth-Sci. Rev.* **52**, 121-173.

84. Trinidade VSF, Carvalho MA, Borghi L (2015) Palynofacies patterns of the Devonian of the Parnaiba Basin, Brazil; paleoenvironmental implications: *J. So. Am. Earth Sci.* 62:164-175.

85. Soreghan GS, Soreghan MJ, Sweet DE, Moore KD (2009) Hot fan or cold outwash? Hypothesized proglacial deposition in the Upper Paleozoic Cutler Formation, western tropical Pangea. *J. Sediment. Res.* 79:495–522. http://doi.org/10.2110/jsr.2009.055

References— Volcanic Ages

86. Williams S, Müller RD, Landgrebe TCW, Whittaker JM (2012) An open-source software environment for visualizing and refining plate tectonic reconstructions using high resolution geological and geophysical data sets. *GSA Today* 22. doi:10.1130/GSATG139A.1

87. deMatos SLF, Yamamoto JK, Riccomini C, Hachiro J, Tassinari CCG (2001) Absolute dating of Permian ash-fall in the Rio Bonito Formation, Paraná Basin, Brazil. *Gondwana Res.* 4:421-426.

88. Guerra-Sommer M, Cazzulo-Klepzig M, Santos JOS, Hartmann LA, Ketzer JM, Formoso MLL (2008) Radiometric age determination of tonsteins and stratigraphic constraints for the Lower Permian coal succession in southern Paraná Basin, Brazil. *Int. J. Coal Geol.* 74:13-27.

89. Guerra-Sommer M, Cazzulo-Klepzig M, Laquintinie Formoso ML, Menegat R, Fo JGM (2008) U-Pb dating of tonstein layers from a coal succession of the southern Paraná Basin (Brazil): A new geochronological approach. *Gondwana Res.* 14:474-482.

90. Guerra-Sommer M, Cazzulo-Klepzig M, Menegat R, Formoso MLL, Basei MAS, Barboza EG, Simas MW (2008) Geochronological data from the Faxinal coal succession, southern Paraná Basin, Brazil: A preliminary approach combining radiometric U-Pb dating and palynostratigraphy. *J South Am. Earth Sci.* 25:246-256.

91. Mori ALO, de Souza PA, Marques JC, Lopes RC (2012) A new U-Pb zircon age dating and palynological data from a Lower Permian section of the southernmost Paraná Basin, Brazil: Biochronostratigraphical and geochronological implications for Gondwanan correlations. *Gondwana Res.* 21:654-669.

92. Cagliari J, Lavina ELC, Philipp RP, Tognoli FMW, Basei MAS, Faccini UF (2014) New Sakmarian ages for the Rio Bonito Formation (Paraná Basin, southern Brazil) based on LA-ICP-MS U-Pb radiometric dating of zircon crystals. *J. South Am. Earth Sci.* 56:265-277.

93. Griffis NP, Mundil R, Montanez IP, Isbell J, Fedorchuk N, Vesely F, Iannuzzi R, Yin QZ, A new stratigraphic framework built on U-Pb single zircon TIMS ages with implications for the timing of the penultimate icehouse (Parana Basin, Brazil). *Geol. Soc. Am. Bull.* (in press).

94. Retallack GJ, Sheldon ND, Carr PF, Fanning M, Thompson CA, Williams ML, Jones BG, Hutton A (2011) Multiple Early Triassic greenhouse crises impeded recovery from Late Permian mass extinction. *Palaeogeogr. Palaeoclimat.* 308:233-251.

95. Roberts J, Offler R, Fanning M (2006) Carboniferous to Lower Permian stratigraphy of the southern Tamworth Belt, southern New England Orogen, Australia: Boundary sequences of the Werrie and Rouchel blocks. *Austral. J. Earth Sci.* 53(2):249-284.

96. Black LP, Kamo SL, William IS, Mudil R, Davis DW (2003) The application of SHRIMP to Phanerozoic geochronology; a critical appraisal of four zircon standards. *Chem. Geol.* 200:171-188.

97. Fildani A, Drinkwater NJ, Weislogel A, McHargue T, Hodgson DM, Flint SS (2007) Age controls on the Tanqua and Laingsburg deep-water systems: new insights on the evolution and sedimentary fill of the Karoo Basin, South Africa. *J. Sediment. Res.* 77:901-908.

98. Fildani A, Weislogel A, Drinkwater NJ, McHargue T, Tankard A, Wooden J, Hodgson D, Flint S (2009) U-Pb zircon ages from the southwestern Karoo Basin, South Africa—Implications for the Permian-Triassic boundary. *Geology* 37:719-722.

99. Lanci L, et al. (2013) Upper Permian magnetic stratigraphy of the lower Beaufort Group, Karoo Basin. *Earth Planet. Sci. Lett.* 375:123-134.

100. Rubidge BS, et al. (2013) High-precision temporal calibration of Late Permian vertebrate biostratigraphy: U-Pb zircon constraints from the Karoo Supergroup, South Africa. *Geology* 41(3):363-366.

101. McKay MP, Coble MA, Hessler AM, Weislogel AL, Fildani A (2016) Petrogenesis and provenance of distal volcanic tuffs from the Permian-Triassic Karoo Basin, South Africa: A window into a dissected magmatic province. *Geosphere* 12:1-14. doi:10.1130/GES01215.1

102. Bowring SA et al. (1998) U-Pb zircon geochronology and tempo of the end-Permian mass extinction. *Science* 280(5366):1039-1045.

103. Mundil R, Ludwig KR, Metcalfe I, Renne PR (2004) Age and timing of the Permian mass extinctions: U-Pb dating of closed-system zircons. *Science* 305(5691):1760-1763.

104. He B, Zhong Y-T, Xu Y-G, Li H-X (2014) Triggers of Permo-Triassic boundary mass extinction in South China: The Siberian Traps or Paleo-Tethys ignimbrite flare-up? *Lithos* 204:258-267.

105. Mao X, Li J, and Zhang H (2014) Zircon U-Pb SHRIMP Ages from the Late Paleozoic Turpan-Hami Basin, NW China. *J. Earth Sci.* 25(5):924-931.

106. Tian W, et al. (2010) The Tarim picrite-basalt-rhyolite suite, a Permian flood basalt from northwest China with contrasting rhyolites produced by fractional crystallization and anatexis. *Contrib. Mineral. Petrol.* 160(3):407-425.

107. Wang Y, et al. (2006) Geochronology and Nd-Sr-Pd isotops of the bimodal volcanic rocks of the Bodga rift. *Acta Petrologica Sinica* 22(5):1215-1224.

108. Xiao Y, et al. (2011) Late Paleozoic magmatic record of East Junggar, NW China and its significance: Implication from zircon U–Pb dating and Hf isotope. *Gondwana Res*. 20:532-542.

109. Shi Y (2013) Zircon U-Pb age, geochemistry and geological implications of granitoids in Tuerkubantao, Xinjiang. *J. Earth Sci*. 24(4):606-618.

110. Zhao Z, et al. (2010) Zircon U-Pb La-ICP-MS dating of Carboniferous volcanics and its geological significance in the northwestern Lesser Xing'an Range. *Acta Petrologica Sinica* 26(8):2542-2464.

111. Allen CM, et al. (1998) Granite genesis and basin formation in an extensional setting: the magmatic history of the northernmost New England Orogen. *Austral. J. Earth Sci*. 45(6), 875-888.

112. Black P, et al. (1994) *U-Pb zircon ion-microprobe ages from the northern Durmmond Basin, northeastern Queensland*. Austral. Geol. Surv.

113. Gulson BL, Diessel CFK, Mason DR, Krough TE (1990) High precision radiometric ages from the northern Sydney Basin and their implication for the Permian time interval and sedimentation rates. Austral. J. Earth Sci. 37(4):459-469.

114 Henderson RA, Davis BK, Fanning CM (1998) Stratigraphy, age relationships and tectonic setting of rift-phase infill in the Drummond Basin, central Queensland. *Austral. J. Earth Sci*. 45:579-595.

115. Opdyke ND, Roberts J, Claoue-Long J, Irving E, Jones PJ (2000) Base of the Kiaman: Its definition and global stratigraphic significance. *Geol. Soc. Am. Bull*. 112(9):1315-1341.

116. Chuvashov BI, et al. (2013) New U-Pb data on the age of rhyolite from Middle Zauralye: Evidence for change of crustal geodynamic regimes. *Doklady Earth Sci*. 45 (1):775-778.

117. Czamanske GK, et al. (2000) Geochemical, isotopic, and SHRIMP age data for Precambrian basement rocks, Permian volcanic rocks, and sedimentary host rocks to the ore-bearing intrusions, Noril'sk-Talnakh District, Siberian Russia. *International Geol. Rev*. 42(10):895-927.

118. Kryza R, et al. (2010) A SIMS zircon age for a biostratigraphically dated Upper Viséan (Asbian) bentonite in the Central-European Variscides (Bardo Unit, Polish Sudetes). *Intl. J. Earth Sci*. 100(6):1227-1235.

119. Schmitz MD, Davydov DI (2012) Quantitative radiometric and biostratigraphic calibration of the Pennsylvanian-Early Permian (Cisuralian) time scale and pan-Euramerican chronostratigraphic correlation. *Geol. Soc. Am. Bull*. 124(3-4):549-577.

120. Vozárová A, Šmelko M, and Paderin I (2009) Permian single crystal U-Pb zircon age of the Rožňava Formation volcanites (Southern Gemeric Unit, Western Carpathians, Slovakia). *Geologica Carpathica* 60(6).

121. Vozárová A, et al. (2012) Permian volcanics in the Northern Gemericum and Bôrka Nappe system: U-Pb zircon dating and the implications for geodynamic evolution (Western Carpathians, Slovakia). *Geologica Carpathica* 63(3).

122. Yarmolyuk VV, et al. (2008) Geochronology of igneous rocks and formation of the Late Paleozoic south Mongolian active margin of the Siberian continent. *Stratigraphy Geol. Correl.* 16(2):162-181.

123. Marocchi M, et al. (2008) Evolution of large silicic magma systems: New U-Pb zircon data on the NW Permian Athesian Volcanic Group (Southern Alps, Italy). *J. Geol.* 116(5):480-498.

124. Nasdala L, et al. (1998) Constraining a SHRIMP U-Pb age: micro-scale characterization of zircons from Saxonian Rotliegend rhyolites. *Contrib. Mineral. Petrol.* 132(3):300-306.

125. Oliveira J, et al. (2013) Geology of the Rosário–Neves Corvo antiform, Iberian Pyrite Belt, Portugal: new insights from physical volcanology, palynostratigraphy and isotope geochronology studies. *Mineralium Deposita* 48(6):749-766.

126. Nawrocki J, et al. (2008) Palaeomagnetism and the age of the Cracow volcanic rocks (S Poland). *Geophys. J. Internat.* 174(2):475-488.

127. Monaghan AA, Parrish RR (2006) Geochronology of Carboniferous-Permian magmatism in the Midland Valley of Scotland: implications for regional tectonomagmtic evolution and the numerical time scale. *J. Geol. Soc. London* 163:15-28.

128. Morelli C, et al. (2012) Volcanic stratigraphy and radiometric age constraints at the northern margin of a mega-caldera system: Athesian Volcanic Group. *GeoActa* 11:51-67.

129. Awdankiewicz MR, Kryza R, Szczepara N (2013) Timing of post-collisional volcanism in the eastern part of the Variscan Belt: constraints from SHRIMP zircon dating of Permian rhyolites in the North-Sudetic Basin (SW Poland). *Geolog. Magazine* 151(04):611-628.

130. Breitkreuz C, Kennedy A, Geibler M, et al. (2007) Far Eastern Avalonia: Its chronostratigraphic structure revealed by SHRIMP zircon ages from Upper Carboniferous to Lower Permian volcanic rocks (drill cores from Germany, Poland, and Denmark). *Geol. Soc. Am. Bull. Spec. Pap.* 423:173-190.

131. Breitkreuz C, Kennedy A (1999) Magmatic flare-up at the Carboniferous-Permian boundary in the NE German Basin revealed by SHRIMP zircon ages. *Tectonophys.* 302:307-326.

132. Eichhorn R, et al. (2000) Multistage Variscan magmatism in the central Tauern Window (Austria) unveiled by U-Pb SHRIMP zircon data. *Contrib. Mineral. Petrol.* 139(4):418-435.

133. Visonà D, et al. (2007) U-Pb SHRIMP zircon dating of andesite from the Dolomite area (NE Italy): geochronological evidence for the early onset of Permian volcanism in the eastern part of the southern Alps. *Swiss J. Geosci.* 100(2):313-324.

134. Dallagiovanna G, Gaggero L, Maino M, Seno S, Tiepolo M (2009) U-Pb zircon ages for post-Variscan volcanism in the Ligurian Alps (Northern Italy). *J. Geol. Soc. London* 166:101-114.

135. Edel JB, et al. (2013) Tectonic evolution of the European Variscan belt constrained by palaeomagnetic, structural and anisotropy of magnetic susceptibility data from the

Northern Vosges magmatic arc (eastern France). *J. Geol. Soc. London* 170(5):785-804.

136. Gretter N, et al. (2013) The transition between the two major Permian tectono-stratigraphic cycles in the central Southern Alps: results from facies analysis and U-Pb geochronology. *Int. J. Earth Sci.* 102(5):1181-1202.

137. Colpron M, et al. (2005) Geology and juxtaposition histroy of the Yukon-Tanana, Slide Mountain, and Cassiar terranes in the Glenlyon area of central Yukon. *Can. J. Earth Sci.* 42(8):1431-1448.

138. Hess JC, Lippolt HJ, Burger K, (1999) High-precision $^{40}Ar/^{39}Ar$ spectrum dating on sanidine from the Donets Basin, Ukraine: evidence for correlation problems in the Upper Carboniferous. *J. Geol. Soc., London*, 156:527-533.

139. Claoue-Long JC (1995) Two Carboniferous ages: A comparison of SHRIMP zircon dating with conventional zircon ages and 40Ar/39Ar analysis. *SEPM Spec. Publ.* 54:3-21.

140. Breitkruez C, Ehling BC, Sergeev S (2009) Chronological evolution of an intrusive extrusive system: the Late Paleozoic Halle Volcanic Complex in the northeastern Saale Basin (Germany). *Z. Dt. Ges. Geowiss.* 160:173-190.

141. Roberts J, Claoue-Long J, Jones PJ, Australian Early Carboniferous time, in *Geochronology Time Scales and Global Stratigraphic Correlation* (SEPM Spec. Publ., Tulsa, 1995) 54:23-40.

142 Schaltegger U, et al. (1996) Precise U-Pb chronometry of 345-340 Ma old magmatism related to syn-convergence extension in the Southern Vosges (Central variscan Belt). *Earth Planet. Sci. Lett.* 144:403-419.

143. Veselá P, Frank S, Friedrich F, Axel G, (2011) Magmato-sedimentary Carboniferous to Jurassic evolution of the western Tauern window, Eastern Alps (constraints from U-Pb zircon dating and geochemistry). *Int. J. Earth Sci. (Geol. Rundsch.)*. 100:993-1027.

144. Schaltegger U, Brack P (2007) Crustal-scale magmatic systems during intracontinental strike-slip tectonics: U, Pb and Hf isotopic constraints from Permian magmatic rocks of the Southern Alps. *Int. J. Earth Sci.* 96(6):1131-1151.

145. Munizaga F, et al. (2008) Late Paleozoic–Early Triassic magmatism on the western margin of Gondwana: Collahuasi area, Northern Chile. *Gondwana Res.* **13**(3), 407-427 (2008).

146. Martina F, Viramonte JM, Astini RA, Pimentel MM, Dantas E (2011) Mississpiian volcanism in the south-central Andes: New U-Pb SHRIMP zircon geochronology and whole-rock geochemistry: *Gondwana Res.* **19**, 524-534 (2011).

147. Simas MW, et al. (2012) Geochronological correlation of the main coal interval in Brazilian Lower Permian: Radiometric dating of tonstein and calibration of biostratigraphic framework. *J. South Am. Earth Sci.* 39:1-15.

148. Rocha-Campos AC, et al. (2011) 30 million years of Permian volcanism recorded in the Choiyoi igneous province (W Argentina) and their source for younger ash fall deposits in the Paraná Basin: SHRIMP U–Pb zircon geochronology evidence. *Gondwana Res.* 19(2):509-523.

149. Santos RV et al. (2006) Shrimp U–Pb zircon dating and palynology of bentonitic layers from the Permian Irati Formation, Paraná Basin, Brazil. *Gondwana Res*. 9(4):456-463.

150. Tabor NJ, et al. (2011) "Ochoan" Quartermaster Formation of north Texas, USA; Part I, Litho- and chemostratigraphy. *Geol. Soc. Am. Bull*. 43(5):383.

151. Shaulis BJ, et al. (2012) Timing and rates of flysch sedimentation in the Stanley Group, Ouachita Mountains, Oklahoma and Arkansas, U.S.A.: Constraints from U-Pb zircon ages of subaqueous ash-flow tuffs. J. Sed. Res. 82(11):833-840.

152. Roots CF, et al. (2002) Constraints on the age of the Klinkit assemblage east of Teslin Lake, northern British Columbia. *Current Res*. A7:1-11.

153. Roots CF, Heaman L (2001) Mississippian U-Pb dates from Dorsey Terrane assemblages in the upper Swift River area, southern Yukon Territory. *Current Res*. A1:1-16.

154. Piercey SJ, et al. (2008) Petrology and U-Pb geochronology of footwall porphyritic rhyolites from the Wolverine volcanogenic massive sulfide deposit, Yukon, Canada: Implications for the genesis of massive sulfide deposits in continental margin environments. *Econ. Geol*. 103:5-33.

155. Ortega-Obregon C, Solari L, Gomez-Tuena A, Elias-Herrera M, Ortega-Gutierrez F, Macias-Romo C (2014) Permian-Carboniferous arc magmatism in southern Mexico: U-Pb dating, trace element and Hf isotopic evidence on zircons of earliest subduction beneath the western margin of Gondwana. *Int. J. Earth Sci*. 103:1287-1300.

156. Lyons PC, et al. (2006) Radiometric ages of the Fire Clay tonstein [Pennsylvanian (Upper Carboniferous), Westphalian, Duckmantian]: A comparison of U–Pb zircon single-crystal ages and $^{40}Ar/^{39}Ar$ sanidine single-crystal plateau ages. *Int. J. Coal Geol*. 67(4):259-266.

157. Dusel-Bacon C, Wooden JL, Hopkins MJ (2004) U-Pb zircon and geochemical evidence for bimodal mid-Paleozoic magmatism and syngenetic base-metal mineralization in the Yukon-Tanana terrane, Alaska. *Geol. Soc. Am. Bull*. **116**(7):989.

158. Alessandretti L, et al. (2013) Provenance, volcanic record, and tectonic setting of the Paleozoic Ventania Fold Belt and the Claromecó Foreland Basin: Implications on sedimentation and volcanism along the southwestern Gondwana margin. *J. South Am. Earth Sci*. 47:12-31.

159. Colpron M, Mortensen JK, Gehrels GE, Villeneuve M (2006) Basement complex, Carboniferous magmatism and Paleozoic deformation in Yukon-Tanana terrane of central Yukon: Field, geochemical and geochronological constraints from Glenlyon map area, in *Paleozoic Evolution and Metallogeny of Pericratonic Terrains at the Ancient Pacific Margin of North America, Canadian and Alaskan Cordillera*. M. Colpron, J. L. Nelson, Eds. *Geol. Assoc. Can. Spec. Pap*. 45:131-151.

160. Dunning GR, Barr SM, Giles PS, McGregor DC, Pe-Piper G, Piper DJW (2002) Chronology of Devonian to early Carboniferous rifting and igneous activity in southern Magdalen Basin based on U-Pb (zircon) dating. *Can. J. Earth Sci*. 39(8): 1219-1237.

161. Murphy DC, et al. (2006) Mid-Paleozoic to early Mesozoic tectonostratigraphic evolution of Yukon-Tanana and Slide Mountain terranes and affiliated overlap assemblages, Finlayson Lake massive sulphide district, southeastern Yukon. *Geol. Assoc. Can. Spec. Pap.* 45:75-105.

162. Roberts J, Offler R, Fanning M (2004) Upper Carboniferous to Lower Permian volcanic successions of the Carroll-Nandewar region, northern Tamworth Belt, southern New England Orogen, Australia. *Austral. J. Earth Sci.* 51:205-232.

163. Claoue-Long JC, Korsch RJ (2003) Geology of the Cranky Corner Basin. *Coal Petrol. Bull.* 4:179-205.

164. Hutton LJ, Withnall IW, Rienks IP, Bultitude RJ, Hayward MA, von Gneilinski FE, Fordham BG, Simpson GA (1999) A preliminary Carboniferous to Permian magmatic framework for the Auburn and Connors Arches, central Queensland, in P. G. Flood, Ed. *New England Orogen* (Univ. New England, Armidale) pp 223-232.

165. Roberts J, Wang X (2003) Stratigraphy and correlation of Carboniferous ignimbrites, Rocky Creek region, Tamworth Belt, Southern New England Orogen, New South Wales. *Austral. J. Earth Sci.* 50:931-954.

166. Li Y, et al. (2014) Geochronology and geochemistry of late Paleozoic volcanic rocks on the western margin of the Songnen–Zhangguangcai Range Massif, NE China: Implications for the amalgamation history of the Xing'an and Songnen–Zhangguangcai Range massifs. *Lithos* 205:394-410.

167. Yang G, et al. (2014) Early Carboniferous volcanic rocks of West Junggar in the western Central Asian Orogenic Belt: implications for a supra-subduction system. *Int. Geol. Rev.* 56(7):823-844.

168. Yu Q, et al. (2014) Petrogenesis of late Paleozoic volcanic rocks from the Daheshen Formation in central Jilin Province, NE China, and its tectonic implications: Constraints from geochronology, geochemistry and Sr–Nd–Hf isotopes. *Lithos* 192-195:116-131.

169. Su Y, et al. (2012) Geochemistry and geochronology of Carboniferous volcanic rocks in the eastern Junggar terrane, NW China: Implication for a tectonic transition. *Gondwana Res.* 22(3-4):1009-1029.

170. Zhang Z, et al. (2009) Late Paleozoic volcanic record of the Eastern Junggar terrane, Xinjiang, Northwestern China: Major and trace element characteristics, Sr–Nd isotopic systematics and implications for tectonic evolution. *Gondwana Res.* 16(2):201-215.

171. Li Y, et al. (2011) Late Carboniferous - Middle Permian arc/forearc-related basin in Central Asian Orogenic Belt: Insights from the petrology and geochemistry of the Shuangjing Schist in Inner Mongolia, China. *Island Arc.* 20(4):535-549.

172. Lai C-K, Meffre S, Crawford AJ, Zaw K, Xue C-D, Halpin JD (2014) The Western Ailaoshan Volcanic Belts and their SE Asia connection: A new tectonic model for the Eastern Indochina Block. *Gondwana Res.* 26:52-7.

173. Bryan SE, Allen CM, Holcombe RJ, Fielding CR (2004) U-Pb zircon geochronology of Late Devonian to Early Carboniferous extension-related silicic volcanism in the northern New England Fold Belt. *Austral. J. Earth Sci.* 51:645-664.

174. Michaelsen P, et al. (2001) Age and significance of the Platypus Tuff Bed, a regional reference horizon in the Upper Permian Moranbah Coal Measures, north Bowen Basin. *Austral. J. Earth Sci.* 48:183-192.

175. Blight JHS, et al. (2010) The Oyut Ulaan Volcanic Group: stratigraphy, magmatic evolution and timing of Carboniferous arc development in SE Mongolia. *J. Geol. Soc., London*. 167(3):491-509.

176. Chen X, et al. (2013) Island arc-type bimodal magmatism in the eastern Tianshan Belt, Northwest China: Geochemistry, zircon U–Pb geochronology and implications for the Paleozoic crustal evolution in Central Asia. *Lithos* 168-169:48-66.

177. Chen X, Shu L, Santosh M (2011) Late Paleozoic post-collisional magmatism in the Eastern Tianshan Belt, northwest China: New insights from geochemistry, geochronology and petrology of bimodal volcanic rocks: *Lithos* 127:581-598.

178. Geng H, et al. (2011) Geochemical and geochronological study of early Carboniferous volcanic rocks from the West Junggar: Petrogenesis and tectonic implications. *J. Asian Earth Sci.* 42(5):854-866.

179. Davydov VI, et al. (2010) High-precision U-Pb zircon age calibration of the global Carboniferous time scale and Milankovitch band cyclicity in the Donets Basin, eastern Ukraine. *Geochem. Geophys. Geosys.* 11(2).

180. Liu J, et al. (2014) Origin of Late Palaeozoic bauxites in the North China Craton: constraints from zircon U-Pb geochronology and in situ Hf isotopes. *J. Geol. Soc. London* 171(5):695-707.

181. Li D, et al. (2013) Early Permian post-collisional magmatic events, East Junggar: Constraints from zircon SHRIMP U-Pb age, geochemistry and Hf isotope of rhyolite in the Yundukala area. *Acta Petrologica Sinica*. 29(1):317-337.

182. Li W, et al. (2013) The geochemical characteristics, geochronology and tectonic significance of the Carboniferous volcanic rocks of the Santanghu area in northeastern Xinjiang, China. *Sci. China Earth Sci.* 56(8):1318-1333.

183. Liu D, et al. (2014) Petrology and geochemistry of Early Permian volcanic rocks in South Tian Shan, NW China: implications for the tectonic evolution and Phanerozoic continental growth. *Int. J. Earth Sci.* 103(3):737-756.

184. Liu H-Q, et al. (2014) Origin of two types of rhyolites in the Tarim Large Igneous Province: Consequences of incubation and melting of a mantle plume. *Lithos* 204:59-72 (2014).

185. Ramezani J, et al. (2007) High-precision U–Pb zircon age constraints on the Carboniferous–Permian boundary in the southern Urals stratotype. *Earth Planet. Sci. Lett.* 256(1-2):244-257.

186. Shu L, et al. (2010) Timing of initiation of extension in the Tianshan, based on structural, geochemical and geochronological analyses of bimodal volcanism and olistostrome in the Bogda Shan (NW China). *Int. J. Earth Sci.* 100(7):1647-1663.

187. Su Y, Zheng J, Griffin WJ, Zhao J, Tang H, Ma Q, Lin X (2012) Geochemistry and geochronology of Carboniferous volcanic rocks in the eastern Junggar terrane, NW China: Implication for a tectonic transition. *Gondwana Res.* 22, 1009-1029.

188. Tang GJ, et al. (2010) Geochronology and geochemistry of Late Paleozoic magmatic rocks in the Lamasu–Dabate area, northwestern Tianshan (west China): Evidence for a tectonic transition from arc to post-collisional setting. *Lithos* 119(3-4):393-411.

189. Wan B, et al. (2011) Contrasting styles of mineralization in the Chinese Altai and East Junggar, NW China: implications for the accretionary history of the southern Altaids. *J. Geol. Soc. London* 168(6):1311-1321.

190. Zhang S-H, et al. (2007) Zircon SHRIMP U–Pb and in-situ Lu–Hf isotope analyses of a tuff from Western Beijing: Evidence for missing Late Paleozoic arc volcano eruptions at the northern margin of the North China block. *Gondwana Res*. 12(1-2):157-165.

191. Zhu Y, et al. (2009) Petrology, Sr-Nd-Hf isotopic geochemistry and zircon chronology of the Late Palaeozoic volcanic rocks in the southwestern Tianshan Mountains, Xinjiang, NW China. *J. Geol. Soc. London* 166(6):1085-1099.

192. Li D, et al. (2012) Genesis of Early Carboniferous volcanic rocks of the Di'nan uplift in Junggar Basin: Constraints to the closure time of Kalamaili ocean. *Acta Petrologica Sinica* 28(8):2340-2354.

193. Li K, et al. (2014) Zircon SHRIMPU-Pb dating and its geological significance of the Late-Carboniferous to Early-Permian volcanic rocks in Bayanwyla area, the central of Inner Monolia. *Acta Petrologica Sinica* 30(7):2041-2054.

194. He D-F, et al. (2013) Geochronology, geochemistry and tectonostratigraphy of Carboniferous strata of the deepest Well Moshen-1 in the Junggar Basin, northwest China: Insights into the continental growth of Central Asia. *Gondwana Res*. 24(2):560-577.

195. Jian P, et al. (2010) Evolution of a Permian intraoceanic arc–trench system in the Solonker suture zone, Central Asian Orogenic Belt, China and Mongolia. *Lithos* 118(1-2):169-190.

196. Luo J, et al. (2008) Geochemical and geochronological characteristics and its tectonic significance of Early Permian acid volcanic rocks of Xiaotikanlike Formation in the southern margin of South Tianshan orogen, NW China. *Acta Petrologica Sinica* 24(10), 2281-2288.

197. Liu D, et al. (2012) The Late Paleozoic tectonic relationship between the Tian Shan orogenic belt and Junggar basin: Constraints from zircon SHRIMP U-Pb dating and geochemistry characteristics of volcanic rocks in Arbasay Formation. *Acta Petrologica Sinica* 28(7):2355-2368.

198. Mao Q, et al. (2014) Geochronology, geochemistry and petrogenesis of Early Permian alkaline magmatism in the Eastern Tianshan: Implications for tectonics of the Southern Altaids. *Lithos* 190-191:37-51.

199. Qian X, et al. (2013) Geochemical and geochronological constrains on the Chiang Khong volcanic rocks (northwestern Thailand) and its tectonic implications. *Frontiers Earth Sci*. 7(4):508-521.

200. Qing M, Tang MG, Ge LS, Han XJ, Feng JB, Yuan SS, Zhao YS (2012) LA-ICP-MS zircon U-Pb age, geochemistry of andesite in Bilihe goldfield, Suniteyouqi, Inner Mongolia and its tectonic significance. *Acta Petrologica Sinica*, 28(2):514-524.

201. Tang G, et al. (2009) LA-ICP-MS zircon U-Pb geochronology, element geochemistry and petrogenesis of the andesites in the wastern Taerbieke gold deposit of the western Tianshan region. *Acta Petrologica Sinica* 25(6):1341-1352.

202. Wainwright AJ, et al. (2010) Devonian and Carboniferous arcs of the Oyu Tolgoi porphyry Cu-Au district, South Gobi region, Mongolia. *Geol. Soc. Am. Bull.* 123(1-2):306-328.

203. Zhang X, et al. (2008) Geochemistry of Permian bimodal volcanic rocks from central Inner Mongolia, North China: Implication for tectonic setting and Phanerozoic continental growth in Central Asian Orogenic Belt. *Chem. Geol.* 249(3-4):262-281.

204. Zhang X, et al. (2011) Early Permian high-K calc-alkaline volcanic rocks from NW Inner Mongolia, North China: geochemistry, origin and tectonic implications. *J. Geol. Soc. London* 168(2):525-543.

205. Zhao Z, et al. (2010) Late Paleozoic arc-related magmatism in Yakeshi region Inner Mongolia: Chronological and geochemical evidence. *Acta Petrologica Sinica* 26(11):3245-3258.

206. Zhu Z-H, Jiang S-Y, Liu G-X, Zhao K-D (2013) Precise dating of the Middle Permian: Zircon U–Pb geochronology from volcanic ash beds in the basal Gufeng Formation, Yangtze region, South China. *Gondwana Res.* 23(4):1599-1606.

207. Zhu Y, et al. (2005) The zircon SHRIMP chronology and trace element geochemistry of the Carboniferous volcanic rocks in western Tianshan Mountains. *Chinese Sci. Bull.* 50(19):2201-2212.

208. Peng T, et al. (2008) Arc-like volcanic rocks from the southern Lancangjiang zone, SW China: Geochronological and geochemical constraints on their petrogenesis and tectonic implications. *Lithos* 102(1-2):358-373.

209. An F, Zhu Y (2008) Study on trace elements geochemistry and SHRIMP chronology of volcanic rocks in Tulasu Basin, Northwest Tianshan. *Acta Petrologica Sinica* 24(12):2741-2748.

210. Blight JHS, Petterson MG, Crowley QG, Cunningham D (2010) The Oyut Ulaan Volcanic Group: stratigraphy, magmatic evolution and timing of Carboniferous arc development in SE Mongolia. *J. Geol. Soc. London* 167:491-509.

211. Chen B, et al. (2007) SHRIMP U-Pb zircon geochronology of igneous rocks from southern margin of the Alataw mountains, Xinjiang, China. *Acta Petrologica Sinica*. **23**(7):1756-1764.

212. An F, Zhu Y (2009) SHRIMP U-Pb zircon ages of tuff in Baogutu Formation and their geological significances. *Acta Petrologica Sinica*. 25(6):1437-1445.

213. Guo L, et al. (2010) The zircon U-Pb LA-ICP-MS geochronology of volcanic rocks in Baogutu areas, western Junggar. *Acta Petrologica Sinica*. 26(2):471-477.

214. Oliver G, Zaw K, Hotson M, Meffre S, Manka T (2014) U–Pb zircon geochronology of Early Permian to Late Triassic rocks from Singapore and Johor: A plate tectonic reinterpretation. *Gondwana Res*. 26(1):132-143.

215. Ruzhentsev SV, et al. (2012) The Baikal-Vitim Fold System: Structure and geodynamic evolution. *Geotectonics* 46(2):87-110.

216. Park AF, Treat RL, Barr SM, White CE, Miller BV, Reynolds PH, Hamilton MA (2014) Structural setting and age of the Partridge Island Block, southern New Brunswick, Canada: a link to the Cobequid Highlands of northern mainland Nova Scotia. *Can. J. Earth Sci*. 51:1-24.

217. Eckoff J, et al. (2013) U-Pb zircon geochronology in the late Devonian Exshaw Formation; global correlation with the Hangenberg black shale and extinction event. *Geol. Soc. Am. Ann. Meet. Abst*. 45(7):581.

218. Erdmer P, et al. (2005) Mississippian volcanic assembblage conformably overlying Cordilleran miogeoclinal strata, Turnagain River area, northern British Columbia, is not part of an accreted terrane. *Can. J. Earth Sci*. 42(8):1449-1465 .

219. Israel S, et al. (2014) New ties between the Alexander terrane and Wrangellia and implications for North America Cordilleran evolution. *Lithosphere* 6(4):270-276.

220. Bailey S (2002) *Geology and geochemistry of the Eagle Bay assemblage in the Johnson Lake area Kootenay Terrane, Southcentral British Columbia*. (MS Thesis, Univ. Victoria Victoria B.C. Canada) 200 pp.

221. Paradis S, et al. (2006) Paleozoic magmatism and syngenetic massive sulphide deposits of the Eagle Bay assemblage, Kootenay terrane, southern British Columbia. *Geol. Assoc. Can., Spec. Pap*. 45:383-414.

222. Richards BC, Ross GM, Utting J (2002) U-Pb geochronology, lithostratigraphy and biostratigraphy of tuff in the upper Famennian to Tournaisian Exshaw Formation: Evidence for a mid-Paleozoic magmatic arc on the northwestern margin of North America. *Can. Soc. Petrol. Geol. Mem*. 19:158-207.

223. Wendt I, et al. (1995) Radiometric dating of volcanic rocks in NW-Saxony by combined use of U-Pb and Sm-Nd zircon dating as well as Sm-Nd and Rb-Sr whole-rock and mineral systematics. *Terra Nostra* 7-95:147-148.

224. Witt WK, et al. (2013) New geochronological results and structural evolution of the Pataz gold mining district: Implications for the timing and origin of the batholith-hosted veins. *Ore Geol. Rev*. 50:143-170.

225. Marcoux E, et al. (2008) Draa Sfar, Morocco: A Visean (331 Ma) pyrrhotite-rich, polymetallic volcanogenic massive sulphide deposit in a Hercynian sediment-dominant terrane. *Ore Geol. Rev*. 33(3-4):307-328.

226. Brownlow J, Cross A (2010) TIMS U-Pb and SHRIMP U-Pb zircon dating of the Dundee Rhyodacite, northern New England, New South Wales. *New England Orogen*, 69-74.

227. Fanning CM, Withnall LJ, Hutton RJ, Bultitude RJ, Von Gnielinski FE, Rienks IP (2005) Shrimp U-Pb Zircon ages from Central Queensland, *Queensland Geology* 12:463-580.

228. Roberts J, Claoue-Long J, Jones PJ, Foster CB (1995) SHRIMP zircon age control of Gondwanan sequences in Late Carboniferous and Early Permian Australia. *Geol. Soc. Spec. Pub.* 89:145-174.

229. Davydov VI, Crowley J, Schmitz MD (2014) Permian-Triassic transition exists in the Phosphoria Basin, eastern Idaho. *Geol. Soc. Am. Abst.* 46(6):418.

230. Martin MW, Walker JD (1995) Stratigraphy and Paleogeographic Significance of Metamorphic Rocks in the Shadow Mountains, Western Mojave Desert, California. *Geol. Soc. Am. Bull.* 107(3):354-366.

231. Thomas WA (2013) The Sabine and Coahuila terranes at the southern margin of Laurentia. *Geol. Soc. Am. Abst.* 45(7):293.

232. Melchor RN (2000) Stratigraphic and biostratigraphic consequences of a new $^{40}Ar/^{39}Ar$ date for the base of the Cochico Group (Permian), Eastern Permian Basin, San Rafael, Mendoza, Argentina. *Rev. Assoc. Paleontol. Argentina* 37(3):271-282.

233. Bruguier O, Becq-Giraudon JF Champenois M, Deloule E, Ludden J, Mangin D (2003) Application of in situ zircon geochronology and accessory phase chemistry to constraining basin development during post-collisional extension: a case study from the French Massif Central. *Chem. Geol.* 201:319-336.

234. Capuzzo N, Bussy F (2000) High-precision dating and origin of synsedimentary volcanism in the Late Carboniferous Salvan-Dorenaz basin (Aiguilles-Rouges Massif, Western Alps). *Schweiz. Mineral. Petrogr. Mitt.* 80:147-167.

235. Goll M, Lippolt HJ (2001) Biotite-geochronology ($^{40}Ar/K$, $^{40}Ar/^{39}Ar$, $^{86}Sr/^{87}Rb$) of Late Variscan magmatic rocks in the Thuringian Forest, Germany. *Neues Jahrbuch Geol. Palaont.* 222(3):353-405.

236. Hess JC, Lippolt HJ (1986) $^{40}Ar/^{39}Ar$ ages of tonstein and tuff sanidines: new calibration points for the improvement of the Upper Carboniferous time scale. *Chem. Geol.* 59:143-154.

237. Mao X, Li JH, Zhang HT (2014) Zircon U-Pb SHRIMP ages from the Late Paleozoic Turpan-Hami Basin, NW China. *J. Earth Sci.* 25(5):924-931.

238. Miao LC, et al. (2004) Zircon SHRIMP geochronology of the Xinkailing-Kele complex in the northwestern Lesser Xing'an Range, and its geological implications. *Chinese Sci. Bull.* 49(2):201-209.

239. Tian W, et al. (2010) The Tarim picrite–basalt–rhyolite suite, a Permian flood basalt from northwest China with contrasting rhyolites produced by fractional crystallization and anatexis. *Contrib. Mineral. Petrol.* 160(3):407-425.

240. Yang TN, et al. (2011) Permo-Triassic arc magmatism in central Tibet: Evidence from zircon U–Pb geochronology, Hf isotopes, rare earth elements, and bulk geochemistry. *Chem. Geol.* 284(3-4):270-282.

241. Awdankiweicz M, Kryza R (2010) The Gory Suche rhyolitic tuffs (Intra-Sudetic Basin, SW Poland): preliminary SHRIMP zircon age. *Mineralogia Spec. Pap.* 37:70.

242. Kirnbauer T, Reischmann T (1999) Pb/Pb ages on zircons from the Hunsruck Slate near Bundenbach (Devonian, Rhenish Massif). Hannover: *Deutsche Geologische Gesellschaft* 7:58.

243. Rosa DRN, et al. (2008) U-Pb geochronology of felsic volcanic rocks hosted in the Gafo Formation, South Portuguese Zone: the relationship with Iberian Pyrite Belt magmatism. *Mineral. Mag.* 72(5):1103-1118.

244. Sundvoll B, Larsen BT (1990) Rb-Sr isotope systematics in the magmatic rocks of the Oslo Rift. *Nor. Geol. Unders. Bull.* 418:27-46.

245. Manaka T, et al. (2014) The Ban Houayxai epithermal Au–Ag deposit in the Northern Lao PDR: Mineralization related to the Early Permian arc magmatism of the Truong Son Fold Belt. *Gondwana Res.* 26(1):185-197.

246. Shen P, et al. (2013) Early Carboniferous intra-oceanic arc and back-arc basin system in the West Junggar, NW China. *Int. Geol. Rev.* 55(16):1991-2007.

247. Zhai W, et al. (2006) SHRIMP dating of zircons from volcanic host rocks of Dahalajunshan Formation in Axi gold deposit, Xinjiang, China, and its geological implications. *Acta Petrologica Sinica* 22(5):1399-1404.

248. Xu C, et al. (2013) Geochronology of ore-bearing andesite in the Kuoerzhenkoula Au deposit, Northern Xinjiang, China. *Goldschmidt Conf. Abstracts* 2524.

249. Bultitude RJ, et al. (1997) Cairns region. *Geosci. Austral. Bull.* 225-325.

250. Childe F, et al. (1998) Primitive Permo-Triassic volcanism in the Canadian Cordillera: Tectonic and metallogenic implications. *Econ. Geol. Bull. Soc. Econ. Geol.* 93(2):224-231.

251. Mihalynuk MG, Friedman RM, Devine F, Heaman LM (2006) Protolith age and deformation history of the Big Salmon Complex, relics of a Paleozoic continental arc in British in *Paleozoic Evolution and Metallogeny of Pericratonic Terrains at the Ancient Pacific Margin of North America, Canadian and Alaskan Cordillera*. M. Colpron M, Nelson JL, Eds. *Geol. Assoc. Can. Spec. Pap.* 45:179-200.

252. Nelson J, Friedman R (2004) Superimposed Quesnel (late Paleozoic-Jurassic) and Yukon-Tanana (Devonian-Mississippian) arc assemblages, Cassiar Mountains, northern British Columbia: field, U-Pb, and igneous petrochemical evidence. *Can. J. Earth Sci.* 41(10):1201-1235.

253. Raterman NS, McClelland WC, Presnell RD (2006) Geochronology and lithogeochemistry of volcanic rocks of the Ambler District, southern Brooks Range, Alaska. *Geol. Soc. Am. Abst.* 38(5):69.

254. Suarez M, de la Cruz R, Fanning M, Etchart H (2008) Carboniferous, Permian and Toarcian magmatism in Cordillera del Viento, Neuquen, Argentina: first U-Pb SHRIMP dates amd tectonic implications. *Congreso Geologico Argentino* XVII:906-907.

255. Bargossi GM, Kloetzli US, Mair V, Marocchi M, Morelli C (2012) The Lower Permian Athesian Volcanic Group (AVG) in the Adige valley between Merano and Bolzano: a stratigraphic, petrographic and geochronological outline. *Int. Geol. Congr.* 32:187.

256. Corfu F, Dahlgren S (2008) Perovskite U–Pb ages and the Pb isotopic composition of alkaline volcanism initiating the Permo-Carboniferous Oslo Rift. *Earth Planet. Sci. Lett.* 265(1-2):256-269.

257. Heeremans M, Faleide JI (2004) Late Carboniferous-Permian tectonics and magmatic activity in the Skagerrak, Kattegat and the North Sea. *Geol. Soc. London Spec. Pub.* 223(1):157-176.

258. Hoffman U, Breitkreuz C, Breiter K, Sergeev S, Stanek K, Tichomirowa M (2013) Carboniferous-Permian volcanic evolution in Central Europe-U-Pb ages of volcanic rocks in Saxony (Germany) and northern Bohemia (Czech Republic). *Int. J. Earth Sci.* 102:73-99.

259. Hofmann H et al. (2009) Timing of dextral strike-slip processes and basement exhumation in the Elbe Zone (Saxo-Thuringian Zone): the final pulse of the Variscan orogeny in the Bohemian Massif constrained by LA-SF-ICP-MS U-Pb zircon data. *Geol. Soc. London Spec. Pub.* 327:197-214.

260. Jirásek J, et al. (2013) The Main Ostrava Whetstone: composition, sedimentary processes, palaeogeography and geochronology of a major Mississippian volcaniclastic unit of the Upper Silesian Basin (Poland and Czech Republic). *Int. J. Earth Sci.* 102(4):989-1006.

261. Koniger S, et al. (2002) Origin, age and stratigraphic significance of distal fallout ash tuffs from the Carboniferous-Permian continental Saar-Nahe Basin (SW Germany). *Int. J. Earth Sci.* 91(2):341-356.

262. Kryza R, Awdankeiwicz M (2012) Ambiguous geological position of Carboniferous rhyodacites in the Intra-sudetic basin (SW Poland) clarified by SHRIMP zircon ages. *Geological Quarterly* 56(1):55-66.

263. Lelkes-Felvari G, Klötzli U (2004) Zircon geochronology of the Kekkut quartz porphyry, Balaton Highland, transdanubian Central Range, Hungary. *Acta Geologica Hungarica* 47(2-3):139-149.

264. Machowiak K, Muszynski A, Armstrong R (2014) High-level volcanic-granodioritic intrusions from Zelezniak Hill (Kaczawa Mountains, Sudetes, SW Poland). *Geol. Soc. London Spec. Pub.* 234:67-74.

265. Shen P, et al. (2012) Northwestern Junggar Basin, Xiemisitai Mountains, China: A geochemical and geochronological approach. *Lithos* 140-141:103-118.

266. Wang Y, et al. (2011) Geochemistry, zircon U–Pb ages and Hf isotopes of the Paleozoic volcanic rocks in the northwestern Chinese Altai: Petrogenesis and tectonic implications. *J. Asian Earth Sci.* 42(5):969-985.

267. Bull KF, et al. (2008) Geochemistry, geochronology and tectonic implications of Late Silurian – Early Devonian volcanic successions, Central Lachlan Orogen, New South Wales. *Austral. J. Earth Sci.* 55(2):235-264.

268. Claoue-Long, JC et al. (1992) The Numerical age of the Devonian-Carboniferous boundary. *Geol. Mag.* 129(3):281-291.

269. Compston W (2004) SIMS U-Pb zircon ages for the Upper Devonian Snobs Creek and Cerberean Volcanics from Victoria, with age uncertainty based on UO2/UO v. UO/U precision. *J. Geol. Soc. London* 161:223-228.

270. Jagodzinski EA, Black LP (1999) U–Pb dating of silicic lavas, sills and syneruptive resedimented volcaniclastic deposits of the Lower Devonian Crudine Group, Hill End Trough, New South Wales. *Austral. J. Earth Sci.* 46:749-76.

271. Cross A, et al. (2008) Joint GSQ-GA NGA geochronology project New England Orogen and Drummond Basin. *Queensland Geological Record 2009* 03:1-35.

272. Hons TRG (2010), *Late Paleozoic Felsic Volcanics in Southern New Brunswick and Related Uranium Mineralization* (Saint Mary's University, Halifax, Heritage Branch).

273. Martens U, Weber B, Valencia VA (2009) U-Pb geochronology of Devonian and older Paleozoic beds in the southeastern Maya block, Central America: Its affinity with peri-Gondwanan terranes. *Geol. Soc. Am. Bull.* 122(5-6):815-829.

274. Park AF, et al. (2014) Structural setting and age of the Partridge Island block, southern New Brunswick, Canada: a link to the Cobequid Highlands of northern mainland Nova Scotia. *Canad. J. Earth Sci.* 51(1):1-24.

275. Thompson MD, Hermes OD (2003) Early Rifting in the Narragansett Basin, Massachusetts–Rhode Island: Evidence from Late Devonian Bimodal Volcanic Rocks. *J. Geol.* 111:597-604.

276. Tucker RD, McKerrow WS (1995) Early Paleozoic chronology: a review in light of new U - Pb zircon ages from Newfoundland and Britain. *Canad. J. Earth Sci.* 32:368-379.

277. Tucker RD, Bradley DC, Ver Straeten CA, Harris AG, Ebert JR, McCutcheon SR (1998) New U–Pb zircon ages and the duration and division of Devonian time. *Earth Planet. Sci. Lett.* 158:175-186.

278. Janoušek V, et al. (2013) Constraining genesis and geotectonic setting of metavolcanic complexes: a multidisciplinary study of the Devonian Vrbno Group (Hrubý Jeseník Mts., Czech Republic). *Int. J. Earth Sci.* 103(2):455-483.

279. Myrow PM, et al. (2014) High-precision U-Pb age and duration of the latest Devonian (Famennian) Hangenberg event, and its implications. *Terra Nova.* 26(3):222-229.

280. Parry SF, et al. (2011) A high-precision U-Pb age constraint on the Rhynie Chert Konservat-Lagerstatte: time scale and other implications. *J. Geol. Soc. London* 168(4):863-872.

281. Peucat JJ, Paris F, Chalet M (1986) U-Pb zircon dating of volcanic rocks, close to the Silurian-Devonian boundary, from Vendee (western France). *Chem. Geol.* 59:133-142.

282. Pin C, Paquette J-L (1997) A mantle-derived bimodal suite in the Hercynian Belt: Nd isotope and trace element evidence for a subduction-related rift origin of the Late Devonian Brevenne metavolcanics, Massif Central (France). *Contrib. Mineral. Petrol.* 129:222-238.

283. Zhang J, Wang J, Ding R (2000) Characteristics and U-Pb ages of zircon in metavolcanics from the Kangbutiebao Formation in the Altay orogen, Xinjiang. *Regional Geol. China* 19(3):281-287.

284. An, F et al. (2013) An Early Devonian to Early Carboniferous volcanic arc in North Tianshan, NW China: Geochronological and geochemical evidence from volcanic rocks. *J. Asian Earth Sci.* 78:100-113.

285. Chai F, et al. (2009) Geochronology and genesis of the meta-rhyolites in the Kangbutiebao Formaion from the Keland basin at the southern margin of the Altay, Xinjiang. *Acta Petrologica Sinica* 25(6):1403-1415.

286. Chen L, et al. (2014) U–Pb zircon ages and geochemistry of the Wuguan complex in the Qinling orogen, central China: Implications for the late Paleozoic tectonic evolution between the Sino-Korean and Yangtze cratons. *Lithos* 192-195:192-207.

287. Demoux A, et al. (2009) Devonian arc-related magmatism in the Tseel terrane of SW Mongolia: chronological and geochemical evidence. *J. Geol. Soc. London* 166(3):459-471.

288. Geng X, et al. (2010) Geochronology and genesis of the bimodal volcanic rocks in Dalawuzi from the southern margin of Altay, Xinjiang. *Acta Petrologica Sinica* 26(10):2967-2980.

289. Li Y, et al. (2012) Confirmation of Devonian volcanic rocks from Yining block, Xinjiang and its geological significations. *Acta Petrologica Sinica* 28(4):1225-1237.

290. Lin W, et al. (2013) Geochronological and geochemical constraints for a middle Paleozoic continental arc on the northern margin of the Tarim block: Implications for the Paleozoic tectonic evolution of the South Chinese Tianshan. *Lithosphere* 5(4):355-381.

291. Liu X, et al. (2013) U-Pb zircon age and geochemical constraints on tectonic evolution of the Paleozoic accretionary orogenic system in the Tongbai orogen, central China. *Tectonophys*. 599:67-88.

292. Lu L, et al. (2010) Zircon U-Pb age for rhyolite of the Maoniushan Formation and its tectonic significance in the East Kunlun Mountains. *Acta Petrologica Sinica*. 26(4):1150-1158.

293. Ru, Y et al. (2012) LA-ICP-MS zircon U-Pb age and tectonic background of the Dahalajunshan Formation colvanic rocks in Wusunshan area, West Tianshan Mountains. *Geol. Bull. China* 31(1):50-62.

294. Shan Q, et al. (2012) Zircon U-Pb ages and geochemistry of the potassic and sodic rhyolites of the Kangbutiebao Formation in the southern margin of Altay, Xinjiang. *Acta Petrologica Sinica* 28(7):2132-2144.

295. Thirlwall MF (1988) Geochronology of Late Caledonian magmatism in northern Britain. *J. Geol. Soc. London* 145:951-967.

296. Zeh A, Bratz H (2000) Radiometrische und morphologische Untersuchungen an Zirkonen aus Granitporphyren, Rhyolithen und Granit-gerollen des nordwestlichen Thuringer Waldes. *Zeitschrift Deutschen Geologischen Geseeschaft* 151(1-2):187-20.

297. Nie F, et al. (2009) Zircon SHRIMP U-Pb dating on rhyolite samples from the Xilimiao Group occurring in the Su-Cha (Sumoqagan Obo) fluorite district, Inner Mongolia. *Acta Geologica Sinica* 83(4):496-504.

298. Warren AA, et al. (2001) Oldest known stereospondylous amphibian from the early Permian of Namibia. *J. Vert. Paleonotol*. 21(1):34-39.

299. Stockar R, Baumgartner PO, Condon D (2012) Integrated Ladinian bio-chronostratigraphy and geochrononology of Monte San Giorgio (Southern Alps, Switzerland). *Swiss J. Geosci*. 105(1):85-108.

300. Schaltegger U, et al. (2008) Precise U–Pb age constraints for end-Triassic mass extinction, its correlation to volcanism and Hettangian post-extinction recovery. *Earth Planet. Sci. Lett*. 267(1-2):266-275.

301. Ozdamer S, Billor MS, Sunal G, Esenli F, Roden MF (2013) First U-Pb SHRIMP zircon and 40Ar/39Ar ages of metarhyolites from the Afyon-Bolkardage Zone, SW Turkey: Implications for the rifting and closure of the Neo-Tethys: *Gondwana Res*. 24:377-391.

302. Furrer H, et al. (2008) U-Pb zircon age of volcaniclastic layers in Middle Triassic platform carbonates of the Austroalpine Silvretta nappe (Switzerland). *Swiss J. Geosci*. 101(3):595-603.

303. Brack P, Rieber H, Mundil R, Blendinger W, Maurer F (2007) Geometry and chronology of growth and drowning of Middle Triassic carbonate platforms (Cernera and Bivera/Clapsavon) in the Southern Alps (northern Italy). *Swiss J. Geosci* 100, 327-347.

304. Brack P, Mundil R, Oberli F, Meier M, Rieber H (1996) Biostratigraphic and radiometric age data question the Milankovitch characteristics of the Latemar cycles (southern Alps, Italy). *Geology* 24:371-375.

305. Akal C, Candan O, Koralay OE, Oberhansli R, Chen F, Prelevic D (2012) Early Triassic potassic volcanism in the Afyon Zone of the Anatolides/Turkey: implications for the rifting of the Neo-Tethys. *Int. J. Earth Sci*. 101:177-194.

306. Wotzlaw JF, et al. (2014) Towards accurate numerical calibration of the Late Triassic: High-precision U-Pb geochronology constraints on the duration of the Rhaetian. *Geology* 42(7):571-574.

307. Spalletti LA, Fanning CM, Rapela CW (2008) Dating the Triassic continental rift in the southern Andes: the Potrerillos Formation, Cuyo Basin, Argentina. *Geologica Acta* 6(3):267-283.

308. Mancuso AC, et al. (2010) Age constraints for the northernmost outcrops of the Triassic Cuyana Basin, Argentina. *J. South Am. Earth Sci*. 30(2):97-103.

309. Boekhout F, et al. (2013) Late Paleozoic to Jurassic chronostratigraphy of coastal southern Peru: Temporal evolution of sedimentation along an active margin. *J. South Am. Earth Sci*. 47:179-200.

310. Barredo S, et al. (2012) Tectono-sequence stratigraphy and U–Pb zircon ages of the Rincón Blanco Depocenter, northern Cuyo Rift, Argentina. *Gondwana Res*. 21(2-3):624-636.

311. Avila JN, et al. (2006) Combined stratigraphic and isotopic studies of Triassic strata, Cuyo Basin, Argentine Precordillera. *Geol. Soc. Am. Bull*. 118(9-10):1088-1098.

312. Riggs NR, et al. (2003) Isotopic age of the Black Forest Bed, Petrified Forest Member, Chinle Formation, Arizona: An example of dating a continental sandstone. *Geol. Soc. Am. Bull*. 115(11):1315-1323.

313. Green D (2001) *Geology of Volcanogenic Massive Sulphide Prospects of the Palmer Property, Haines Area, Southeastern Alaska*. (Ottawa, Department of Earth Sciences, Carleton University).

314. Childe FC, Thompson JFH (1997) Geological setting, U-Pb geochronology, and radiogenic isotopic characteristics of the Permo-Triassic Kutcho Assemblage, north-central British Columbia. *Can. J. Earth Sci.* 34:1310-1324.

315. Donskaya TV, et al. (2012) The Late Triassic Kataev volcanoplutonic association in western Transbaikalia, a fragment of the active continental margin of the Mongol-Okhotsk Ocean. *Russian Geol. Geophys.* 53(1):22-36.

316. Czamanske GK, Wooden JL, Walker RJ, Fedorenko VA, Simonov ON, Budahn JR, Siems DF (2002) Geochemical, isotopic, and SHRIMP age data for Precambrian basement rocks, Permian volcanic rocks, and sedimentary host rocks to the ore-bearing intrusions, Noril'sk-Talnakh District, Siberian Russia. *Int. Books Series* 5:238-270.

317. Zi JW, et al. (2012) Triassic collision in the Paleo-Tethys Ocean constrained by volcanic activity in SW China. *Lithos* 144-145:145-160.

318. Zhu WG, et al. (2011) Petrogenesis of the basalts and rhyolite porphyries of the Minle copper deposit, Yunnan: Geochronological and geochemical constraints. *Acta Petrologica Sinica* 27(9):2694-2708.

319. Zhang C, et al. (2007) Tectonic evolution of the Western Kunlun orogenic belt in northern Qinghai-Tibet Plateau: Evidence from zircon SHRIMP and LA-ICP-MSU-Pb geochronology. *Sci. China Ser. D: Earth Sci.* 50(6):825-835.

320. Zeng Q, et al. (2012) Geological and thermochronological studies of the Dashui gold deposit, West Qinling Orogen, Central China. *Mineralium Deposita* 48(3):397-412.

321. Yu Y, et al. (2009) Chronology and Geochemistry of Mesozoic Volcanic Rocks in the Linjiang Area, Jilin Province and their Tectonic Implications. *Acta Geologica Sinica* 83(2):245-257.

322. Yin H, et al. (2007) An accurately delineated Permian-Triassic boundary in continental successions. *Sci. China Ser. D: Earth Sci.* 50(9):1281-1292.

323. Yang TN, Zhang HR, Liu YX, Wang ZL, Song YC, Yang ZS, Tian SH, Xie HQ, Hou KJ (2011) Permo-Triassic arc magmatism in central Tibet: Evidence from zircon U-Pb geochronology, Hf isotopes, rare earth elements, and bulk geochemistry. *Chem. Geol.* 284:270-282.

324. Wang D, et al. (2014) Zircon SHRIMP U-Pb age and geological implications of tuff at the bottom of Chang-7 Member of Yanchang Formation in the Ordos Basin. *Sci. China Earth Sci.* 57(12):2966-2977.

325. Barr SM, et al. (2000) Petrochemistry, U-Pb (zircon) ages, and palaeotectonic setting of the Lampang volcanic belt, northern Thailand. *J. Geol. Soc. London* 157:553-563.

326. Barr SM, et al. (2006) Age, tectonic setting and regional implications of the Chiang Khong volcanic suite, northern Thailand. *J. Geol. Soc. London* 163:1037-1046.

327. Guo X, et al. (2012) Middle Triassic arc magmatism along the northeastern margin of Tibet: U-Pb and Lu-Hf zircon characterization of the Gangcha complex in the West Qinling terrane, central China. *J. Geol. Soc. London* 169(3):327-336.

328. Hu J, et al. (2005) SHRIMP U-Pb dating for zircons from pyroxene andesite of Shuiquanguo Formation in western Liaoning province and its tectonic significance. *Geol. Bull. China* 24(2):104-109.

329. Kawagoe Y, et al. (2013) Evidence for late Permian-Triassic volcanism in the Hida Gaine belt, southwest Japan: New U-Pb ages from the Motodo, Ashidani, and Otani Formation. *Mem. Fukui Prefectural Dinosaur Museum* 12:17-33.

330. Leng C-B, et al. (2012) Zircon U–Pb and molybdenite Re–Os geochronology and Sr–Nd–Pb–Hf isotopic constraints on the genesis of the Xuejiping porphyry copper deposit in Zhongdian, Northwest Yunnan, China. *J. Asian Earth Sci.* 60:31-48.

331. Li C, et al. (2007) Geochronology evidence of the closure of Longmu Co-Shuanghu suture, Qinghai-Tibet plateau: Ar-Ar and zircon SHRIMP geochronology from ophiolite and rhyolite in Guoganjianian. *Acta Petrologica Sinica* 23(5):911-918.

332. Liu C, et al. (2011) Characteristics of volcanic rocks from Late Permian to Early Traissic in Ailaoshan tectomo-magmatic belt and implications for tectonic setting. *Acta Petrologica Sinica* 27(12):3590-3602.

333. Ma Q, et al. (2012) Triassic "adakitic" rocks in an extensional setting (North China): Melts from the cratonic lower crust. *Lithos* 149:159-173.

334. Peng T, et al. (2013) Mid-Triassic felsic igneous rocks from the southern Lancangjiang Zone, SW China: Petrogenesis and implications for the evolution of Paleo-Tethys. *Lithos* 168-169:15-32.

335. Qin X, et al. (2011) Geochronology and geochemistry of Early Mesozoic acid volcanic rocks from Southwest Guangxi: constraints on tectonic evolution of the southwestern segment of Qinzhou-Hangzhou joint belt. *Acta Petrologica Sinica* 27(3):794-808.

336. Srichan W, Crawford AJ, Berry RF (2009) Geochemistry and geochronology of Late Triassic volcanic rocks in the Chiang Khong region, northern Thailand. *Island Arc* 18(1):32-51.

337. Wang Q, et al. (2011) Late Triassic high-Mg andesite/dacite suites from northern Hohxil, North Tibet: Geochronology, geochemical characteristics, petrogenetic processes and tectonic implications. *Lithos* 126(1-2):54-67.

338. Wang B-Q, et al. (2013) Petrogenesis and tectonic implications of the Triassic volcanic rocks in the northern Yidun Terrane, Eastern Tibet. *Lithos* 175-176:285-301.

339. Wang J, et al. (2008) Chronology and geochemistry of the volcanic rocks in Woruo Mountain region, northern Qiangtang depression: Implications to the Late Triassic volcanic-sedimentary events. *Sci. China Ser. D: Earth Sci.* 51(2):194-205.

340. Wang F, Xu W-L, Gao F-H, Meng E, Cao H-H, Zhao L, Yang Y (2012) Tectonic history of the Zhangguangcailing Group in eastern Heilongjiang Province, NE China: Constraints from U–Pb geochronology of detrital and magmatic zircons. *Tectonophys.* 566-567:105-122.

341. Wu F, et al. (2010) Zircon U-Pb ages for rhyolitic tuffs of the Naocangjianguo Formation in the east Kulun orogenic belt and their implications. *J. Geomech.* 16(1):44-50.

342. Xu W-L, et al. (2009) Triassic volcanism in eastern Heilongjiang and Jilin provinces, NE China: Chronology, geochemistry, and tectonic implications. *J. Asian Earth Sci.* 34(3):392-402.

343. Xu W-L, et al. (2013) Spatial–temporal relationships of Mesozoic volcanic rocks in NE China: Constraints on tectonic overprinting and transformations between multiple tectonic regimes. *J. Asian Earth Sci.* 74:167-193.

344. Quick JE, Sinigoi S, Peressini G, Demarchi G, Wooden JL, Sbisá A (2009) Magmatic plumbing of a large Permian caldera exposed to a depth of 25 km. *Geology* 37(7):603-606.

345. Michel LA, Tabor N, Montanez IP, Davydov VI (2015) Chronostratigraphy and paleoclimatology of the Lodève Basin, France: Evidence for a pan-tropical aridification event across the Carboniferous – Permian boundary. *Palaeogeogr. Palaeoclimatol.* 430. doi:10.1016/j.palaeo.2015.03.020

346. Chen C, Zhang Z, Li K, Chen Y, Tang W, Li J, (2015) Geochronology, geochemistry, and its geological significance of the Damaoqi Permian volcanic sequences on the northern margin of the North China Block. *J. Asian Earth Sci.* 97:307-319.

347 Li D, He D, Qi X, Zhang N (2015) How was the Carboniferous Balkhash-West Junggar remnant ocean filled and closed? Insights from the well Tacan-1 strata in the Tacheng Basin, NW China. *Gondwana Res.* 27:342-362.

348. Li D, He D, Santosh M, Ma D, Tang J (2015) Tectonic framework of the northern Junggar basin part I: The eastern Luliang Uplift and its link with the East Junggar terrane. *Gondwana Res.* 27:1089-1109.

349. Qian X, Feng Q, Yang W, Wang Y, Chonglakmani C, Monjai D (2015) Arc-like volcanic rocks in NW Laos: Geochronological and geochemical constraints and their tectonic implications. *J. Asian Earth Sci.* 98:342-357.

350. Ovtcharova M, Goudemand N, Hammer O, Guodun K, Cordey F, Galfetti T, Schaltegger U, Bucher H (2015) Developing a strategy for accurate definition of a geological boundary through radio-isotopic and biochronological dating: The Early-Middle Triassic boundary (South China). *Earth-Sci. Rev.* 146:65-76.

351. Zhao SQ, Tan J, Wei JH, Tian N, Zhang DH, Liang SN, Chen JJ (2015) Late Triassic Batang Group arc volcanic rocks in the northeastern margin of Qiangtang terrane, northern Tibet: partial melting of juvenile crust and implications for Paleo-Tethys ocean subduction. *Int. J. Earth Sci.* 104:369-387.

352. Berra F, Tiepolo M, Caironi V, Siletto GB (2015) U-Pb zircon geochronology of volcanic deposits from the Permian basin of the Orobic Alps (Southern Alps, Lombardy): chronostratigraphic and geological implications. *Geol. Mag.* 152:(3), 429-443.

353. Rossi P, Cocherie A, Fanning CM (2015) Evidence in Variscan Corisca of a brief and voluminous Late Carboniferous to Early Permian volcanic-plutonic event

contemporaneous with a high-temperature/low-pressure metamorphic peak in the lower crust. *Bulletin de la Societe Geologique de France* 186 :171-192.

354. Wang F, Xu WL, Xu YG, Gao F, Ge W (2015) Late Triassic bimodal igneous rocks in eastern Heilongjiang Province, NE China: Implications for the initiation of subduction of the Paleo-Pacific Plate beneath Eurasia. *J. Asian Earth Sci*. 97:406-423.

355. Lanik A, Over DJ, Schmitz M, Kirchgasser WT (2016) Testing the limits of chronostratigraphic resolution in the Appalachian Basin, Late Devonian (middle Frasnian), eastern North America: New U-Pb zircon dates for the Belpre Tephra Suite. *Geol. Soc. Am. Bull*. 128:1813-1821.

356. Xei W, Luo Z-Y, Xu Y-G, Chen Y-B, Hong L-B, Ma L, Ma Q (2016) Petrogenesis and geochemistry of the Late Carboniferous rear-arc (or back-arc) pillow basaltic lava in the Bogda Mountains, Chinese North Tianshan. *Lithos*. 244:30-42 (2016).

357. Creixell C, et al. (2016) Geodynamics of Late Carboniferous-Early Permian forearc in north Chile (28°30'-29°30'S). *J. Geol. Soc. London* 173:757-772.

358. Rice CL, Belkin HE (1994) The Pennsylvanian Fire Clay tonstein of the Appalachian basin-Its distribution, biostratigraphy, and mineralogy. *Geol. Soc. America Spec. Pap*. 294: 87-104.

359. Monaghan AA, Pringle S (2004) $^{40}Ar/^{39}Ar$ geochronology of Carboniferous-Permian volcanism in the Midland Valley, Scotland. *Geol. Soc. London Spec. Pub*. 223:219-241.

360. Gunning MH (1996), *Definition and interpretation of Paleozoic volcanic domains, northwestern Stikinia, Iskut River Area, British Columbia* (University of Western Ontario, Canada) 515 pp.

361. Murphy DC, et al. (2006) Mid-Paleozoic to early Mesozoic tectonostratigraphic evolution of Yukon-Tanana and Slide Mountain terranes and associated overlap assemblages, Finlayson Lake massive sulphide district, southeastern Yukon. *Geol. Assoc. Can. Spec. Pap*. 45:75-105.

362. Dusel-Bacon C, Wooden JL, Hopkins MJ (2004) U-Pb zircon and geochemical evidence for bimodal mid-Paleozoic magmatism and syngenetic base-metal mineralization in the Yukon-Tanana terrane, Alaska. *Geol. Soc. Am. Bull*. 116**:**989-1015. doi:10.1130/B25342.1

363. Dusel-Bacon C, Hopkins MJ, Mortensen JK, Dashevsky SS, Bressier JR, Day WC (2006) Paleozoic tectonic and metallogenic evolution of the pericratonic rocks of east-central Alaska and adjacent Yukon, in *Paleozoic Evolution and Metallogeny of Pericratonic Terranes at the Ancient Pacific margin of North America, Canadian and Alaskan Cordillera*. M. Colpron, J. L. Nelson, Eds. *Geol. Assoc. Can. Spec. Pap*. 45:25-74.

364. Aleinikoff JN, Nokleberg WJ (1989) Age of deposition of the Cleary Sequence of the Fairbanks Schist Unit, Yukon Tanana terrane, East Central Alaska, in *Geologic Studies in Alaska 1988*. J. H. Dover J. P. Galloway, Eds. *U. S. Geol. Surv. Bull*. B 1903:75-83.

365. Roots CF, Nelson JL, Simard R-L, Harms TA (2006) Continental fragments, mid-Paleozoic arcs and overlapping late Paleozoic arc and Triassic sedimentary strata in

the Yukon Tanana terrane of northern British Columbia and southern Yukon, in *Paleozoic Evolution and Metallogeny of Pericratonic Terrains at the Ancient Pacific Margin of North America, Canadian and Alaskan Cordillera*. M. Colpron, J. L. Nelson, Eds. *Geol. Assoc. Can. Spec. Pap.* 45:153-177.

366. Mackenzie DE (1993) Geology of the Featherbed Cauldron Complex, North Queensland: Part 1-Eruptive Rocks and Post-Volcanic Sediment. *Austral. Geol. Surv. Org. Record* 1993/82:103 pp.

367. Withnall IW, Mackenzie DE, Denaro TJ, Bain JHC, Oversby BS, Ichutson J, Donchak PJT, Champion DC, Wellman P, Chikshank BI, Sun SS, Pain CF (1997) Chapter 3-Georgetown Region in *North Queensland Geology*. J. H. C. Bain, J. J. Draper, Eds. *Austral. Geol. Surv. Org. Bull.* 240:19-116.

368. Black LP, McCulloch MT (1990) Isotopic evidence for the dependence of recurrent felsic magmatism on new crust formation: An example from the Georgetown region of Northeastern Australia. *Geochim. Cosmochim. Acta* 54:183-196.

369. Blewett RS, Denaro TJ, Knewtson J, Welmman P, Mackenzie DE, Cruikshank BI, Wilford JR, von Gnielinski FE, Pain CF, Sun SS, Bultitude RJ (1997)Chapter 4-Coen Region in *North Queensland Geology*. J. H. C. Bain, J. J. Draper, Eds. *Austral. Geol. Surv. Org. Bull.* 240:117-158.

370. Hutton LJ, Draper JJ, Rienks IP, Withnall IW, Knewtson J (1997) Chapter 6-Charter Towers Region in *North Queensland Geology*. J. H. C. Bain, J. J. Draper, Eds. *Austral. Geol. Surv. Org. Bull.* 240:165-224.

371. Perkins C, Walshe CJL, Morrison G (1995) Metallogenic Episodes of the Tasman Fold Belt System, Eastern Australia. *Econ. Geol.* 90:1443-1460.

372. Bruguier O, Becq-Girandon JF, Bosch D, Lancelot JR (1998) Late Visean hidden basins in the internal zones of the Variscan belt: U-Pb zircon evidence from the French Massif Central. *Geology* 26:627-630.

373. Dahlgren S, Corfu F (2001) Northward sediment transport from the late Carboniferous Variscan mountains: zircon evidence from the Oslo Rift, Norway. *J. Geol. Soc. London* 158:29-36.

374. Larson O (1972) K-Ar datering af prover fra danske dybdeboringer: in the Dansk Geologisk forenings. *Arsskrift* 1971:91-94.

375. Burger K, Hess JC, Lippolt HJ (1997) Tephrochronologie mit Kaolin-Kohlentonsteinen: Mittel zur Korrelation paralischer und limnicher Ablagerungen des Oberkarbons. *Geologisches Jahrbuch* A147:3-39.

376. Lippolt HJ, Hess JC (1989) Isotopic evidence for the stratigraphic position of the Saar-Nahe Rotliegende volcanism. III. Synthesis of results and geological implications. *Neues Jahrbuch fuer Geologie und Palaeontologie* 1989.9:553-559.

377. Conte JC, Gasgcon F, Lago M, Carls P (1987) Materiales Stephano-Permicos en la fosa de Fombuena (Provincia de Zaragoza): *Boletin Geologico y Minero* XCVIII:460-470.

378. Diakow LJ, Rogers C (1997) Geology of the McConnell Range- Serrated Peak to Jensen Creek, parts of NTS 94E/2 and 94D/15. *British Columbia Geol. Soc. Pap.* 1998-1:14 pp.

379. Gehrels GE, McClelland WC, Samson SD, Patchett PJ, Geology of the western flank of the Coast Mountains between Cape Fanshaw and Taku Inlet, southeastern Alaska. *Tectonics* 11:567-585.

380. McClelland WC, Gehrels GE, Samson SD, Patchett PJ (1992) Protolith relations of the Gravina belt and Yukon-Tanana terrane in central Southeastern Alaska. *J. Geol.* 100:107-123.

381. Cagliari J, Philipp RP, Buso VV, Netto RG, Hillebrand PK, Lopes RC, Basei MAS, Faccini UF (2016) Age constraints of the glaciation in the Parana Basin: Evidence fromU-Pb dates. *J. Geol. Soc. London* 173:871-874.

382. Conte JC, Gasgcon F, Lago M, Carls P (1987) Materiales Stephano-Permicos en la fosa de Fombuena (Provincia de Zaragoza). *Boletin Geologico y Minero* XCVIII (IV):460-470.

383. Hernando S, Schott J-J, Thuizat R, Montigny R (1980) Age des andesites et des sediments interstratifies de la region d'Atienza (Espagne): Etude stratigraphique, geochronologique et paleomagnetique. *Sci. Geol. Bull.* 33(2) :119-128.

384. Pereira MF, Castro A, Chichorro M, Fernandez C, Diaz-Alvarado J, Marti J, Rodriguez C (2014) Chronological link between deep-seated processes in magma chambers and eruptions: Permo-Carboniferous magmatism in the core of Pangaea (Southern Pyrenees). *Gondwana Res.* 25:290-308.

385. Xie W, Xu Y-G, Chen Y-B, Luo Z-Y, Hong L-B, Ma L, Liu H-Q (2016) High-alumina basalts from the Bogda Mountains suggest an arc setting for Chinese Northern Tian Shan during the Late Carboniferous. *Lithos*, 256-257:165-181.

386. Liu D, Cheng F, Guo Z, Jolivet M, Song Y (2015) Lahar facies of the Latest Paleozoic Arbasan Formation: Geomorphological characters and paleoenvironmental reconstruction of northern Tian Shan NW China. *J. Asian Earth Sci.* 113:282-292.

387. Fu D, Huang B, Peng S, Kusky TM, Zhou Z, Ge M (2016) Geochronology and geochemistry of late Carboniferous volcanic rocks from northern Mongolia, North China: Petrogenesis and tectonic implications. *Gondwana Res.* 36:545-560.

388. Liao Z, Hu W, Cao J, Wang X, Yao S, Wan Y (2016) Permian-Triassic boundary (PTB) in the Lower Yangtze Region, southeastern China: A new discovery of deep-water archive based on organic carbon isotopic and U-Pb geochronological studies. *Palaeogeogr. Palaeoclimatol.* 451:124-139.

389. Fraser GL, Gilmore PJ, Fitzherbert JA, Trigg SA, Campbell LM, Deyssing L, Thomas OD, Berton GR, Greenfield JE, Blevin PE, Simpson CJ (2014) New SHRIMP U-Pb zircon ages from the Lachlan, Southern Thomson and New England Orogens, New South Wales. *Geol. Surv. New South Wales Rpt.* GS 2014/0829 Maitland NSW Australia 217 pp.

390. Liu HT (2001) Qimantage terrestrial volcanics: petrologic evidence of active continental margin of Tarim Plate during late Indo-China epoch. *Acta Petrologica Sinica* 17(3):337-351.

391. Pei F-P, Zhang Y, Wang Z-W, Cao H-H, Zu W-L, Wang Z-J, Wang F, Yang C (2016) Early-Middle Paleozoic subduction-collision history of the south-eastern

Central Asian Orogenic Belt: Evidence from igneous and metasedimentary rocks of central Jilin Province, NE China. *Lithos* 261:164-180.

392. Sorokin AA, Kotov AB, Kudryashov NM, Kovach VP, Early Mesozoic granitoid and rhyolite magmatism of the Bureya Terrane of the Central Asian Orogenic Belt: Age and geodynamic setting. *Lithos* 261:181-194.

393. Wang C, Ding L, Zhang LY, Kapp P, Pullen A, Yue YH (2016) Petrogenesis of Middle-Late Triassic volcanic rocks from the Gangdese belt, southern Lhasa terrane: Implications for early subduction of Neo-Tethyan oceanic lithosphere. *Lithos* 262:320-333.

394. Kositcin N, Purdy DJ, Brown DD, Bultitude RJ, Carr PA (2015) Summary of results joint GSQ-GA geochronology project: Thomson Orogen and Hodgkinson Province, 2012-2013. *Queensland Geological Record* 68 pp.

395. Demko R, Hrasko L (2013) Rhyolite body Gregova near the Telgart village (Western Carpathians). *Minerella Slovaca* 45:161-174.

396. Machowiak K, Muszynski A, Armstrong R, High-level volcanic-granodioritic intrusions from Zelezniak Hill (Kaczawa Mountains, Sudetes, SW Poland). *Geol. Soc. London Spec. Pub.* 68-74.

397. Thomson B, Aftalion M, McIntyre RM, Rice C (1995) Geochronology and tectonic setting of silicic dike swarms and related silver mineralization at Candelaria, western Nevada. *Econ. Geol.* 90:2182-2196.

398. Franzese JR, Pankhurst RJ, Rapela CW, Spalletti LA, Fanning M, Muravchik M (2002) Nuevas evidencias geocronologicas sobre el magmatismo Gondwanico en el noroeste del Macizo Norpatagonico. *Actas del XV Congreso Geologico Argentino*. El Calafate.

399. Ottone EG, Monti M, Marsicano CA, de la Fuenta MS, Naipauer M, Armstrong R, Mancuso AC (2014) A new Late Triassic age for the Puesto Viejo Group (San Rafael depocenter, Argentina): SHRIMP U-Pb zircon dating and biostratigraphic correlations across southern Gondwana. *J. South Am. Earth Sci.* 56:186-199.

400. Hess JC (1990) Numerischae stratigraphie permokarbonischer vulkanite zentraleuropas. Allgemeine Einfuhrung und Teil I: Sudtirol: *Zeitschrift Deutschen Geologischen Gesellschaft* 141:1-11.

401. Schaltegger U (1997) The age of an upper Carboniferous/Lower Permian sedimentary basin and its hinterland as constrained byU-Pb dating of volcanic and detrital zircons (Northern Switzerland). *Schweiz. Mineral. Petrogr. Mitt.* 77:101-111.

402. Yu X, Wang Z, Zhou X, Xiao W, Yang X (2016) Zircon U-Pb geochronology and Sr-Nd isotopes of volcanic rocks from the Dahalajunshan Formation: implications for Late Devonian-Middle Carboniferous tectonic evolution of the Chinese western Tianshan. *Int. J. Earth Sci.* 105:1637-1661.

403. Zhao X, Xue C, Symons DTA, Zhang Z, Wang H (2014) Microgranular enclaves in island-arc andesites: A possible link between known epithermal Au and potential prophyry Cu-Au deposits in the Tulasu ore cluster, western Tianshan, Xinjang, China. *J. Asian Earth Sci.* 85:210-283.

404. Duan S, Zhang Z, Jiang Z, Zhao J, Zhang Y, Li F, Tian J (2014) Geology, geochemistry, and geochronology of the Dunde iron-zinc ore deposit in western Tianshan, China. *Ore Geol. Rev.* 57:441-461.

405. Lippolt HJ, Hess JC (1985) $^{40}Ar/^{39}Ar$ dating of sanidines from upper Carboniferous tonsteins. *Compte Rendu* 10:175-181.

406. Bodorkos S (2008) Summary of results for the joint GSNSW-GA geochronology project: Eastern Lachlan Orogen. *Geological Survey of New South Wales*.

407. Zhang FR (2009) LA-ICP-MS zircon U-Pb dating of volcanic rocks from the Dahalajunshan formation, Wusun Mountains in west Tianshan. *Xinjiang Geology* 27:231-235.

408. An F, Zhu Y, Wei S, Lai S (2013) An Early Devonian to Early Carboniferous volcanic arc in North Tianshan, NW China: Geochronological and geochemical evidence from volcanic rocks. *J. Asian Earth Sci.* 78:100-113.

409. He B, Xu Y, Huong X, Luo Z, Shi Y, Yang Q, Yu S (2007) Age and duration of the Emeishan flood volcanism, SW China: Geochemistry and SHRIMP zircon U-Pb dating of silicic ignimbrites, post volcanic Xuanwei Formation and clay tuff at the Chaotian section. *Earth Planet. Sci. Lett.* 255:306-323.

410. He B, Zhong Y, Xu Y, Li X (2014) Triggers of Permo-Triassic boundary mass extinctions in South China: the Siberian Traps or Paleo-Tethys ignimbrite flare-up? *Lithos* 204:258-267.

411. Clemens JD, Frei D, Finger F (2014) A new precise date for the Tolmie Igneous Complex in northeastern Victoria. *Austral. J. Earth Sci.* 61:951-958.

412. Roberts J, Claoue-Long JC, Foster CB (1996) SHRIMP zircon dating of the Permian system of eastern Australia. *Austral. J. Earth Sci.* 43(4):401-421.

413. Breitkreuz C (1996) U-Pb geochronology and significance of Late Permian ignimbrites in Northern Chile. *J. South Am. Earth Sci.* 9:281-293.

414. Meng E, Xu WL, Pei FP, Yang DB, Wang F, Zhang XZ (2011) Permian bimodal volcanism in the Zhangguangcai Range of the eastern Heilongjian Province NE China; Zircon and U-Pb-Hf isotopes and geochemical evidence. *J. Asian Earth Sci.* 41:119-132.

415. Meng QA, Wan CB, Zhu DF, Zhang YL, Ge WC, Wu FY (2013) Age assignment and geological significance of the "Budate Group" in the Hailar Basin. *Science China* 56:970-979.

416. Nie F, Xu D, Jiang S, Hu P (2009) Zircon SHRIMP U-Pb dating on rhyolite samples from the Xilimiao Group in the Sumoqagan Obo fluorite deposit, Inner Mongolia. *Acta Geologica Sinica* 83:496-504.

417. Seltmann R, Konopelko D, Biske G, Divaev F, Sergeer S (2011) Hercynian post-collisional magmatism in the context of Paleozoic magmatic evolution of the Tian Shan orogenic belt. *J. Asian Earth Sci.* 42:821-838.

418. Su CQ, Jiang CY, Xia MZ, Wei W, Pan R (2009) Geochemistry and zircons SHRIMP U-Pb age of volcanic rocks of the Aguishan Formation in the eastern area of north Tianshan, China. *Acta Petrologica Sinica* 24:901-915.

419. Zhai W, Sun XM, Gao J, He XP, Liang JL, Miao LC, Wu YL (2006) SHRIMP dating of zircons from volcanic host rocks of Dahalajunshan Formation in Axi gold deposit, Xinjiang, China, and its geological implications. *Acta Petrologica Sinica* 22:1399-1404.

420. Zhang SH, Zhao Y, Song B, Yang YH (2007) Zircon SHRIMP U-Pb and in-situ Lu-Hf isotope analyses of a tuff from western Beijing: Evidence for missing Late Paleozoic arc volcano eruptions at the northern margin of the North China Block. *Gondwana Res*. 12:157-165.

421. Kunk MJ, Rice CL (1994) High-precision ^{40}Ar-^{39}Ar age spectrum dating of sanidine from the middle Pennsylvanian fire clay tonstein of the Appalachian Basin, in *Elements of Pennsylvanian Stratigraphy, Central Appalachian Basin,* C. L. Rice, Ed., *Geol. Soc. Am. Spec. Pap*. 294:105-113.

422. Briqueu L, Innocent C (1993) Datation U-Pb sur zircon et geochimie isotopique Sr et Nd du volcanisme Permien des Pyrenees occidentales (ossau et Anayetl). *C.R. Academia Sci. Paris)* 316 series II :623-628.

423. Kryza R, Muszer J, August C, Haydukiewicz J, Jurasik M (2008) Lower Carboniferous bentonites in the Bardo Structural Unit (central Sudetes): geological context petrology and palaeotectonic setting. *Geologia Sudetica* 40:19-31.

424. Pointon MA, Chew DM, Ovtcharova M, Sevastopulo GD, Delcambre B (2014) High-precision zircon CA-ID-TIMS dates from the western European late Visean bentonites. *J. Geol. Soc. London* 171:649-658.

425. Gastaldo RA, Purkynova E, Simunek Z, Schmitz MD (2009) Ecological persistence in the late Mississippian (Serpukhovian Namurian A) megafloral record of the Upper Silesian basin, Czech Republic. *Palaios* 24:336-350.

426. Pointon MA, Chew DM, Ovtcharova M, Sevastopulo GD, Crowley QG (2012) New high-precision U-Pb dates from western European Carboniferous tuffs; implications for time-scale calibration, the periodicity of Late Carboniferous cycles and stratigraphical correlation. *J. Geol. Soc. London* 169:713-721.

427. Wang B, Wang L, Chen J, Liu H, Yin F, Li X (2017) Petrogenesis of Late Devonian-Early Carboniferous volcanic rocks in northern Tibet: New constraints on the Paleozoic tectonic evolution of the Tethyan Ocean. *Gondwana Res*. 41:142-156.

428. Rosa DRN, Finch AA, Anderson T, Inverno CMC (2009) U-Pb geochronology and Hf isotope ratios of magmatic zircons from the Iberian Pyrite Belt. *Mineral. Petrol*. 95:47-69.

429. Trapp E, Kaufmann B, Mezger K, Korn D, Weyer D (2004) Numerical calibration of the Devonian-Carboniferous boundary: TWD new U-Pb isotope dilution-thermal ionization mass spectrometry single-zircon ages from Hasselbactel (Sauerland, Germany). *Geology* 32:857-860.

430. Valverde-Vaquero P, Cuesta Fernandez A, Gallastegui G, Suarez O, Corretge G, Dunning GR (1999) U-Pb dating of Late Variscan magmatism in the Cantabrian Zone (northern Spain). *Europ. Union Geosci. Abst*. 4:101.

431. GreiE (1995) U-Pb zircon geochronology of Lower Jurassic and Paleozoic Stikinian strata and Tertiary intrusions, northwestern British Columbia. *Can. J. Earth Sci.* 32:1155-1171.

432. Chai F, Mao J, Dong L, Yang F, Liu F, Geng X, Zhang Z (2009) Geochronology of metarhyolites from the Kangbutiebao Formation in the Kelang Basin, Altay Mountains, Xinjiang: Implications for tectonic evolution and metallogeny. *Gondwana Res.* 16:189-200.

433. Gao R, Xiao L, Wang H, Wang G, Luo Y, Liu H (2012) Geochemical characteristics and LA-ICP-MSU-Pb zircon ages of volcanic rocks in Kaidu River, South Tianshan, Xinjiang, and their geological significance. *Acta Petrologica et Mineralogica* 31:541-553.

434. Guo Q, Xiao W, Hou Q, Mindley BF, Han, Tian Z, Song D (2014) Construction of Late Devonian Dundunshan arc in the Beishan orogen and its implications for tectonics of Southern Central Asian Orogenic Belt. *Lithos* 184-187:361-378.

435. Tang GJ, Wang Q, Wyman DA, Sun M, Li ZX, Zhao ZH, Sun WD, Jia WH, Jiang ZQ (2008) Geochronology and geochemistry of late Paleozoic magmatic rocks in the Lamasu-Dabate area, northwestern Tianshan (west China): Evidence for a tectonic transition from arc to post-collisional setting. *Lithos* 119:393-411.

436. Barr SM, Mortenson JK, Thompson MD, Hermes OD, White CE (2011) Early to Middle Devonian granitic and metamorphic rocks from the Central Gulf of Maine. *Lithos* 126:455-465.

437. Parrish CB (2013) *Insights into the Appalachian Basin Middle Devonian Depositional System from U-Pb Zircon Geochronology of Volcanic Ashes in the Marcellus Shale and Onondaga Limestone* (MS Thesis, West Virginia University, Morgantown WV) 140 pp.

438. Kaufman B, Trapp E, Mezger K, Weddige K (2005) Two new Erusian (Early Devonian) U-Pb zircon ages from volcanic rocks of the Rheruish Massif (Germany): implications for the Devonian time scale: *J. Geol. Soc. London* 162:363-371.

439. Lehrman DJ, Ramezani J, Bowring SA, Martin P, Montgomery P, Enos P, Payne JL, Orchard MJ, Hongmei W, Jiayong W (2006) Timing of recovery from the end-Permian extinction: Geochronologic and biostratigraphic constraints from South China. *Geology* 34:1053-1056.

440. Qiu X, Liu C, Mao G, Deng Y, Wang F, Wang J (2014) Late Triassic tuff intervals in the Ordos Basin, central China: Their depositional, petrographic, geochemical characteristics and regional implications. *J. Asian Earth Sci.* 80:148-160.

441. Liu S, Fan W, Luo M, Tang F, Zhu H, Chen W (2014) Zircon U-Pb dating and geochemistry characteristics of the bimodal volcanic rocks in Phlaythong area, southern Laos. *J. Jihin Univ. Earth Sci. Ed.* 44:540-553.

442. Barrinvero M, Arnosio M, Llambias EJ (2013) Nuevos datos geocronologicos en subsvelo y afloramientos del Grupo Choiyoi en el oeste de La Pampa: Implicancias estratigráficas. *Revista de la Asociacion Geologica Argentina* 70:31-39.

443. Liu J, Li J, Chi X, Qu J, Chen J, Hu Z, Feng Q (2016) The tectonic setting of early Permian bimodal volcanism in Central Inner Mongolia: Continental rift, post-collisional extension, or active continental margin?. *Int. Geol. Rev*. 58:737-755.

444 Domeier M, Vandervoo R, Tomezzoli RN, Tohver E, Hendriks BWH, Torsvik TH, Vizan H, Dominguez A (2011) Support for an "A-type" Pangea reconstruction from high-fidelity Late Permian and Early to Middle Triassic paleomagnetic data from Argentina: *J. Geophys. Res*. 116. Doi:10.1029/2011JB008495

445. Lehrmann DJ, et al. (17 coauthors) (2015) An interated biostratigraphy (conodonts and foraminfers) and chronostratigraphy (paleomagnetic reversals, magnetic susceptibility, elemental chemistry, carbon isotopes, and geochronology) for the Permian-Upper Triassic strata of Guandao section, Nanpaujiang Basin, South China. *J. Asian Earth Sci*. 108:117-135.

446. Gulbranson EL, Ciccioli PL, Montanez IP, Marenssl SA, Limarino CO, Schmitz MD, Davydov VI (2015) Paleoenvironments and age of the Talampaya Formation: The Permo-Triassic boundary in northwestern Argentina. *J. South Am. Earth Sci*. 63:310-322.

447. Hamilton MA, Soreghan GS, Carvajal CP, Isaacson PE, Grader GW, Di Pasquo MM (2016) A precise U-Pb zircon age from volcanic ash in the Pennsylvanian Copacabana Formation, Bolivia. *Geol. Soc. Am. Mtg. Abst*. 48(6), 276278. doi: 10.1130/abs/2016RM-276278

448. Bai J, Li Z, Xu X, Ru Y, Ting L (2011) The chronology of Tulasu-Yelimodun Volcanic Belt: Constraints of the metallogenic epoch of the Jiamante gold deposit, western Tianshan Mountains of Xinjiauy. *Acta Geoscientica Sinica* 32:322-330.

449. Dunning GR, Diez Montes A, Matas J, Martin Parra LM, Almarza J, Donaire M (2002) Geocronología U/Pb del volcanismo ácido y granitoides de la Faja Pirítica Ibérica (Zona Surportuguesa). *GEOGACETA* 32:127-130.

450. Shauggvau S, Peate IU, Tian W, Xu Y (2015) Re-evaluating the geochronology of the Permian Tarim magmatic province: implications for temporal evolution of magmatism. *J. Geol. Soc. London* 173:228-239.

451. Maino M, Dallagiovanna G, Gaggero L, Seno S, Tiepolo M (2012) U-Pb zircon geochronological and petrographic constraints on Late to post-collisonal Variscan magmatism and metamorphism in the Ligurian Alps, Italy. *Geol. J*. 47:632-652.

452. Waters CN, Condon DJ (2012) Nature and timing of Late Mississippian to Mid-Pennsylvanian glacio-eustatic sea-level changes of the Pennine Basin, UK. *J. Geol. Soc. London* 169:37-51.

453. Davydov VI, Biakov AS, Isbell JL, Crowley JL, Schmitz MD, Vedernikov IL (2016) Middle Permian U-Pb zircon ages of the "glacial" deposits of the Atkan Formation, Ayan-yuryakh anticlinorium, Magadan Province, NE Russia: Their significance for global climatic interpretations. *Gondwana Res*. 38:74-85.

454. Kurchavov AM, Shatagin KN (2002) Rb-Sr and Sm-Nd isotopic studies of the Upper Paleozoic ignimbrites from the Tokrau, Kazakstan. *Geologiya Kzakhstana* 3(6):40-48.

455. Logan JM, Drobe JR, McClelland WC (2000) Geology of the Forrest Kerr-Mess Creek Area, northwestern British Columbia (NTS 104 B/10, 15 & 104G/2 & 7W). *British Columbia Geol. Surv. Bull.* 104:164 pp.

456. Yu J, Mo X, Dong G, Yu X, Li Y, Huang X (2011) Felsic volcanic rocks from northern Tarim, NW China: Zircon U-Pb dating and geochemical characteristics. *Acta Petrologica Sinica* 27:2184-2194.

457. Kilian TM, Swanson-Hysell NL, Bold U, Crowley J, Macdonald F (2016) Paleomagnetism of the Teel basalts from the Zavkhan terrane: Implications for Paleozoic paleogeography in Mongolia and the growth of continental crust. *Lithosphere* 8:699-715.

458. Zhang Y, Yuan C, Long X, Sun M, Huang Z, Du L, Wang X (2017) Carboniferous bimodal volcanic rocks in the Eastern Tianshan, NW China: Evidence for arc rifting. *Gondwana Res.* 43:92-106.

459. Yu, Q, Ge W-C, Zhang J, Zhao G-C, Zhang Y-L, Yang H (2017) Geochronology, petrogenesis, and tectonic implication of late Paleozoic volcanic rocks from the Dashizhai Formation in Inner Mongolia, NE China. *Gondwana Res.* 42:164-177.

460. Zhang W, Chen H, Han J, Zhao L, Huang J, Yang J, Yan X (2015) Geochronology and geochemistry of igneous rocks in the Bailingshan are: Implications for the tectonic setting of late Paleozoic magmatism and iron skarn mineralization in the eastern Tianshan, NW China. *Gondwana Res.* 38:40-59.

461. Oplustil S, Schmitz MD, Cleal CJ, Martinek K (2016) A review of the Middle-Late Pennsylvanian west European regional substages and global biozones, and their correlation to the Geological Time Scale based on new U-Pb ages. *Earth Sci. Rev.* 154:301-335.

462. Waltenberg K, Blevin PL, Bull KF, Cronin DE, Armistead SE (2016) New SHRIMP U-Pb zircon ages from the Lachlan Orogen and the New England Orogen, New South Wales. *Geol. Surv. New South Wales Rep.* GS2016/810:97 pp.

463. Bodorkos S, Blevin PL, Simpson CJ, Gilmore PJ, Glen RS, Greenfield JE, Hegarty R, Quinn CD (2013) New SHRIMP U-Pb zircon ages from the Lachlan, Thomson and Delamerian orogens, New South Wales. *Geol. Surv. New South Wales Rec.* 2013/29:124 pp.

464. Luthardt L, Robler R, Schneider JW (2016) Palaeoclimatic and site-specific conditions in the early Permian forest of Chemnitz— Sedimentological, geochemical, and paleobotanical evidence. *Palaeogeogr. Palaeoclimatol.* 441:627-652.

465. Cross AJ, Purdy DJ, Bultitude RJ, Dhnaram CR, Gnielinski FE (2009) Joint GSQ-GA NGA geochronology project New England Orogen and Drummond Basin, 2008. *Queensland Geol. Rec.* 2009/03:1-35.

466. Visonà D, Fioretti AM, Poli ME, Zanferrari A, Fanning M (2007) U-Pb SHRIMP zircon dating of andesite from the Dolomite area (NE Italy): geochronological evidence for the early onset of Permian volcanism in the eastern part of the southern Alps. *Swiss J. Geosci.* 100(2):313-324.

467. Shaulis BJ, Lapen TJ, Casey JF, Staszyc A, Newberry AS (2012) Timing of flysch sedimentation in the Ouachita remnant ocean basin; constraints from U-Pb ages of zircon in subaqueous tuff deposits. *Am. Geophys. Union Abst* T51A-2552.

468. Qian X, Wang Y, Srithai B, Feng Q, Zhang Y, Zi J-W, He H (2017) Geochronological and geochemical constraints on the intermediate-acid volcanic rocks along the Chiang Khong-Lampang-Tak igneous zone in NW Thailand and their tectonic implications. *Gondwana Res*. 45:87-99.

469. Wang Y, Luo Z, Santosh M, Wang S, Wang N (2017) The Liuyuan Volcanic Belt in NW China revisited: evidence for Permian rifting associated with the assembly of continental blocks in the Central Asian Orogenic Belt. *Geol. Mag*. 154:265-285.

470. Chisholm E-K, Blevin P, Simpson C (2014) New SHRIMP U-Pb zircon ages from the New England Orogen, New South Wales July 2010-Jume 2012. *Geol. Surv. New South Wales Report* GS2013/1838 http://dx.doi.org/10.11636/Record.2014.013.

471. Vesela P, Lammerer B, Wetzel A, Sollner F, Gerdes A (2008) Post-Variscan to Early Alpine sedimentary basins in the Tauern Window (eastern Alps), in *Tectonic Aspects of the Alpine-Dinaride-Carpathian System*, S. Siegemund, B. Fugenschuh, N. Froitzheim, Eds., *Geol. Soc. London Spec. Pub*. 298:83-100.

472. Vesela P, Lammerer B (2008) The Pfitsch-Morchner Basin, an example of the post-Variscan sedimentary evolution in the Tauern Window (Eastern Alps). *Swiss J. Geosci*. 101, Supplement 1:S73-S88.

473. Engwell S, Eychenne J (2016) in *Volcanic ash: hazard observation*, S. Mackie, Ed. (Elsevier, Amsterdam), pp 67–85.

References for Estimating the Intensity of Past Volcanism

474. Crosweller HS et al. (2012) Global database on large magnitude explosive volcanic eruptions (LaMEVE). *J. Appl. Volcan*. 1:4. doi:10.1186/2191-5040-1-4

475. Brown SK et al. (2014) Characterisation of the Quaternary eruption record: Analysis of the Large Magnitude Explosive Volcanic Eruptions (LaMEVE) database. *J. Appl. Volcan*. 3:5. doi: 10.1186/2191-5040-3-5

476. Matthews KJ et al. (2016) Global plate boundary evolution and kinematics since the late Paleozoic, *Glob. Planet. Change* 146:226–250.

477. Wilson CJN et al. (1995) An exceptionally widespread ignimbrite with implications for pyroclastic flow emplacement. *Nature* 378:605–607.

478. Toohey M, Sigl M (2017) Volcanic stratospheric sulphur injections and aerosol optical depth from 500 BCE to 1900 CE, *Earth Sys. Sci. Data Discuss*. https://doi.org/10.5194/essd-2017-31.

479. Thordarson Th, Self S (1993) The Laki (Skaftár Fires) and Grímsvötn eruptions in 1783–1785. *Bull. Volcanol*. 55:233–263.

480. Thordarson Th, Self S (2003) Atmospheric and environmental effects of the 1783–1784 Laki eruption: A review and reassessment. *J. Geophys. Res*. 108:4011.

481. D'Arrigo R et al. (2011) The anomalous winter of 1783–1784 : Was the Laki eruption or an analog of the 2009–2010 winter to blame? *Geophys. Res. Lett.* 38:L05706.

482. Lanciki A et al. (2012) Sulfur isotope evidence of little or no stratospheric impact by the 1783 Laki volcanic eruption. *Geophys. Res. Lett.* 39:L01806.

483. Schmidt A et al. (2012) Climatic impact of the long-lasting 1783 Laki eruption: Inapplicability of mass-independent sulfur isotopic composition measurements. *J. Geophys. Res.* 117:D23116.

484. Cole-Dai J, et al. (2014) Comment on "Climatic impact of the long-lasting Laki eruption: Inapplicability of mass-independent sulfur isotope composition measurements" by Schmidt et al. *J. Geophys Res. Atmos.* 119:6629–6635.

485. Schmidt A, Mills MJ, Ghan S, Gregory JM, Allan RP, Andrews T, et al. (2018) Volcanic radiative forcing from 1979 to 2015. *J. Geophys. Res. Atmos.* 123:12491-12508. https://doi.org/10/1029/2019JD028776

486. Gough DO (1981) Solar Interior Structure and Luminosity Variations. *Solar Phys.* 74:21–34.

487. Guenther DB (1989) Age of the Sun. *Astrophys. J.* 339:1156–1159.

488. Norman GS and Campbell JM (1998) *An Introduction to Environmental Biophysics* (Springer, New York, ed. 2), Chapter 11.

489. Ubertoli G (2017) Solar Irradiation Model, *Matlab Central*, https://uk.mathworks.com/matlabcentral/fileexchange/49701-solar-irradiation-model, Last accessed: 22 September 2017 (updated 21 Feb 2017).

490. Aubry TJ, Jellinek AM, Degruyter W, Bonadonna C, Radić V, Clyne M, Quainoo A (2016). Impact of global warming on the rise of volcanic plumes and implications for future volcanic aerosol forcing. *J. Geophys. Res. Atmos.* 121(22).

491. Watt, SFL, Pyle DM, Mather TA (2013) The volcanic response to deglaciation: Evidence from glaciated arcs and a reassessment of global eruption records. *Earth-Sci. Rev.* 122:77-102 https://doi.org/10.1016/j.earscirev.2013.03.007

492. Schindlbeck JC, et al. (2018) 100-kyr cyclicity in volcanic ash emplacement: evidence from a 1.1 Myr tephra record from the NW Pacific. *Sci. Reports* 8 doi:10.1038/s41598-018-22595-0

493. WMO (1999) Scientific assessment of ozone depletion: 1998 global ozone research and monitoring project, Report No. 44, WMO, Geneva, Switzerland.

494. Byrne B, Goldblatt C (2014) Radiative forcing at high concentrations of well-mixed greenhouse gases. *Geophys. Res. Lett.* 41:152–160.

495. Foster GL, Royer DL, Lunt DJ (2017) Future climate forcing potentially without precedent in the last 420 million years. *Nat. Comm.*, 8:14845.

Supplementary Data Table S1: Glacial Deposits (Devonian-Triassic)

Unit	Location	Basin	Plate	*Stages w/ Glacial Deposits	SI Reference Citation #
Agoula/N'Khom	Gabon	Gabon Interior	Africa	Bas, Mos, Kas, Gzh, Ass, Sak	1, 6
Lukuga Gp (Lower Subgp)	Congo (Zaire)	Congo	Africa	Ass, Sak	1, 7
Lutoe Series	Angola	Baixa do Cassanje	Africa	[Bas, Mos, Kas, Gzh, Ass, Sak, Art, Kun]	1
Serie Tilitica/Kondo Pools Fm	Mozambique/Zimba	Cabora Bassa/Mana Pools	Africa	Mos, Kas, Gzh, Ass	1, 8
Dwyka Series	Zimbabwe-Zambia	Zambezi	Africa	Mos, Kas, Gzh, Ass	1, 26
Dwyka Gp	Zimbabwe	Tuli	Africa	Mos, Kas, Gzh, Ass, Sak	1
Dwyka Gp	Namibia-Botswana	South Kalahari	Africa	Mos, Kas, Gzh, Ass, Sak	1, 6, 10, 11
Dwyka Gp	Namibia	Karasburg	Africa	Mos, Kas, Gzh, Ass, Sak	1, 10, 11
Dwyka Gp	South Africa	Main Karoo	Africa	Mos, Kas, Gzh, Ass, Sak	1, 10, 11
Siankondobo Sandstone Fm	Zambia	Lukusashi	Africa	Gzh, Ass, Sak	12
Mukumba Siltstone	Zambia	Luangwa	Africa	Bas, Mos, Kas, Gzh, Ass, Sak	6
Sakoa Gp	Madagascar	Morondava	Africa	Mos, Kas, Gzh, Ass	1, 13
Teragh Sandstone Fm	Niger	Iullumeden	Africa	E Vis	1, 14
Songea Gp / Idusi Fm / Lisimba M	Tanzania	Ruhuhu	Africa	Mos, Kas, Gzh, Ass	15, 16
Unnamed tillites	Niger		Africa	L Fam, E Tou	14
Mambere Fm	Central African Rep.	Congo?	Africa	L Fam, E Tou	17, 18
Edaga Arbi Glacials/Upper Entich	Ethiopia	Northern Ethiopian/Ogaden	Africa	Mos, Kas, Gzh, Ass, Sak	19
Northern Wadi Malik Fm	SW Egypt	Gilf Kebir-Abu Ras area	Africa	Mos, Kas, Gzh	20, 21, 22
Unnamed glacial strata (=Norther	Sudan		Africa	Mos, Kas, Gzh	22, 23
Songea Gp/ Idusi Fm	Tanzania	Ruhuhu	Africa	Mos, Kas, Gzh, Ass	15
Akbarah / Kunlun Fm	Yemen	South Arabian Peninsula	Africa	Mos, Kas, Gzh, Ass	23, 24
Al Khlata Fm	Oman	South Oman Salt B. (East Arabian Penin.)	Africa	Mos, Kas, Gzh, Ass	23, 24
Juwayl Mbr/Wajid Fm; Unayzah B	Saudi Arabia	Central Arabian Peninsula	Africa	Ser, Bas, Mos, Kas, Gzh, Ass, Sak	25
Tahara Fm	Libya	Ghadames	Africa	L Fam	26
Witteburg Fm/Perdepoort Mbr	South Africa	Karoo	Africa	L Fam	26
Beacon Supergp	Antarctica	Heimefrontfjella	Antarctica	[Bas, Mos, Kas, Gzh, Ass, Sak, Art, Kun]	1
Gale Mudstone	Antarctica	Transantarctic Mtns	Antarctica	[Ass, Sak, Art, Kun]	1, 27
Pagoda/Scott Glacier/Buckeye Fm	Antarctica	Central Transantarc. Mtns	Antarctica	Ass, Sak	1, 27
Darwin Tillite	Antarctica	Darwin Mtns	Antarctica	Ass, Sak	27
Metschel Tillite	Antarctica	South Victoria Land	Antarctica	Ass, Sak	1, 27
Permian tillites/Lanterman Fm	Antarctica	North Victoria Land	Antarctica	Ass.	1, 29
Whiteout Conglomerate	Ant- Ellsworth Mtns	Ellsworth Mountains	Antarctica	[Bas, Mos, Kas, Gzh, Ass, Sak, Art, Kun]	1, 30
Tobra Fm	Pakistan	Salt Range	Asia	Kas, Gzh, Ass	1, 31, 32
Thini Chu Gp - Bangba Fm	Nepal	Lesser Himalaya	Asia (India)	Bas, Mos	1, 49
Golabgarh Boulder Fm	Nepal	Lesser Himalaya	Asia (India)	Ass, Sak	1, 34
Agglomeratic Slate	Nepal	Lesser Himalaya-Darjeeling	Asia (India)	Ass	1, 35, 32
Garu Fm	Nepal	E. Himalaya Gondwana Belt	Asia (India)	Sak, Art	1, 44
Rangit Pebble Slate	Kashmir	Intra-Gondwanan Basins	Asia (India)	Ass	1, 36
Ganmachidam Diamictite	Kashmir-Tibet	Intra-Gondwanan Basins	Asia (India)	[Bas, Mos, Kas, Gzh, Ass, Sak, Art, Kun]	47, 13
Talchir Boulder Beds	India	Peninsular India	Asia (India)	Ass, Sak	1, 5
Singa Formation/Ular Mbr	Malaysia	Yunnan-Malaya Orogenic Belt	Asia	Ser, Bas, Mos, Kas, Gzh, Ass, Sak	1, 39, 40
Kaeng Krachan/Phuket Gp/Ko Sire	Thailand	Sibumasu	Asia	Ass, Sak	1, 40, 41

Zhanjin Fm	Tibet	Tethys Himalayan Zone	Asia	Bas, Mos, Kas, Gzh, Ass, Sak	42, 43
Rakyang Fm	Tibet	Tethys Himalayan Zone	Asia	Vis, Ser	36
Pondo Gp	Tibet	Lhasa Block	Asia	[Bas, Mos, Kas, Gzh] Ass, Sak	44
Kongshuhe/Zizhi (Bangdu) Fm	China/Myanmar	Tengchong Block	Asia	Kas, Gzh, Ass, Sak	45
Cameng Fm	Tibet	Qiangtang Block	Asia	Gzh, Ass, Sak	44
Dingjiazhai Fm	China	Baoshan Block	Asia	Gzh, Ass, Sak	44
Jilong Fm/Zhadari Diamictite	Tibet	Yarlung-Zangbo Suture-High Himalayan Cryst	Asia	Gzh, Ass	36, 44
Bohorok Fm	Sumatra	northern Sumatra	Asia	[Bas, Mos, Kas, Gzh] Ass	13
Chepor Mbr	Malaya	NW Peninsula	Asia	L Vis	46, 47
[Keep Inlet Beds] / Kuriyippi Fm	W. Australia	Bonaparte	Australia	Ass	1, 49, 51
Grant Fm/Wye Worry Mbr	W. Australia	Canning	Australia	Ass, Sak	1, 66
Paterson Fm/Betty Fm	W. Australia	Canning	Australia	Gzh, Ass, Sak	1, 49
Lyons Fm	W. Australian	Carnarvon	Australia	Ass, Sak	1, 51
Nangetty Fm	W. Australia	Perth	Australia	Ser, Bas, Mos, Kas, Gzh, Ass, Sak	1, 52
[Stockton Gp] Shotts Fm	W. Australia	Collie	Australia	Gzh, Ass	1, 48, 49
Paterson Fm	W. Australia	Officer	Australia	Ass, Sak	1
Boorthanna Fm	S. Australia	Arckaringa	Australia	Ass, Sak	1, 49
Crown Point Fm	S. Australia	Pederka	Australia	[Bas, Mos, Kas, Gzh] Ass	1, 49
Unnamed diamictite	S. Australia	Polda	Australia	Sak	1
Cape Jervis Beds	S. Australia	Troubridge	Australia	Sak	1
[Joe Joe Gp]/Jericho Fm	E. Australia	Galilee	Australia	Ser, Bas, Mos	1, 53
[Joe Joe Gp]/Boonderoo Beds	E. Australia	Galilee	Australia	Sak	5
[Joe Joe Group]/Lake Galilee Ss	E. Australia	Galilee	Australia	Ser, Bas	5
Betts Creek Beds	E. Australia	Galilee	Australia	Wor	5
Reids Dome Beds	E. Australia	Galilee	Australia	Sak, Art	5
Ingelara/Peawaddy Fm	E. Australia	Bowen	Australia	Roa	1, 54
Youlambie Conglomerate	E. Australia	New England Fold Belt	Australia	Ass, Sak	5
Rocky Creek Cgl/Currabubula	E. Australia	New England Fold Belt	Australia	Ser, Bas, Mos	1, 5
Spion Kop Cgl	E. Australia	New England Fold Belt	Australia	Ser	1, 55
Johnsons Creek	E. Australia	New England Fold Belt	Australia	Ser	5
Seaham Fm	E. Australia	Cranky Corner/Gresford Block	Australia	Ser, Bas, Mos, Kas	1, 49
Beckers Fm	E. Australia	Cranky Corner/Gresford Block	Australia	Ass, Sak	5
Maitland Gp	E. Australia	Cranky Corner/Gresford Block	Australia	Roa	5
Youdale/Kullatine Fm	E. Australia	Northern Hastings Block	Australia	Ser	5
Unnamed diamictite	E. Australia	Sydney	Australia	Sak, Art	1, 5
Talaterang Group (Tallong/Burraw	E. Australia	Sydney	Australia	Sak, Art	1, 5
Glen Davis/Newnes/Baal Bone Fn	E. Australia	Sydney	Australia	Cap	5
Coleraine Fm/Bacchus Marsh/Wil	E. Australia	Murray	Australia	Sak	1, 72
Wynyard Tillite	Tasmania		Australia	Gzh, Ass	1, 57
Itararé SubGp	Brazil	Paraná	South America	Bas, Mos, Kas, Gzh	1, 58, 59, 60
San Gregorio/Cerro Pelado Fm	Uruguay	Paraná	South America	Kas, Gzh, Ass	1, 11, 62
Santa Fe Gp/Brocotó/Brejo de Arr	Brazil	Sanfranciscana	South America	Bas, Mos, Kas, Gzh	60, 63
Mulungu Mbr/Batinga Fm	Brazil	Sergipe-Alagoas	South America	Bas, Mos, Kas, Gzh	1, 60, 63
Macharetí Gp	Argentina-Bolivia	Tarija-Chaco	South America	Bas, Mos, Kas	1, 64, 65
Mandiyuti Gp/San Telmo Fm	Bolivia	Tarija-Chaco	South America	Gzh, Ass	64, 65

Itacua Fm	Bolivia	Tarija-Chaco	South America	Tou, E-M Vis	64, 65
Charata Fm	Argentina	Chaco Parana	South America	[Bas, Mos, Kas, Gzh, Ass, Sak, Art, Kun]	1
Guandacol, Quebrada Larga (lwr)	Argentina	Paganzo	South America	Ser, Bas	1, 65, 67
Jejenes Fm	Argentina	Paganzo	South America	Ser, Bas	1, 68, 69
Bajo de Veliz Fm	Argentina	Paganzo	South America	Ass	1, 70, 71
Tupe Fm	Argentina	Paganzo	South America	Mos	66
Jaguel/Cortaderas/Malimán Fm	Argentina	Rio Blanco	South America	M Vis	1, 66
Rio del Peñon (lower)	Argentina	Rio Blanco	South America	Ser, Bas	66
Valle Chico	Patagonia	Tepuel-Genoa	South America	L Tou, E Vis	72
Pampa de Tepuel	Patagonia	Tepuel-Genoa	South America	L Vis	72
Pampa de Tepuel	Patagonia	Tepuel-Genoa	South America	Ser, Bas	72
Pampa de Tepuel	Patagonia	Tepuel-Genoa	South America	Mos	72
Pampa de Tepuel	Patagonia	Tepuel-Genoa	South America	Gzh, Ass	72
Mojón de Hierro	Patagonia	Tepuel-Genoa	South America	Sak	72
El Paso Fm	Argentina	Calingasta-Uspallata	South America	L Vis	1, 68
Hoyada Verde	Argentina	Callingasta-Uspallata	South America	Bas	1, 66
El Imperial	Argentina	San Rafael	South America	Bas	73
Sauce Grande Fm	Argentina	Sauce Grande	South America	Kas, Gzh, Ass, Sak	1, 74, 75
Tepuel Gp/Las Salinas Fm	Argentina	Patagonian	South America	Ser, Bas, Mos	1, 76
Cumaná Fm	Bolivia	Titicaca	South America	L Fam	8, 26, 11
Saipuru Fm	Bolivia	Subandes	South America	L Fam	8, 26, 11
Ccatcca Fm	Peru	Urubamba area	South America	L Fam	8, 26, 11
Toregua Fm	Bolivia	Madre de Dios	South America	L Fam, E Tou	8, 26, 11
Jaragui Fm	Brazil	Solimoes	South America	L Fam	8, 26, 11
U. Curiri	Brazil	Amazonas	South America	L Fam	8, 11
Faro Fm	Brazil	Amazon	South America	M-L Vis	26, 79
U. Oriximina Fm	Brazil	Amazonas	South America	M Tou	26
Curuá Formation	Brazil	Amazon	South America	L Fam	1, 80
Jaraqui Mbr	Brazil	Solimoes	South America	L Fam	8, 26
Poti Fm	Brazil	Paranaíba	South America	M-L Vis	55, 79
Longa Fm	Brazil	Paranaíba	South America	M Tou	26
Cabecas Fm	Brazil	Paranaíba	South America	L Fam	1, 82, 83, 11
Jandiatuba Fm	Brazil	Solimoes	South America	M Tou	26
Cortaderas Fm	Argentina	Rio Blanco	South America	M-L Vis	26
Unnamed diamict dikes	Argentina	Falklands	South America	L Vis	26
Spechty Kopf Fm	Eastern U.S.	Appalachian	North America	L Fam	26
Cutler Fm	Western U.S.	Paradox	North America	Mos, Kas, Gzh, Ass, Sak	85

*Stages (including partial Stage) reported with glacial deposits. If age is resolved only to Period , then all Stages in that Period are listed (w/ brackets signaling lower resolution -- see Methods].

Stage Abbreviations

Abbreviation	**Stage Name**
L Fam	late Famennian
E Tou	early Tournaisian
M Tou	middle Tournaisian
L Tou	late Tournaisian

E Vis	early Visean
M Vis	middle Visean
L Visean	late Visean
Ser	Serpukhovian
Bas	Bashkirian
Mos	Moscovian
Kas	Kasimovian
Gzh	Gzhelian
Ass	Asselian
Sak	Sakmarian
Art	Artinskian
Kun	Kungerian
Roa	Roadian
Wor	Wordian
Cap	Capitanian

Supplementary Data Table 2: Volcanic Units (Devonian-Triassic)

Site No.	Age / Ma	Age Error / ± Ma	Age (Stage)	Plate ID	PaleoLat	PaleoLong	Modern Latit	Modern Long.	Reference #	Unit Name	Sample Name	*Composition	Ignimbrite?	Pyroclastic?
3	268.4	3.8	Wordian	701	-61	-34	-32.50	20.25	99	Waterford Formation	OPA151			P
4	263.3	3.3	Capitanian	701	-59	-31	-32.50	20.25	99	Waterford Formation	OPA160			P
5	261.241	0.32	Capitanian	701	-60	-24	-32.75	24.41	114	Koonap Formation	Bruce-1			P
6	260.407	0.32	Capitanian	701	-60	-23	-32.75	24.41	114	Koonap Formation	K220307-2			P
7	259.262	0.31	Capitanian	701	-60	-23	-32.75	24.41	114	Middleton Formation	Tortoise			P
8	259.433	0.31	Capitanian	701	-60	-23	-32.75	24.41	114	Middleton Formation	K150307-2B			P
9	259.58	0.39	Capitanian	701	-60	-23	-32.75	24.41	114	Middleton Formation	K150307-2T			P
10	256.247	0.32	Wuchiapingian	701	-60	-21	-32.62	25.27	114	Middleton Formation	Bruintjieshoogte			P
13	283.9	2.7	Artinskian	451	50	81	43.35	93.80	106	Unnamed volcanics	Well Baocan 1	R		
14	286.6	3.3	Artinskian	580	50	59	41.12	81.50	106	Unnamed volcanics	YM5-8	R		
15	271.7	2.2	Roadian	580	53	71	40.80	81.50	106	Unnamed volcanics	MN1	R		
16	282.9	2.5	Kungurian	580	51	63	41.28	82.17	106	Unnamed volcanics	YM16	R		
17	277.3	2.5	Kungurian	580	52	68	41.25	82.29	106	Unnamed volcanics	NK1	R		
18	290.9	4.1	Sakmarian	580	50	55	41.30	81.80	106	Unnamed volcanics	YM30	R		
19	340.3	3.4	Visean	451	36	45	43.60	91.80	107	Qijiaojing	Bogda rhyolites	R		
20	400	5	Emsian	450	39	24	45.00	88.10	108	Unnamed tuff	BJG10			P
21	315	4	Moscovian	450	39	33	45.00	88.10	108	Unnamed rhyolite	BLG14	R		
22	323	5	Bashkirian	450	36	33	45.00	88.10	108	Unnamed rhyolite	BLG15	R		
23	332	9	Visean	450	37	28	44.95	88.15	108	Unnamed rhyolite	ZPG-3	R		
24	295.9	1.4	Asselian	401	53	36	47.55	86.80	109	Unnamed rhyolite	K5b	R		
25	306.9	2.2	Kasimovian	430	71	107	50.42	125.74	110	Honghutuhe Group	HH32-82	R		P
26	353.1	2	Tournaisian	430	68	52	49.48	125.05	110	Honghutuhe Group	HH39-105	R		P
27	353.8	2.4	Tournaisian	430	68	52	49.25	125.10	110	Honghutuhe Group	HH41-108	R		P
28	307.5	2.1	Moscovian	430	71	107	49.50	126.42	110	Honghutuhe Group	HH6-15	R		P
29	352.5	3	Tournaisian	430	68	51	49.48	125.10	110	Honghutuhe Group	HH36-96	R		P
30	294.2	2.8	Sakmarian	801	-46	134	-21.13	149.15	111	Dumbleton Ignimbrite	CB45Z		I	P
32	304.7	3.2	Kasimovian	801	-44	129	-21.00	147.50	112	Locharwood Rhyolite	88502032	R		
33	293.5	5.6	Sakmarian	801	-46	132	-20.55	147.20	112	Arundel Rhyolite	89503028	R		
35	297.4	2.9	Asselian	801	-45	130	-21.00	147.35	112	Conway	89302132	D-A	I	P
36	309	3	Moscovian	801	-53	143	-32.80	151.33	113	Matthews Gap Dacitic Tuff Membe	MGD-1	D		P
37	256	4	Wuchiapingian	801	-68	145	-32.90	151.51	113	Awaba Tuff	AT-1			P
38	371.2	6.1	Famennian	801	-18	-180	-23.05	147.25	114	Silver Hills Volcanics	sample 1	R		P
39	343.7	5.3	Visean	801	-39	133	-24.05	147.25	114	Silver Hills Volcanics	sample 2		I	P
40	349.2	7.1	Tournaisian	801	-37	143	-22.90	147.25	114	Silver Hills Volcanics	sample 5	T		
41	344.1	4.5	Visean	801	-38	134	-22.90	147.26	114	Silver Hills Volcanics	sample 7	R		
42	355.7	5.9	Tournaisian	801	-33	167	-23.50	147.51	114	Silver Hills Volcanics	sample 10	R	I	P
43	365.3	4.6	Famennian	801	-24	171	-23.50	147.50	114	Silver Hills Volcanics	sample 12	R		
44	387	7	Givetian	801	-20	166	-20.95	147.05	114	St Anns Formation	sample 13		I	P
45	362.4	8	Famennian	801	-25	162	-20.92	147.15	114	St Anns Formation	sample 14		I	P
46	321.3	3.2	Bashkirian	801	-51	140	-30.09	150.37	115	Ermelo Pyroclastics	Ermelo			P
47	319.2	2.8	Bashkirian	801	-43	147	-30.59	150.35	115	Wanganui Andesite	Wanganui	A		
48	317.8	2.8	Bashkirian	801	-45	146	-30.53	150.39	115	Eastons Arm Rhyolite	Eastons Arm	R		
49	318	3.4	Bashkirian	801	-44	146	-30.19	150.29	115	Peri Rhyolite	Peri	R		
50	322.3	3.2	Bashkirian	801	-42	148	-31.30	150.37	115	Unnamed Dacite	Unnamed	D		
51	313.6	3.6	Moscovian	801	-49	144	-31.12	150.59	115	Figtree Creek unnamed ignimbrite	Figtree Creek		I	P
52	306	4.2	Kasimovian	801	-52	140	-31.17	150.64	115	Piallaway Trig Ignimbrite	Piallaway Trig		I	P
53	235	2	Carnian	390	51	39	56.50	62.55	116	Unnamed rhyolite	2926-3	R		
54	270	3	Roadian	401	58	19	69.00	88.00	117	Maslov's Diatreme	19F-57	R-D		
55	333.7	3.4	Visean	375	-1	-15	50.46	16.66	118	Paprotnia Beds	bentonite layer			P
56	288.36	0.35	Artinskian	302	34	28	53.88	56.53	119	Dal'ny Tulkas roaduct section	DTR905			P
57	308.36	0.38	Moscovian	302	27	15	53.92	56.53	119	Usolka section	01DES-481			P
58	308.5	0.36	Moscovian	302	27	15	53.88	56.54	119	Dal'ny Tulkas quarry section	01DES-351			P
59	317.54	0.38	Bashkirian	390	22	13	56.42	61.81	119	Kljuch section	Bed 32			P
60	304.39	0.36	Kasimovian	302	29	18	52.29	58.92	119	Verkjnyaya Kardailovka section	02VD-1			P
61	273.3	2.8	Kungurian	334	7	22	48.92	20.80	120	Roznava Formation	8-SM	R	I	P
62	275.3	2.9	Kungurian	334	6	22	48.92	20.80	120	Roznava Formation	2-Sm	R	I	P
63	272.4	7.3	Roadian	334	8	22	48.95	20.85	120	Petrova Hora Fromation		A		
64	275.2	4	Kungurian	334	6	22	48.81	20.91	120	Petrova Hora Fromation	38/SM	R-D		
65	331	1	Visean	453	57	51	43.08	107.33	122	Khan-Bogd rhyolites	KHB-1802	R		
66	274.1	1.6	Kungurian	308	2	21	46.48	11.05	123	Ora Formation	26CM411 (1)	R	I	P
67	274.2	2.9	Kungurian	308	2	21	46.54	11.16	123	Ora Formation	26CM405 (2)	R	I	P
68	277	2	Kungurian	307	1	21	46.43	11.28	123	Ora Formation	26CM413 (3)	R	I	P
69	274.6	2.1	Kungurian	308	2	21	46.54	11.18	123	Andriano Formation	26CM404 (4)	R		
70	276.9	2.3	Kungurian	307	1	21	46.49	11.29	123	Gries Formation	26CM412 (5)	R	I	P
71	276.7	1.1	Kungurian	307	1	21	46.54	11.19	123	Nalles Formation	26CM407 (6)	R	I	P
72	276.5	1.1	Kungurian	308	1	21	46.58	11.15	123	Gargazzone Formation	26CM403 (8)	R-D	I	P
73	278.4	1.5	Kungurian	308	0	21	46.61	11.13	123	Monte Luco Formation	26CM012 (9)	R-D		
74	279.6	4.5	Kungurian	308	0	21	46.54	11.07	123	Monte Luco Formation	26CM410 (10)	R-D	I	P
75	279.6	1.1	Kungurian	308	-1	21	46.54	11.08	123	Monte Luco Formation	26CM409 (11)	R-D		
76	284.9	1.6	Artinskian	308	-2	17	46.57	11.04	123	Basal Conglomerate	26CM293/2 (12)	R	I	P
77	276.1	1.5	Kungurian	307	1	21	46.56	11.24	123	Subvolcanic Terlano Body	26CM408 (7)	R-D		
78	284.5	1.7	Artinskian	308	-2	17	46.57	11.08	123	Plazzoles Laccolite	26CM396/2 (15)	R-D		
79	274.5	3.7	Kungurian	308	1	21	46.59	11.10	123	Megafeldspar porphyritic dikes	26CM393/2 (18)	R-D		
80	281.5	0.7	Kungurian	308	-2	20	46.56	11.05	123	Rhyodacitic dikes	26CM502 (13)	R-D		
81	282.3	1.3	Kungurian	308	-2	19	46.58	11.06	123	Rhyodacitic dikes	26CM501 (14)	R-D		
82	278	5	Kungurian	375	13	14	50.71	12.83	124	Saxonian Rotliegend rhyolites	64	R		
83	278	5	Kungurian	375	14	20	50.95	12.60	124	Saxonian Rotliegend rhyolites	4	R		
84	364	2	Famennian	304	-12	-56	37.62	-8.13	125	unnamed volcanics	R1	R-D		
88	359	3	Famennian	304	-15	-57	37.65	-8.13	125	unnamed volcanics	R14	R-D		
89	359	1	Famennian	304	-15	-57	37.59	-8.13	125	unnamed volcanics	C6	R-D		
90	358	2	Tournaisian	304	-15	-56	37.68	-8.13	125	unnamed volcanics	MD2-106	R-D		
91	354	2	Tournaisian	304	-15	-54	37.62	-8.13	125	unnamed volcanics	CP2-366	R-D		
97	294.2	2.1	Sakmarian	302	12	11	50.10	19.60	126	Cracow igneous rocks	Zalas	R-D		
99	343.4	1	Visean	315	-1	-43	55.97	-2.82	127	Garleton Hills Volcanic Formation	ASW124	T-A		P
100	335.2	0.8	Visean	315	-3	-32	55.84	-4.73	127	Clyde Plateau Volcanic Formation	ASW131	T-A		
101	334.7	1.7	Visean	315	-3	-30	55.72	-4.40	127	Clyde Plateau Volcanic Formation	ASW142	T		
103	276	1.2	Kungurian	308	1	21	46.68	11.25	128	Athesian Volcanic Group	13AM93	R-D	I	P
105	293.3	1.5	Sakmarian	308	-4	9	46.68	11.12	128	Athesian Volcanic Group	13CM300		I	P
108	287.9	3.5	Artinskian	375	13	15	51.03	15.87	129	Wielławka Rhyolites	2	R		
109	292.4	1.8	Sakmarian	375	11	11	51.06	15.86	129	Rózana Rhyolites	775	R		
110	292.8	2.1	Sakmarian	375	11	11	50.94	16.11	129	Bolków Rhyolites	776	R		
111	294.1	3.1	Sakmarian	375	11	9	51.03	15.88	129	Sedzlzowa Rhyolites	891	R		
112	298.5	3.3	Asselian	315	12	5	52.90	17.00	130	unnamed volcanics	Pniewy-3		I	P
113	294.6	2.3	Sakmarian	330	13	6	54.20	15.00	130	unnamed volcanics	Wysoka Kamienska-2			P
114	293	2.3	Sakmarian	302	14	8	54.40	16.90	130	unnamed volcanics	Daszewo-12	R		
115	302.6	9.6	Gzhelian	330	10	-4	56.70	7.60	130	unnamed volcanics	C-1	R		
116	296	2	Asselian	315	10	3	53.00	9.80	130	unnamed volcanics	Dageförde Z1a	R		
117	295.3	2.3	Asselian	330	12	4	54.71	11.98	130	unnamed volcanics	Fehmarn Z1	R		

118	289.8	2.6	Artinskian	315	13	9	54.90	11.60	130	unnamed volcanics	Rodby-2	R-D			
119	296	3	Asselian	315	11	7	52.00	17.00	130	unnamed volcanics	Zdrój-1	D			
120	293.8	2.7	Sakmarian	315	11	7	53.00	11.70	130	unnamed volcanics	Salzwedel 2/64	R			
121	299.7	5.3	Gzhelian	330	11	2	54.10	14.80	130	unnamed volcanics	Penkun 1/71	D			
122	301	3	Gzhelian	315	9	2	52.52	13.38	131	Landsberg Unit	Spitzberg	R			
123	298	3	Asselian	315	10	3	52.52	13.38	131	Lobejun Unit	Ha 4/3	R			
125	292	3	Sakmarian	315	12	8	52.52	13.38	131	Petersberg Unit	Ha 2/7(4 zircons exclu	R			
127	307	3	Kasimovian	315	6	0	52.52	13.38	131	Schwerz Unit	Ha 5/5	R			
128	302	3	Gzhelian	315	8	1	52.52	13.38	131		Fl 34		I		P
129	300	3	Gzhelian	315	10	1	53.56	12.83	131	Mirow 1/74 core	MiY1		I		P
130	297	3	Asselian	315	11	3	53.56	12.83	131	Mirow 1/74 core	MiH1	R			P
131	299	3	Gzhelian	315	10	2	53.57	13.38	131	Friedland 1/71 core	FrB2	R-D			
132	297	4	Asselian	315	11	4	53.57	13.38	131	Friedland 1/71 core	FrD2				P
133	297	3	Asselian	315	10	4	52.83	12.67	131	Kotzen 4/74 core	KoE5	R-D			
134	300	5	Gzhelian	305	6	5	48.08	13.33	132	Peitingalm gneiss (metavolc)	11	D			P
135	299	4	Gzhelian	334	-1	0	47.83	13.67	132	Heuschartenkopf gneiss (metavolc)	12	R			P
136	279	9	Kungurian	305	11	23	48.00	13.58	132	Schonbachwald gneiss (metavolc)	14	R			P
137	290.7	3	Asselian	307	-4	11	46.58	11.53	133	Ponte Gardena/Waidbruck	TPZ 159	A			
138	289	3	Artinskian	307	-3	13	46.58	11.53	133	Ponte Gardena/Waidbruck	TPZ 160	A			
139	272.7	2.2	Roadian	344	10	22	44.25	7.95	134	Lithozone C	LIC	R	I		P
140	274.1	2.6	Kungurian	344	9	22	44.08	7.94	134	Lithozone D	LID	R	I		P
141	334	4	Visean	305	-6	-21	48.13	6.33	135	Saint-Nabor	SL1	R	I		P
142	277.9	2.1	Kungurian	307	0	20	45.80	10.60	136	Ponte Murandin lava	GN01	D			
143	279.2	1.9	Kungurian	307	-1	20	45.80	10.60	136	Malga Plan Ignimbrites	MP01	R-D	I		P
144	267.8	1.5	Wordian	16106	38	-36	62.00	-134.00	137	Tummel fault zone	KG02-048	A			
145	305.5	1.5	Kasimovian	302	16	15	48.50	39.00	138	Kashirsky group	coal tonstein horizon I $^{1}_{3}$				P
146	311	3.4	Moscovian	315	1	-3	51.32	7.62	139	Carboniferous tonstein	Z1				P
147	327.7	2	Serpukhovian	801	-41	150	-32.60	151.80	139	Paterson Volcanics	Z850				
148	294.8	1.7	Sakmarian	375	10	7	51.50	12.00	140	Wettin Subformation	1390	R			
151	342.1	3.2	Visean	801	-43	141	-32.08	151.17	141	lower Isismurra Formation			I		P
167	332.3	2.2	Visean	801	-41	147	-32.25	151.53	141	Martins Creek Ignimbrite			I		P
155	345	2	Visean	305	-5	-34	48.08	6.32	142	Low-K rhyolite, Trmontkopf	SU-93-11	R			
158	336	5	Visean	305	-6	-32	48.08	6.32	142	Molkenrian Rhyolite Breccia	SU-94-5	R	I		P
159	279	4.8	Kungurian	308	0	22	47.60	12.10	143	unnamed meta-andesite	SNA1	A			
161	304	3	Kasimovian	308	-8	3	47.10	11.30	143	unnamed metarhyolite	VE1	R			
162	309.8	1.5	Moscovian	308	-10	1	47.30	11.60	143	Grierkar meta-rhyodacite	GKAR	R-D			
163	280.5	2.6	Kungurian	308	-1	22	47.00	11.50	143	Pfitsch meta-rhyolite	PFJ	R			P
166	280.53	0.48	Kungurian	307	-1	21	46.20	169	144	Val Calamento	SU-99-7	R-D			
167	277.59	0.55	Kungurian	307	-1	21	46.20	11.10	144	Albiano	SU-99-8	R	I		P
168	277	5	Kungurian	307	0	21	46.40	11.40	144	San Lugano	SU-99-6	R	I		P
170	307.9	2.8	Moscovian	201	-40	-78	-21.16	-68.84	145	Collahuasi Group	CLL-75	R			
171	297.6	2.4	Asselian	201	-41	-69	-21.03	-68.66	145	Collahuasi Group	CLL-85	R			
172	304.6	3.2	Kasimovian	201	-41	-75	-20.97	-68.70	145	Collahuasi Group	CLL-114	R			
173	296.9	4.3	Asselian	201	-41	-68	-20.99	-68.63	145	Collahuasi Group	CLL-221	D			
174	298.3	2.1	Asselian	201	-41	-70	-20.97	-68.70	145	Collahuasi Group	CLL-223	R			
175	303.9	3	Kasimovian	201	-41	-75	-20.97	-68.70	145	Collahuasi Group	CLL-237	R			
176	308.5	2.2	Moscovian	201	-40	-78	-20.97	-68.70	145	Collahuasi Group	CLL-238	R			
177	244.8	2.5	Anisian	201	-32	-38	-21.01	-68.61	145	Collahuasi Group	CLL-30	D			
178	342	0.97	Visean	202	-45	-104	-27.33	-68.17	146	unnamed volcanics	FLPCG	R			
179	348	3	Tournaisian	202	-44	-98	-28.77	-67.81	146	unnamed volcanics	FLPDAT	R			
180	291	1.2	Sakmarian	201	-40	-63	-31.30	-52.90	147	Rio Bonito Formation	G-RECREIO				P
182	281.4	2.5	Kungurian	2901	-52	-61	-34.75	-68.50	148	Yacimiento Los Reyunos Formatior	CH-1		I		P
183	264.8	2.3	Capitanian	2901	-48	-47	-34.75	-68.50	148	Agua de los Burros Formation	CH-4		I		P
184	264.7	2.9	Capitanian	2901	-48	-47	-34.75	-68.50	148	Cerro Carrizalito Formation	CH-9	R	I		P
187	278.4	2.2	Kungurian	201	-48	-31	-25.50	-51.00	149	Irati Formation	SM3				P
188	252.2	0.6	Changhsingian	101	9	-32	34.90	-101.66	150	Quatermaster Formation	unnamed				P
189	320.7	2.5	Bashkirian	101	-15	-54	34.70	-93.40	151	Stanley Group	Chickasaw Creek Tuff				P
190	324.8	2.1	Serpukhovian	101	-14	-60	34.30	-94.80	151	Stanley Group	Upper Mud Creek				P
191	322.4	2.4	Bashkirian	101	-14	-58	34.30	-94.80	151	Stanley Group	Lower Mud Creek Tuff				P
192	326.1	3.7	Serpukhovian	101	-14	-62	34.20	-94.70	151	Stanley Group	Hatton Tuff				P
193	328.5	2.7	Serpukhovian	101	-13	-65	34.20	-94.70	151	Stanley Group	Beaver's Bend Tuff				P
194	281	2	Kungurian	16113	32	-36	60.00	-133.00	152	Butsih volcanic unit	96-DY-58Z	A			P
195	355.6	2.7	Tournaisian	16113	22	-101	60.00	-133.00	153	Dorsey Assemblage	99RAS-31-1				P
196	346	2.2	Visean	16104	27	-88	61.48	-130.22	154	Wolverine Volcanogenic Massive S	Fisher (P98-69A)	R			
199	356.9	0.5	Tournaisian	16104	22	-100	61.38	-130.07	154	Wolverine Volcanogenic Massive S	Puck	R			
200	270.5	2.5	Roadian	215	-14	-51	17.38	-97.10	155	Sosola rhyolite	unnamed	R			
206	293	1.6	Sakmarian	201	-50	-44	-23.50	-50.00	88	Lower Candiota Coal Seam	LowCand2				P
207	288.4	1.2	Artinskian	201	-49	-39	-23.50	-50.00	88	Upper Candiota Coal Seam	UppCand1				P
208	293.8	3.5	Sakmarian	201	-50	-45	-23.50	-50.00	88	Upper Candiota Coal Seam	UppCand2				P
209	314.6	0.9	Moscovian	101	-14	-44	37.63	-82.55	156	Fire Clay Tonstein	USGS field sample				P
210	372	3	Famennian	16105	20	-116	63.95	-147.30	157	Totatlanika Schist	97ADb57F	R	I		P
211	280.8	1.9	Kungurian	290	-57	-54	-38.00	-62.00	75	Tunas Formation	Tunas Fm tuff				P
213	284	15	Artinskian	290	-58	-58	-38.21	-61.48	158	Tunas Formation	VE-19				P
214	344.5	5.2	Visean	16104	30	-86	62.95	-135.83	159	Little Kalzas Formation	98MC063a	R			
215	365	2	Famennian	108	-13	-81	47.01	-60.61	160	Fisset Brook Formation	SMB95-18	R			
216	371	2	Famennian	108	-15	-84	46.55	-61.01	160	Fisset Brook Formation	B82	R			
217	374	2	Frasnian	108	-16	-85	46.52	-60.96	160	Fisset Brook Formation	KP95-21	R			
218	371	3	Famennian	108	-16	-84	45.78	-61.48	160	Fisset Brook Formation	GAM93-33	R			
219	370	1.5	Famennian	108	-16	-85	45.84	-61.94	160	McAras Brook Formation	A15	R			
220	358	1	Tournaisian	108	-13	-77	45.58	-63.33	160	Upper Byers Brook Formation	C7357	R			
222	356	2	Tournaisian	108	-12	-76	45.47	-64.20	160	Fountain Lake Group	C7358	R			
223	356.2	0.9	Tournaisian	401	57	-18	61.67	-131.00	161	Wolverine Lake Group	FV-21				
224	320	4.5	Bashkirian	801	-42	148	-30.68	150.33	162	Mihi Rhyolite	429-1	R			
225	315	3.5	Moscovian	801	-47	145	-30.61	150.28	162	Bunaleer Dacite	432-7	D			
226	315.2	2.8	Moscovian	801	-47	145	-30.87	150.34	162	Birken Head Volcanic	511-2	D	I		
227	297.1	3.4	Asselian	801	-54	139	-30.73	150.31	162	Unnamed rhyolite	512-2	R			
228	319.3	2.8	Bashkirian	801	-43	148	-31.17	150.65	162	Taggarts Mountain Ignimbrite	206-4	D	I		P
229	287.6	2.8	Artinskian	801	-56	145	-31.74	150.96	95	Brogans Rhyodacite	287-2A	R-D			
230	339.6	3	Visean	801	-43	142	-31.67	150.93	95	Burnewang Ignimbrite	456-13A		I		P
231	314.7	3.5	Moscovian	801	-45	148	-31.70	150.91	95	Unnamed Ignimbrite C4	466-15		I		P
232	324.1	3.7	Serpukhovian	801	41	149	-31.76	150.99	95	Wheelihans Ignimbrite	469-43		I		P
233	348.9	3	Tournaisian	801	-40	159	-31.80	151.04	95	Isismede Ignimbrite	470-13		I		P
236	351.9	2	Tournaisian	801	-37	163	-31.84	150.79	95	Isismede Ignimbrite	488-16C		I		P
237	308.4	2.9	Moscovian	801	-51	143	-31.70	150.87	95	Allawa Ignimbrite	490-2		I		P
238	305.8	2.8	Kasimovian	801	-52	142	-31.71	151.00	95	Kankool Ignimbrite	493-3		I		P
239	348.2	3.2	Tournaisian	801	-40	157	-31.58	150.87	95	Isismede Ignimbrite	501-4		I		P
240	315.9	2.9	Bashkirian	801	-43	149	-31.88	151.00	95	Unnamed Ignimbrite C3	503-1		I		P
241	312.1	3.5	Moscovian	801	-47	146	-31.54	150.78	95	White Rocks Ignimbrite	505-1		I		P
242	343.3	2.1	Visean	801	-42	148	-31.92	151.03	95	Unnamed Ignimbrite D	527-24		I		P
243	342.8	2.7	Visean	801	-42	148	-31.92	151.03	95	Unnamed Ignimbrite B	532-1A		I		P

244	323.1	2.6	Bashkirian	801	-41	149	-31.97	150.97	95	Elmswood Ignimbrite	538-40		I		P
245	302.6	2.7	Gzhelian	801	-53	141	-32.18	150.95	95	Well Gully Ignimbrite	556-5		I		P
247	306.5	2.1	Kasimovian	850	-62	146	-41.50	148.00	163	Mt Durham Tuff Member	Z2815 +Z2450		I		P
248	291	6	Sakmarian	801	-46	135	-21.09	148.31	164	Lizzie Creek Volcanics	RSC011	D	I		P
249	303	5	Gzhelian	801	-45	132	-22.41	149.26	164	Connors Volcanics (Cycle 2?)	RSC074a	R	I		P
250	350	7	Tournaisian	801	-36	146	-22.85	149.43	164	Connors Volcanics (Cycle 1?)	RSC093	R	I		P
251	313	6	Moscovian	801	-44	139	-25.31	150.36	164	Torsdale Volcanics	RSC171	R	I		P
253	298	3	Asselian	801	-47	134	-24.00	150.12	164	Camboon Volcanics	IWGG809	R	I		P
254	308	6	Moscovian	801	-47	136	-25.15	150.29	164	Camboon Volcanics	BB2535		I		P
258	321.1	1.9	Bashkirian	801	-42	147	-30.19	150.05	165	unnamed ignimbrite	198-1		I		P
259	327.2	2.9	Serpukhovian	801	-40	147	-30.04	150.38	165	Bexley Rhyolite Member	202-6	R			
260	326.4	2.9	Serpukhovian	801	-40	147	-30.13	150.30	165	Plagyan Rock Rhyodacite Member	203-1	R-D	I		P
261	320	2.8	Bashkirian	801	-42	148	-30.19	150.18	165	Pound Rock Rhyodacite Member	213-3	R-D			
262	319	2.7	Bashkirian	801	-43	147	-30.43	150.50	165	Plagyan Ignimbrite Member	234-5		I		P
263	316.3	2.1	Bashkirian	801	-45	145	-29.85	150.28	165	The Tops Rhyolite Member	239-3	R			
264	351	3	Tournaisian	430	67	52	49.98	127.12	166	Kunaerhe Formation	HSW10	R			
265	319	3	Bashkirian	455	75	70	49.04	127.04	166	Wudaoling	HSW4	R			
266	319	3	Bashkirian	455	75	70	49.05	127.04	166	Wudaoling	HSW 5	D			
267	295	2	Sakmarian	430	65	118	49.33	127.14	166	Wudaoling	12HSW4	R			
268	293	2	Sakmarian	430	66	119	49.98	127.18	166	Hetaoshan	HSW8	R			
269	331	3	Visean	462	35	26	46.47	84.24	167	west Junggar dacite	wk01	D			
270	300	2	Gzhelian	601	26	74	43.37	124.72	168	Daheshan Formation	DH002	D			
271	302	2	Gzhelian	601	23	74	43.37	126.73	168	Daheshan Formation	DH006	D			
272	299	2	Gzhelian	601	25	76	43.37	126.73	168	Daheshan Formation	DH008	R			
273	301	2	Gzhelian	601	24	74	43.37	126.74	168	Daheshan Formation	DH020	R			
274	300	2	Gzhelian	601	25	75	43.36	126.75	168	Daheshan Formation	DH037	R			P
275	300	2	Gzhelian	601	25	75	43.35	126.75	168	Daheshan Formation	DH041	R			
276	314.3	1.9	Moscovian	450	41	33	45.00	89.25	169	BN Formation	09LSG-6	R			
277	306.5	1.5	Kasimovian	450	46	33	45.02	89.03	169	BN Formation	09BJE-79	R			
278	275.6	2.8	Kungurian	450	55	60	44.98	89.28	170	BN Formation		R			
281	298	2	Asselian	601	31	74	43.33	118.17	171	Shuangjing Schist		R-D			
282	288.5	3.3	Artinskian	60401	0	87	23.04	102.00	172	Baliu	K10-56	R	I		P
283	364.3	7.2	Famennian	801	-22	169	-21.71	149.45	173	Campwyn Volcanics	GH1	R	I		P
284	373.6	2.9	Frasnian	801	-15	177	-21.40	149.29	173	Campwyn Volcanics	SB11C	R	I		P
285	354.7	3.3	Tournaisian	801	-30	152	-20.88	148.95	173	Campwyn Volcanics	FI11	R	I		P
286	354.3	4.1	Tournaisian	801	-31	150	-20.62	148.68	173	Campwyn Volcanics	WC31	R	I		P
287	364.6	3.4	Famennian	801	-22	164	-21.33	149.30	173	Campwyn Volcanics	PV2/3	R			P
288	350.9	2.7	Tournaisian	801	-36	149	-24.62	151.12	173	Rockhampton group	SB283	R	I		P
289	258.9	2.7	Wuchiapingian	801	-57	138	-21.83	148.00	174	Platypus tuff bed	WB1	R	I		P
290	323.1	0.6	Bashkirian	430	61	56	43.95	109.08	175	Tsagaan Nuruu Formation	95.3A	R	I		P
291	344.4	1.9	Visean	451	37	46	43.44	91.41	176	Hongshankou rhyolite	618-2	R			
292	293.3	1.7	Sakmarian	451	53	70	43.64	88.02	177	Permian volcanics	642	R			
293	294.6	2	Sakmarian	451	50	70	43.49	91.48	177	Permian volcanics	647	R			
294	293.6	2.3	Sakmarian	451	50	70	43.42	92.07	177	Permian volcanics	652	R			
295	293.6	2.2	Sakmarian	451	51	71	43.44	91.41	177	Permian volcanics	650	R			
296	344	3	Visean	450	36	22	45.50	84.50	178	Carboniferous volcanics	FYD1	A			
297	336	3	Visean	450	36	24	45.90	85.00	178	Carboniferous volcanics	HS13	D			
298	307.26	0.11	Moscovian	302	14	14	48.07	37.79	179	Isaevsky	n1 coal				P
299	310.55	0.1	Moscovian	302	12	13	48.05	37.79	179	Gorlovsky	nm3 coal				P
300	312.01	0.08	Moscovian	302	10	13	48.36	37.24	179	Mar'evsky	13(a) coal				P
301	312.18	0.07	Moscovian	302	11	14	48.13	38.27	179	Mar'evsky	13(b) coal				P
302	312.23	0.09	Moscovian	302	11	14	48.13	38.35	179	Mar'evsky	11 coal				P
303	313.16	0.08	Moscovian	302	10	14	48.45	38.80	179	Kamensky	k7 coal				P
304	314.4	0.06	Moscovian	302	9	14	48.45	38.80	179	Krasnodonsky	k3 coal				P
305	328.14	0.11	Serpukhovian	302	7	3	47.78	37.25	179	Samarsky	c11 coal				P
306	342.01	0.1	Visean	302	8	-17	47.73	37.65	179	Sty'lsky	c1ve2				P
307	345	0.08	Visean	302	9	-21	47.72	37.65	179	Glubokinsky	c1vc				P
308	345.17	0.07	Visean	302	9	-21	47.73	37.65	179	Glubokinsky	3/2002				P
309	357.26	0.08	Tournaisian	302	13	-37	47.64	37.89	179	Karakubsky	5/2002				P
321	335.99	0.39	Visean	202	-46	-104	-28.50	-68.90	66	Punta del Aqua Formation	O7VD-36	A			
322	319.57	0.39	Bashkirian	202	-45	-96	-28.50	-68.90	66	Lower Rio del Penon Formation	07VD-35				P
323	310.63	0.37	Moscovian	202	-45	-86	-28.50	-68.90	66	Middle Rio del Penon Formation	RPTIgn-1		I		P
324	310.93	0.37	Moscovian	202	-45	-86	-28.50	-68.80	66	Patquia Formation	GPIgn-1		I		P
325	309.89	0.08	Moscovian	202	-46	-86	-29.50	-68.80	66	Patquia Formation	07VD-26		I		P
326	318.79	0.38	Bashkirian	202	-46	-97	-30.00	-68.90	66	Guandacol Formation	07VD-13				P
327	315.46	0.37	Bashkirian	202	-47	-93	-30.00	-68.90	66	Tupe Formation	07VD-5				P
328	312.82	0.38	Moscovian	202	-47	-90	-30.00	-68.90	66	Tupe Formation	07VD-6				P
329	310.71	0.38	Moscovian	202	-46	-88	-30.00	-68.90	66	Patquia Formation	07VD-8				P
330	296.09	0.35	Asselian	202	-49	-74	-30.00	-67.60	66	Las Colinas Formation	PPAsh-1				P
331	304	3	Kasimovian	601	27	67	40.54	117.75	180	G' layer bauxites	LT-1				P
332	296	2	Asselian	601	34	71	40.05	113.15	180	'G' layer bauxites	D01				P
333	316	5	Bashkirian	601	16	64	40.09	119.59	180	'G' layer bauxites	ZY-2				P
334	303	2	Gzhelian	601	28	66	39.95	115.93	180	'G' layer bauxites	WYS-1				P
335	308	17	Moscovian	601	22	66	41.11	120.66	180	'G' layer bauxites	08065-1				P
336	311	7	Moscovian	601	26	61	39.49	111.41	180	'G' layer bauxites	P02				P
337	302	15	Gzhelian	601	30	63	37.87	113.65	180	'G' layer bauxites	T14				P
338	279.8	2.5	Kungurian	401	56	57	46.47	89.38	181	Batmayineishan Formation	K28-5-1	R			
339	276	3	Kungurian	450	55	57	46.38	89.45	181	Batmayineishan Formation	k28-16-1	R			
340	276.2	3.1	Kungurian	450	55	57	46.33	89.48	181	Batmayineishan Formation	k28-18-1	R			
341	328.9	1.9	Serpukhovian	451	33	54	42.70	94.20	182	Haerjiawu Formation	DH103	A			
342	331.5	2.3	Visean	451	34	53	42.80	94.25	182	Haerjiawu Formation	ML05	D			
343	295	2.8	Sakmarian	580	50	49	42.04	81.63	183	Xiaotilanlike Formation	NJ1-004	R			
344	286.8	0.5	Artinskian	467	47	50	42.91	82.87	184	Wenquan rhyolites	WQ09-2	R			
345	298.05	0.44	Asselian	302	31	19	53.50	56.35	185	Usolka section	01DES-202				P
346	298.49	0.13	Asselian	302	32	-74	53.50	56.35	185	Usolka section	01DES-194				P
347	299.22	0.13	Gzhelian	302	31	18	53.50	56.35	185	Usolka section	01DES-144				P
348	298.92	0.52	Gzhelian	302	31	19	53.50	56.35	185	Usolka section	01DES-143				P
349	296.6	1.8	Asselian	451	52	67	43.68	88.05	186	Baiyanggou olistostrome	2891	R			
350	306.5	1.5	Kasimovian	450	39	25	45.03	89.12	187	BN Formation	09BJE-79	R			
352	316	4	Bashkirian	461	34	32	44.80	81.40	188	Dabate	06XJ04	D			
353	375	3	Frasnian	450	35	27	45.00	90.00	189	Ashele Rhyolite	?	R			
354	401	3	Emsian	450	40	25	45.00	90.00	189	Keyinbulake Rhyolite	?	R			
355	296	4	Asselian	601	32	72	39.95	115.92	190	Hongmioaling Formation	T3S-1				P
356	324	4.9	Serpukhovian	459	33	34	43.18	84.56	191	Laerdundaban volcanics	TS04	T-A			
357	316	2.5	Bashkirian	459	36	34	43.18	84.56	191	Yuximolegai rhyolite	TS1618	R			
359	337.2	4.1	Visean	450	38	25	45.17	87.42	192	Carboniferous tuff	Dixi-14	R			P
360	307.1	6.3	Moscovian	450	42	33	44.37	113.26	193	Baolige Formation	NM08-140	R			
361	308.9	1.8	Moscovian	455	64	84	44.41	113.19	193	Baolige Formation	NM10-25	R			
362	331.7	3.8	Visean	450	36	28	45.00	86.50	194	Well Moshen-1	J08-14	A			P
367	250.2	2.4	Olenekian	601	41	108	42.53	110.63	195	Hugiert–Chaganhadamiao proto-a	SLS03	A			

369	289.4	5.5	Artinskian	467	44	48	41.70	79.69	196	Xiaotikanlike Formation	?	R			
370	307.2	1.3	Moscovian	450	42	33	43.93	85.10	197	Arbasay Formation	TS-09-9	R			
371	286.7	2.1	Artinskian	451	51	77	42.48	91.82	198	Shaerhu alkaline complex	?	R			
372	241.2	4.6	Ladinian	60301	-5	101	19.75	100.25	199	Doi Yao Volcanics	TL-1-B	A			
373	241.7	2.9	Ladinian	60301	-5	101	20.00	100.38	199	Doi Yao Volcanics	TL-31-B	A			
374	238.3	3.8	Ladinian	60301	-2	100	20.25	100.38	199	Doi Khun Ta Khuan Volcanics	TL-32-B1	R			
375	281	4.3	Kungurian	601	36	92	42.74	114.65	200	unnamed	09WJ-I-001	A			
376	343	3	Visean	801	-43	143	-31.77	151.01	95	Burnewang Ignimbrite	465-13A		I	P	
378	328.1	2.9	Serpukhovian	801	-41	148	-31.54	150.79	95	Unnamed Ignimbrite M4	488-16C		I	P	
379	320.5	2.8	Bashkirian	801	-43	150	-32.18	150.97	95	Kewell Creek Volcanics	284-2		I	P	
380	347.2	1.6	Tournaisian	461	33	21	44.20	81.60	201	Eastern Taerbieke		A			
381	367	3	Famennian	453	62	45	43.03	106.99	202	Devonian volcanics	AJW-03-148	D	I	P	
382	354	2	Tournaisian	453	55	43	43.03	106.99	202	Carboniferous volcanics	AJW-04-246	A		P	
383	346	8	Visean	453	54	38	43.03	106.99	202	Carboniferous volcanics	AJW-04-270	A			
384	339	2	Visean	430	54	34	45.03	106.99	202	Carboniferous volcanics	AJW-03-221	R		P	
385	339	2	Visean	430	55	33	46.03	106.99	202	Carboniferous volcanics	AJW-03-192	D		P	
386	345	2	Visean	430	57	33	47.03	107.99	202	Carboniferous volcanics	AJW-03-183	A			
388	282	4	Kungurian	453	55	112	44.50	117.50	203	Xilinhot volcanics	XW04-40	R			
389	289	4	Artinskian	455	59	101	44.50	113.25	204	Baolige Formation	BY04-20	A			
390	287	4	Artinskian	455	58	103	44.33	113.33	204	Baolige Formation	BY04-1	R			
391	306.9	2.2	Kasimovian	430	71	105	50.42	125.73	205	Honghutuhe Group	HH32-82	R			
392	307.5	2.1	Moscovian	430	71	107	49.49	126.43	205	Honghutuhe Group	HH6-15	R			
393	353.1	2	Tournaisian	430	68	52	49.44	125.05	205	Honghutuhe Group	HH39-105	R			
394	353.8	2.4	Tournaisian	430	68	53	49.25	125.08	205	Honghutuhe Group	HH41-108	R			
395	352.5	3	Tournaisian	430	68	51	49.45	125.07	205	Honghutuhe Group	HH36-95	R			
396	272	5.5	Roadian	601	26	88	31.64	117.83	206	Gufeng Formation	Bed 5a			P	
397	312.8	4.2	Moscovian	459	38	34	43.18	84.56	207	Dahalajunshan Formation	TS02	T-A			
398	248.5	6.3	Olenekian	60301	-96	99	21.94	100.93	208	Akelaozhai	20SM-408	A			
399	386.4	9.3	Givetian	459	32	21	43.67	82.25	209	Dahalajunshan Formation	JX9-1	R			
400	323.1	0.6	Bashkirian	430	61	55	43.83	107.67	209	Tsagaan Nuruu Formation	95:3A	R	I	P	
403	300	5	Gzhelian	462	45	30	47.20	82.20	211	Unnamed	1642-1	R			
404	336.5	1.6	Visean	453	61	51	44.96	118.58	212	Baogtou Formation	07TS166			P	
405	342.6	0.76	Visean	457	60	43	44.96	118.58	212	Baogtou Formation	07TS167			P	
406	328.4	0.72	Serpukhovian	453	65	65	44.96	118.58	212	Baogtou Formation	07TS169			P	
407	332.1	3	Visean	453	63	60	44.96	118.58	213	Baogutu Formation	B-71			P	
408	336.3	2.5	Visean	453	61	51	44.96	118.58	213	Xibeikulas Formation	B-3			P	
411	274.8	5.2	Kungurian	64701	-36	104	2.40	104.00	214	Sibu		R		P	
413	290.8	4.1	Sakmarian	315	7	3	51.50	110.00	215	Surkhebt Formation	?	T-R			
414	358.9	5.8	Tournaisian	108	-13	-79	45.30	-66.00	216	Taylors Island Formation	?	R			
415	360.2	0.1	Famennian	154	7	-108	50.75	-115.00	217	Exshaw Formation				P	
416	339.7	0.6	Visean	16106	21	-77	58.50	-128.80	218	Mississippian volcanics	PE00-75	A			
418	352.84	0.29	Tournaisian	16110	58	-78	61.50	-140.00	219	lower Station Creek	08SI-090-1			P	
420	360.6	4.7	Famennian	16107	8	-110	51.14	-119.83	220	Eagle Bay Assemblage		A-D			
421	345.8	5.3	Visean	16107	14	-90	51.24	-119.90	221	Eagle Bay Assemblage		D			
422	363.34	0.39	Famennian	101	6	-110	54.30	-121.00	222	Exshaw Formation	Nordegg Tuff		I	P	
424	287	3	Artinskian	302	19	8	60.00	13.18	223	NW-Saxonian; Wurzen IIA	HBG7, TBN-1		I	P	
425	334.3	1.8	Visean	201	-27	-93	-7.99	-77.64	224	Lavasen Volcanics	WWGA6	R		P	
426	331.7	7.9	Visean	701	-79	-26	-8.00	32.20	225	Draa Sfar		R			
428	252.4	0.3	Changhsingian	602	14	121	30.00	104.00	103	Meishan boundary clay	D3t			P	
430	265.3	0.2	Wordian	602	12	134	31.90	-104.80	102	Bell Canyon Formation	Nipple Hill			P	
431	253.4	0.2	Changhsingian	602	12	134	31.00	120.00	102	Changhsing	MD96-7			P	
432	254.34	0.34	Wuchiapingian	315	24	16	-29.20	151.90	226	Dundee		R-D	I	P	
433	314.9	2.9	Moscovian	801	-44	140	-25.87	150.32	227	Torsdale Volcanics	IRAU613	R	I	P	
434	298.2	5.1	Asselian	801	-48	135	-24.42	150.28	227	Torsdale Volcanics	IWGN145	R	I	P	
435	325	4	Serpukhovian	801	-36	143	-24.89	150.41	227	Torsdale Volcanics	LHT322	R			
436	308.1	5.1	Moscovian	801	-47	136	-25.31	150.36	227	Torsdale Volcanics	RSC171	R	I	P	
437	311.6	3.8	Moscovian	801	-46	138	-25.71	150.35	227	Torsdale Volcanics	RSC218A	R	I	P	
438	308.2	5	Moscovian	801	-47	136	-25.15	150.29	227	Camboon Volcanics	BB2535	R	I	P	
439	297.1	3.3	Asselian	801	-47	135	-24.00	150.12	227	Camboon Volcanics	IWGG809	R	I	P	
440	321.3	4.4	Bashkirian	801	-42	151	-32.50	151.50	228	Mirannie Ignimbrite	Z845		I	P	
441	274.1	3.4	Kungurian	801	-61	150	-32.50	151.50	228	Lakes Road Rhyolite	Z772	R			
442	260.57	0.07	Capitanian	178	19	-38	42.00	-113.50	229	Meade Peak Formation	10VD-2			P	
443	281	8	Kungurian	178	9	-49	35.50	-117.75	230	El Paso Mountains andesite	And-A	A			
444	328.5	2.7	Serpukhovian	101	-15	-62	35.00	-91.00	231	Sabine	?			P	
445	320.7	2.5	Bashkirian	101	-16	-54	35.00	-91.00	231	Sabine	?			P	
446	266.31	0.82	Wordian	2901	-49	-49	-34.70	-68.50	232	Yacimiento Los Reyunos Formation	SR26		I	P	
449	296.2	7.2	Asselian	305	-1	4	43.50	3.00	233		Ci5			P	
450	297.9	5.1	Asselian	305	0	4	44.20	3.80	233		Ci7			P	
451	295.3	4.8	Asselian	305	0	6	43.50	3.50	233		Ci9			P	
452	296	6.8	Asselian	305	1	5	44.40	4.80	233		Ci12			P	
453	297.4	4.4	Sakmarian	305	0	4	44.00	4.50	233		Ci13			P	
455	295	4	Sakmarian	305	3	6	46.00	7.00	234		CN 118			P	
456	307	2	Kasimovian	305	-2	0	46.00	7.00	234	Mont-Blanc	FB 947	R			
457	282	2	Kungurian	375	10	13	50.60	10.60	235	Oberhof	TW 50	R		P	
458	287	2	Artinskian	375	10	13	50.60	10.60	235	Oberhof	TW89A/TW95A/TW97	R			
459	292	2	Sakmarian	375	9	8	50.60	10.50	235	Liebebsteiner Gneis	TW61	R			
460	293	2	Sakmarian	375	9	7	50.60	10.60	235	Mohrenbach	TW4/TW86/TW1	T-A			
461	300.3	0.6	Gzhelian	305	2	0	49.30	8.30	236	Stephanian C	159/71S			P	
462	309.3	4.6	Moscovian	375	7	3	50.80	15.50	236	Upper Westphalian	COT-KR1			P	
463	283.9	2.7	Artinskian	451	50	81	43.20	93.50	237	Sanpu sag	T79	R			
464	292	6	Sakmarian	430	64	118	49.25	125.70	238	Kele complex	2002NJ-2				
465	290.9	4.1	Sakmarian	580	50	55	40.90	81.80	239		YM30-1	R			
466	286.6	3.3	Artinskian	580	50	60	40.75	81.90	239		YM5-8	R			
467	272	3	Roadian	616	-34	82	33.13	95.70	240	Nayixiong Formation	TB060-6	A		P	
468	270	4	Roadian	616	-30	83	33.12	95.74	240	Nayixiong Formation	TB071-2	R			
469	262	4	Capitanian	616	-20	88	33.11	95.74	240	Nayixiong Formation	TB071-3	A			
470	273.3	2.3	Kungurian	616	-35	82	33.12	95.69	240	Nayixiong Formation	TB066-2	D			
471	238.6	3	Ladinian	616	0	93	33.12	95.69	240	Nayixiong Formation	TB066-3	D			
472	275.4	0.8	Kungurian	616	-39	81	33.09	95.71	240	Nayixiong Formation	TB065-1	A		P	
473	273	0.76	Kungurian	616	-35	82	33.12	95.73	240	Nayixiong Formation	TB0123-1	R			
476	300	4	Gzhelian	302	5	-30	52.00	20.90	241	Gory Suche Rhyolitic Tuff		R	I	P	
477	388.2	3.2	Eifelian	315	0	-72	49.83	7.35	242	Hunsruck Slate	HU-38	R		P	
478	309.8	1.5	Moscovian	308	-11	1	47.10	11.85	143	Grierkar	GKAR	R-D			
479	304	3	Kasimovian	308	-8	3	47.00	11.80	143	Venntal	VE1	R			
480	280.5	2.6	Kungurian	308	-1	22	47.00	11.82	143	Pfitscher Joch	PEJ	R			
481	279	4.8	Kungurian	308	-1	22	47.15	12.10	143	Schonach	SNA1	A			
482	356.5	1.4	Tournaisian	304	-15	-55	37.80	-7.80	243		VA12	R-D			
483	354.9	2.5	Tournaisian	304	-15	-54	37.80	-7.80	243		VA15	R-D			
484	356.4	1.5	Tournaisian	304	-15	-55	37.80	-7.80	243		VA16	R-D			
485	288	4	Artinskian	302	17	6	59.60	10.17	244	Vestfold	T1	T			

486	285	7	Artinskian	302	18	9	59.60	10.17	244	Vestfold	T2	T			
487	274	3	Kungurian	302	22	14	59.60	10.17	244	Drammen	R-lava	R	I		P
488	286	4	Artinskian	604	-3	93	18.80	102.70	245		HSD01	A			
489	283	4	Kungurian	604	-3	96	18.80	102.70	245		HSD04				P
490	324	2.8	Serpukhovian	450	34	30	45.90	84.30	246	Hatu area	HTP57				P
491	324.9	3.4	Serpukhovian	450	34	30	45.90	84.30	246	Hatu area	HTP65				P
492	363.2	5.7	Famennian	461	30	25	44.25	81.55	247	Dahalajunshan Formation	04A5	A			
493	339.4	4.8	Visean	450	38	21	47.00	86.45	248	Sawur		A			
495	281	2	Kungurian	801	-45	137	-16.67	144.66	249	Lumma		R			
496	242	1	Ladinian	154	36	-37	58.10	-125.50	250	Kutcho Assemblage		R			
497	242	1	Ladinian	16104	38	-44	58.10	-127.50	250	Kucho Assemblage		R			
498	325.1	3	Serpukhovian	101	-18	-54	59.87	-125.69	251	Mt. Francis	MM 197-35-1a				P
499	336.4	3.6	Visean	16106	22	-72	59.60	-130.50	252	Ram Creek Complex	96JN34-5	D			P
500	332	4	Visean	16104	28	-76	59.50	-131.40	252	Ram Creek Complex	96JN9-12	D			P
501	376	3	Frasnian	18103	22	-109	67.00	-171.83	253			R			
502	327.9	2	Serpukhovian	283	-53	-116	-39.83	-69.33	254	Arroyo del Torreon Formation		R-D			
503	284.9	1.6	Artinskian	308	-2	17	46.66	11.00	255	Maso Argento		R	I		P
504	276.5	1.1	Kungurian	308	1	21	46.66	11.00	255	Gargazzone Formaion		R			P
505	278.4	1.5	Kungurian	308	0	21	46.66	11.00	255	Monte Luco Formation		R-D	I		P
506	299.9	0.9	Gzhelian	302	13	-4	58.95	9.90	256	Brunlanes			I		P
507	298.9	0.7	Asselian	302	14	-2	59.00	9.67	256	Skien	Porsgrunn				P
508	274	4	Kungurian	302	20	17	56.50	11.50	257	Zechstein Group		R			
511	326.8	4.3	Serpukhovian	375	-4	-7	50.70	13.70	258	Mikulov Ignimbrite	TAVC-1	R	I		P
512	308.8	4.9	Moscovian	375	4	1	50.70	13.70	258	Teplice Ignimbrite	TAVC-2	R	I		P
513	302.9	2.5	Gzhelian	375	7	2	51.17	13.33	258	Leutewitz Ignimbrite	MVC-1	R	I		P
514	296	3	Asselian	375	9	6	51.00	13.34	258	Unkersdorf Formation	DB-1	R			
515	292	13	Sakmarian	375	10	9	51.00	13.53	258	Zauckerode Tuff	DB-2	R			P
516	296.6	3	Asselian	375	9	6	50.67	12.50	258	Planitze Ignimbrite	CB-1	R	I		P
517	294.4	1.8	Sakmarian	375	10	7	51.10	12.67	258	Rochlitz Ignimbrite	NSVC-2	R	I		P
518	305	3	Kasimovian	375	7	3	51.05	15.57	259	Elbe Tuff	Elbe 1				P
519	327.35	0.15	Serpukhovian	302	-1	-6	51.17	19.00	260	Main Ostrava Whetstone	MOW				P
520	297	3.2	Asselian	315	6	3	49.70	7.80	261	Pappelberg Tuff	6212/109				P
521	306	6	Kasimovian	375	2	-1	49.50	7.50	261	Humberg Tuff	6410/1				P
522	306.1	2.8	Kasimovian	375	6	2	51.00	15.70	262	Sady Gome Formation	SG	R-D			
523	291.4	4.7	Sakmarian	334	-1	9	46.90	17.95	263	Kekkut quartz porphyry	Kekkut-4	R			
524	315	1.8	Moscovian	375	-1	2	50.95	15.92	264	Zelezniak Hill		R-D			
525	419.9	3.3	Pridoli	450			46.53	85.67	265	Devonian volcanics	S24TC1	R			
526	418.2	2.8	Lochkovian	450			46.53	85.67	265	Devonian volcanics	S24TC44	A			
527	422.5	1.9	Pridoli	450			46.53	85.67	265	Devonian volcanics	S24A10	R			
528	411.2	2.9	Lochkovian	450			46.53	85.67	265	Devonian volcanics	BE4	A			
529	419.2	3.9	Lochkovian	450			46.53	85.67	265	Devonian volcanics	BE10	A			
530	316	4	Bashkirian	461	34	32	44.60	81.45	265	Dabate	06XJ04	D			
534	411	4	Lochkovian	315	5	-94	48.50	7.20	266		BH39	D-R			
535	409	9	Pragian	801	-45	157	-32.98	146.00	267	Mt Hope Volcanics- Coan Rhyolite	KB502	R			
536	408.6	3.6	Pragian	801	-45	157	-32.98	146.00	267	Mt Hope Volcanics	KB511b				
537	415.3	4.7	Lochkovian	801	-47	138	-32.98	146.00	267	Mt Hope Volcanics- Mt Victor Rhyc	KB426	R			
538	355.8	5.6	Tournaisian	315	0	-51	51.50	7.48	268	Kingsfield Formation	Z830				P
539	352.8	4	Tournaisian	315	0	-47	51.50	7.48	268	Hangenberg Limestone	Bed79				P
540	373.2	1.8	Frasnian	801	-26	-170	-37.25	145.90	269	Snobs Creek Volcanics	GA838	R			
541	375	2	Frasnian	801	-27	-172	-37.38	145.73	269	Cerberean Volcanics	GA842	R-D			
542	404.8	4.8	Emsian	801	-39	166	-33.01	149.70	270	Merrions Formation	94843524	A			
543	406.2	5.1	Emsian	801	-41	164	-33.01	149.70	270	Merrions Formation	94843526	D			
544	405.5	4.6	Emsian	801	-40	165	-33.01	149.70	270	Merrions Formation	94843523	R			
545	406	4.3	Emsian	801	-41	164	-33.20	149.66	270	Merrions Formation-Limekilns	94843525	R			
546	409.6	4.6	Pragian	801	-43	160	-33.01	149.70	270	Merrions Formation	94843522	A			
547	411.5	4.1	Lochkovian	801	-44	159	-33.00	149.67	270	Turondale Formation	93844559B	D			
548	409.5	4.3	Pragian	801	-43	160	-33.01	149.70	270	Turondale Formation	94843520	D			
549	362.8	2.7	Famennian	801	-24	165	-21.43	147.45	271	Silver Hills Volcanics	200701501	R			
550	360.2	2.5	Famennian	801	-27	172	-21.03	147.38	271	Bimurra Volcanics	200701503	R			
551	253	2.4	Changhsingian	801	-64	145	-28.90	151.91	271	Wallangarra Volcanics	200701541	R	I		P
552	361	7	Famennian	108	-14	-80	45.50	-63.50	272	Cherry Hill	17				
553	406	6	Emsian	205	-19	-48	17.00	-89.20	273	Bladen Formation	BZ01	R			
554	358.9	5	Tournaisian	466	24	15	45.40	66.00	274	Taylors Island Formation	NB11-20A	R			
555	373	2	Frasnian	108	-21	-92	41.90	-71.40	275	Wamsutta	DH02-17-98	R			
559	420.2	3.9	Pridoli				52.33	-2.68	276	Upper Whitcliffe Formation					P
562	417.6	1	Lochkovian	101	-17	-125	36.90	-81.10	277	Kalkberg formation					P
563	408.3	1.9	Pragian	101	-18	-107	42.67	-74.75	277	Esopus formation					P
564	391.4	1.8	Eifelian	101	-24	-99	42.67	-74.75	277	Tioga K-bentonite					P
565	381.1	1.3	Frasnian	101	-28	-104	36.50	-83.16	277	Little war gap					P
566	374	1.7	Frasnian	374	-1	-38	50.00	14.50	278	Western Volcanic Belt	GV-20a	R			
567	371	1.4	Famennian	374	1	-41	50.00	14.50	278	Eastern Volcanic Belt	GV-7a	R			
568	359.97	0.46	Famennian	302	5	-49	50.80	20.55	279	Wocklumeria Limestone	A2KQ-5				P
569	358.97	0.11	Famennian	302	5	-49	50.80	20.55	279	Wocklumeria Limestone	A2KQ-1				P
570	358.89	0.2	Tournaisian	302	5	-49	50.80	20.55	279	above Hangenberg Shale	A2KQ-2				P
572	411.5	1.3	Lochkovian	315	6	-94	57.40	-2.80	280	Milton of Noth Andesite	RM-15XX	A			
573	405	5	Emsian	305	-20	-6	45.50	0.50	281	Porphyroides	7615	R			
574	366	5	Famennian	305	-5	40	45.67	4.75	282	Brevenne		R			
576	407.3	9.2	Pragian	401	46	11	47.99	88.14	283	Kangbuticbao Formation	Tmp—1	R			
577	356.2	2	Tournaisian	461	32	23	44.30	81.75	284	Axi	AX12	A			
578	408.7	5.3	Pragian	401	46	11	47.99	88.14	285	Tiebao formation	Abg53	R			
579	412.6	3.5	Lochkovian	401	45	12	47.99	88.14	285	Kangbutiebao Formation	Abg178	R			
580	406.7	4.3	Emsian	401	46	11	47.99	88.14	285	Kangbutiebao Formation	Tm51	R			
581	368	3	Famennian	601	11	57	33.58	110.65	286	Wuguan complex	WG03-5	A			
582	396.3	3.3	Emsian	430	69	5	44.53	97.81	287	Tseel terrane	M3883	R			
583	397	3.2	Emsian	430	69	3	44.92	97.83	287	Tseel terrane	M3884	R			
584	365.6	1.6	Famennian	401	39	16	47.13	89.30	288	Aletaizhen Formation		R			
585	369.7	4.9	Famennian	461	30	26	44.00	82.58	289	Yining	TW-6-1	R			
586	363.4	2.5	Famennian	461	30	26	44.00	82.58	289	Yining	TW-13-1	R			
587	388	6.7	Eifelian	401	45	13	46.12	90.48	289	Jiangzeer Kuduke Formation		B-A			
588	403.5	2.1	Emsian	580	24	36	42.18	85.35	290	Liushugou volcanics	XJ045-2	R			
589	403.9	2	Emsian	580	25	36	42.22	85.72	290	Liushugou volcanics	XJ050	D			
590	356	8	Tournaisian	601	14	52	32.50	113.39	291	Zhupeng	DH03-1				
593	423.2	1.8	Ludfordian				35.97	94.91	292	Maoniushan Formaion	B743-2	R			
594	408.2	2.4	Pragian	456	20	42	35.94	94.86	292	Maoniushan Formaion	B820-1	R			
595	404.9	4.8	Emsian	456	20	43	35.96	94.84	292	Maoniushan Formaion	B705-1	R			
596	399.6	2.8	Emsian	401	46	10	35.93	94.98	292	Maoniushan Formaion	B656-1	R			
597	353.9	6.5	Tournaisian	459	32	23	43.43	81.90	293	Dahalaunshan Formation	10TK05-2	A			
598	356.3	4.4	Tournaisian	459	31	25	43.40	81.89	293	Dahalaunshan Formation	10TK08-2	A			P
599	396.7	1.4	Tournaisian	401	45	10	47.94	88.11	294	Kangbutiebao Formation	10DG-1A	R			
600	394	6	Eifelian	401	45	11	47.35	89.19	294	Kangbutiebao Formation	KKTL-1A	R			

604	415.5	5.8	Lochkovian	315	7	-99	55.80	-4.25	295	Northern Midland Valley, ORS	ignimbrite			I	P
605	412.6	5.7	Lochkovian	315	-4	5	55.80	-4.25	295	South Midland Valley, ORS volcani	PE4	R-D			
607	411.9	1.9	Lochkovian	315	5	-94	55.80	-4.00	295	The Tinto Felsite	PE27				
608	408	2	Pragian	315	5	-91	55.80	-2.00	295	Southern Upland-Northern part ORS	volcanics				
609	287	5	Artinskian	375	10	13	50.60	10.75	296	Ilmenau Formation	98002	R			
610	271	8	Roadian	178	14	-40	43.00	-111.70	297	Xilmiao Group		R			
611	272	1.8	Roadian	701	-52	-24	-20.73	14.25	298	Gai-As formation					P
612	265	2.5	Capitanian	701	-48	-20	-20.73	14.25	298	Gai-As formation					P
613	241.07	0.13	Ladinian	307	11	22	45.95	9.00	299	Meride Limestone	RS09/4				P
614	239.51	0.15	Ladinian	307	11	21	45.95	9.00	299	Meride Limestone	RS09/5a				P
615	240.63	0.13	Ladinian	307	11	22	45.95	9.00	299	Meride Limestone	Ca31				P
616	201.58	0.28	Rhaetian	201	-2	-44	-6.18	-77.85	300	Aramachay Formation	86				P
618	230	2	Carnian	522	1	29	39.25	33.75	301		OK2	R			
619	229	2	Carnian	522	2	29	39.25	33.75	301		OK4	R			
624	240.91	0.26	Ladinian	308	11	23	46.67	9.90	302	Prosanto Formation	DUCAN-I				P
625	239.89	0.21	Ladinian	308	11	23	46.67	9.90	302	Altein Formation	DUCAN-II				P
626	242.4	0.2	Anisian	307	10	25	46.50	12.00	303	Bivera Formation	BIV-1				P
627	242.8	0.2	Anisian	307	10	25	46.50	12.00	303	Latemar	LAT30				P
628	241.2	0.8	Ladinian	307	10	24	46.50	12.00	304	Buchenstein Beds					P
629	238	0.7	Ladinian	307	11	23	46.50	12.00	304	Buchenstein Beds					P
630	247.6	5.8	Olenekian	522	-1	35	38.10	32.40	305	L. Triassic metavolcanics	1196/21	T-A			
631	251.6	5.3	Induan	522	-2	36	38.10	32.40	305	L. Triassic metavolcanics	1199	T-A			
632	205.7	0.15	Rhaetian	201	-5	-45	-6.30	-77.90	306	Pucara Group	LP2010-3a				P
633	205.4	0.09	Rhaetian	201	-4	-45	-6.30	-77.90	306	Pucara Group	LP2010-1b				P
634	205.3	0.14	Rhaetian	201	-4	-45	-6.30	-77.90	306	Pucara Group	LP2010-1d				P
635	203.71	0.11	Rhaetian	201	-3	-45	-6.30	-77.90	306	Pucara Group	LM4-23B				P
636	202.38	0.16	Rhaetian	201	-3	-44	-6.30	-77.90	306	Pucara Group	LM4-50/51				P
637	202.16	0.27	Rhaetian	201	-3	-44	-6.30	-77.90	306	Pucara Group	LM4-58/59				P
638	201.87	0.17	Rhaetian	201	-2	-44	-6.30	-77.90	306	Pucara Group	LM4-76/77				P
639	201.51	0.15	Rhaetian	201	-2	-44	-6.30	-77.90	306	Pucara Group	LM4-86				P
642	239.7	2.2	Ladinian	2901	-45	-46	-32.95	-69.20	307	Potreillos Formation	PTR 1				P
643	230.3	2.3	Carnian	2901	-46	-48	-32.95	-69.20	307	Potreillos Formation	PTR 2				P
644	243.8	1.9	Anisian	202	-42	-43	-30.86	-69.17	308	Cerro Puntudo Formation	CP-01				P
648	215.9	0.82	Norian	201	-23	-41	-17.75	-69.90	309	Chocolate Formation	09FB88			I	P
649	266.8	7.1	Wordian	202	-44	-48	-31.30	-69.30	310	Del Salto Formation	RB-01	A			
650	238	5.4	Ladinian	202	-43	-45	-31.50	-69.30	310	Corral de Piedra Formation	RB-03				P
651	246.4	1.1	Anisian	202	-42	-43	-31.50	-69.30	310	Cienaga Redondo Formation	RB-06	R			
652	243	5	Anisian	2901	-45	-45	-33.00	-69.30	311	Rio Mendoza Formation	CUY-7			I	P
653	213	1.7	Norian	101	18	-43	34.30	-107.50	312	Black Forest Bed					P
655	213	5	Norian	16124	48	-50	59.24	-135.48	313	Glacier Creek		R			
656	242	1	Ladinian	16113	37	-39	58.15	-128.50	314	Kutcho Creek	KC-GC-01	R			
657	246	7	Anisian	16113	37	-37	58.15	-128.50	314	Kutcho Creek	KC-GC-04	R			
663	226	3	Norian	401	75	78	50.28	106.60	315	Kataev Formation	5167	R			
664	270	3	Roadian	401	58	18	69.33	88.24	316	Maslov Diatreme rhyolite	19F-57	R			
665	247	3	Anisian	602	21	114	28.50	99.00	317	Pantiange rhyolite	SJ22	R			
666	246	3	Anisian	602	22	114	28.50	99.00	317	Pantiange rhyolite	SJ33	R			
667	242	3	Ladinian	602	26	112	27.30	99.25	317	Lower Cuiyibi rhyolite	SJ4	R			
668	239	3	Ladinian	602	30	111	27.30	99.25	317	Upper Cuiyibi rhyodacite	SJ44	R-D			
669	234.8	2.4	Carnian	60401	34	104	23.75	100.50	318	Songjiapo Formation	SJP0901-0912	R			
670	228.4	2.1	Carnian	590	12	76	37.87	75.28	319	unnamed	KL021	R			
672	213.6	3.8	Norian	457	46	121	35.10	102.00	320	Dashui gold deposit	DS-1			I	P
673	222	1.2	Norian	601	48	146	41.90	127.00	321	Naozhigou formation	TH7-10	R			
676	252.6	2.8	Changhsingian	602	15	118	26.70	103.80	322	Chahe Assemblage	GWC68a				P
677	253	3	Changhsingian	616	-12	93	33.10	95.68	323	Nayixiong Formation	TB060-6	A			
678	254	4	Changhsingian	616	-12	93	33.09	95.90	323	Nayixiong Formation	TB071-2	R			
679	241.3	2.4	Ladinian	601	41	108	36.94	107.45	324	Chang-7 Member of Yanchang Form	L-1（Luo-36）				P
680	239.7	1.7	Ladinian	601	41	110	35.89	107.97	324	Chang-7 Member of Yanchang Form	L-3（Zhuang-211）				P
681	240	1	Ladinian	60301	-4	102	18.08	99.75	325	Mae Man Group	LP-3A	R			P
682	232.9	0.4	Carnian	60301	1	99	20.10	100.42	326	Chiang Khong volcanic suite	Th00-26	R			P
683	242.1	1.2	Anisian	456	42	102	35.58	102.38	327	Gangcha Complex	09XK30	A			
684	230.4	3.1	Carnian	601	48	133	40.91	119.35	328	Shuiquangou Formation	Nangoushang-1	A			
685	254.2	2.5	Wuchiapingian	630	24	122	35.86	136.52	329	Motodo Formation	11110801	A			P
686	253	3.6	Changhsingian	630	21	108	35.86	136.48	329	Motodo Formation	12082601	A			P
687	218.5	1.6	Norian	602	41	113	28.00	99.83	330	Xuejiping Porphyry	X07-20	A			
688	214	4	Norian	616	13	93	33.58	86.04	331	Jianianshan	1695T	R			
689	247.3	1.8	Olenekian	60401	20	109	22.93	102.77	332	Lychun Rhyolite	?	R			
690	220	4	Norian	601	50	139	40.90	119.22	332	Shuiquangou Formation	09BD-3	T			
691	221	3	Norian	601	50	138	40.88	119.21	332	Shuiquangou Formation	09BG-12	A			
692	259.5	0.9	Capitanian	602	2	130	32.33	105.47	103	Lower Wuchiapingian ash horizon	SH01(7)				P
693	260.4	0.8	Famennian	602	1	132	32.33	105.47	103	Lower Wuchiapingian ash horizon	SH03（8）				P
694	257.3	0.3	Tournaisian	602	6	127	32.33	105.47	103	Vocanic-ash layer(Upper Wuchiapi	SH08(15)				P
695	253.2	0.3	Changhsingian	602	14	123	32.33	105.47	103	ash layer	SH27(23)				P
696	252.5	0.3	Changhsingian	602	16	122	32.33	105.47	103	ash layer	SH09(25)				P
697	252.2	0.4	Changhsingian	602	16	122	32.33	105.47	103	ash layer	SH10(27)				P
698	252.5	0.2	Changhsingian	602	16	122	32.33	105.47	103	ash layer	SH32(29)				P
699	230	2	Carnian	60301	3	97	22.50	100.50	334	Manghuai Formation	DX-92	R			
700	231	5	Carnian	60401	40	101	24.50	100.33	334	Manghuai Formation	02DX-95	R			
701	246	2	Anisian	602	14	119	22.28	106.71	335	Beisi Formation	D1070	D			
702	250	2	Olenekian	602	9	121	21.68	107.62	335	Banba Formation	BAN8	R			
703	220	4	Norian	60301	7	104	19.32	100.23	336	Chiang Khong-Lampang-Tak Volcan	16′ /10(1)	R			
704	223	6	Norian	60301	6	102	20.31	100.28	336	Chiang Khong-Lampang-Tak Volcan	14/2(1)				
705	210.4	1.9	Norian				90.50	35.00	337	high-Mg andesite/dacite suites	2406a	D			
706	210.9	1.6	Norian				90.50	35.00	337	high-Mg andesite/dacite suites	2406b	D			
707	211	2	Norian				90.50	35.00	337	high-Mg andesite/dacite suites	2121--6	A			
709	227.9	1.5	Carnian	603	4	94	25.90	99.83	338	Xiangcheng volcanics	XC09	D			
710	230.6	1.3	Carnian	602	45	107	31.20	99.54	338	Changtai volcanics	GB47	D			
711	230	2.5	Carnian	602	45	106	31.08	99.31	338	Changtai volcanics	GB89	R			
712	216.1	4.5	Norian	616	12	93	33.73	87.75	339	volcanics above Xiaochaka Formati	OP-2				P
713	219	1	Norian	453	51	166	45.07	129.30	340	Zhangguangcailing Group	HDY21-1	D			
714	317	2	Bashkirian	453	73	92	45.21	129.29	340	Zhangguangcailing Group	HDY3-1	R			
715	243.5	1.7	Anisian	456	45	95	36.83	95.25	341		DG25-4	R			P
716	217	1	Norian	454	49	154	43.67	131.13	342	Tuopangou Formation	HS13-1	R			
717	214	2	Norian	454	49	156	43.72	131.13	342	Tuopangou Formation	HS14-1	R			
718	208	1	Rhaetian	454	49	158	44.00	131.10	342	Tianqiaoling Formation	HS15-1	R			
723	214	3	Norian	453	51	155	45.73	129.29	343	Zhangguangcailing Group	HDL1-2	R			
724	211	2	Norian	453	50	156	45.08	129.26	343	Zhangguangcailing Group	HDY16-1	A			
725	228	2	Carnian	453	49	147	45.08	129.26	343	Qinglongtun Formation	HB31-2	A			
726	285	2	Artinskian	307	-2	14	45.60	8.30	344	Sesia Valley Volcanics	R16	R			
727	281.7	2.6	Kungurian	307	-1	17	45.50	8.40	344	Sesia Valley Volcanics	R4	R			
728	282.86	0.13	Kungurian	305	3	17	43.65	3.30	345	Salagou Formation (Octon Membe	T12				P

729	283.53	0.1	Artinskian	305	3	16	43.66	3.33	345	Salagou Formation (Octon Membe	T9				P
730	284.46	0.1	Artinskian	305	3	15	43.67	3.36	345	Salagou Formation (Octon Membe	T2				P
731	284.4	0.07	Artinskian	305	3	15	43.67	3.35	345	Salagou Formation (Octon Membe	T1				P
732	290.96	0.19	Sakmarian	305	1	10	43.69	3.35	345	Viala Formation	III				P
733	293.85	0.1	Sakmarian	305	0	7	43.69	3.18	345	Tulieres-Loiras Formation	VI				P
734	293.94	0.08	Sakmarian	305	0	7	43.69	3.17	345	Tulieres-Loiras Formation	V				P
735	270.2	2.7	Roadian	601	22	62	41.77	110.43	346	Suji Volcanic Sequence	NM08-42	R			
736	268	3.8	Wordian	601	37	96	41.75	110.55	346	Suji Volcanic Sequence	NM08-58	D			
737	315.3	1.6	Bashkirian	464	36	30	46.30	83.20	347	Carboniferous section	TCA-1				P
738	322.9	5.6	Bashkirian	450	36	31	46.00	87.50	348	Batamayineishan Formation	J08-14-7				P
740	330.4	2.2	Serpukhovian	604	-14	73	18.65	102.15	349	Muang Feuang andesite	LV-5	A			
741	334.9	1.7	Visean	604	-16	67	18.80	102.13	349	Muang Feuang rhyolite	LV-8	R			
742	349.6	1.7	Tournaisian	604	-23	69	18.70	102.13	349	Muang Feuang tuff	LV-14				P
744	315.4	3.8	Bashkirian	60401	-12	75	18.16	101.36	349	Pak Lay basaltic andesite	LV-25	A			
745	247.41	0.12	Olenekian	602	16	121	25.80	107.00	350	Luolou Formation	CHIN47				P
751	247.35	0.11	Olenekian	602	16	120	25.80	107.00	350	Luolou Formation	CHIN52				P
752	246.43	0.17	Anisian	602	17	120	25.80	107.00	350	Luolou Formation	CHIN51				P
753	247.36	0.06	Olenekian	602	15	120	24.60	106.80	350	Luolou Formation	MOW103				P
754	247.25	0.06	Olenekian	602	15	120	24.60	106.80	350	Luolou Formation	MOW104				P
755	246.87	0.09	Anisian	602	16	120	24.60	106.80	350	Transition beds	MOW105				P
756	247.1	0.15	Anisian	602	15	120	24.60	106.80	350	Transition beds	MOW106				P
757	246.78	0.07	Anisian	602	16	120	24.60	106.80	350	Transition beds	MOW107				P
758	246.44	0.14	Anisian	602	16	120	24.60	106.80	350	Transition beds	MOW109				P
759	221	1	Norian	616	11	96	33.80	95.17	351	Batang Group	GS3	D			
785	280	2.5	Kungurian	307	-1	20	45.98	9.85	352	Cabianca Volcanite	VZ1				P
786	291	4	Sakmarian	307	-4	10	45.98	9.85	352	Cabianca Volcanite	VZ3		I		P
787	272	3	Roadian	307	3	20	46.00	9.86	352	Cabianca Volcanite	LG4		I		P
788	270	2	Roadian	307	4	21	46.00	9.86	352	Cabianca Volcanite	LG5		I		P
794	308.1	2.9	Moscovian	306	-11	-3	42.32	8.63	353	Osani Andesite	RC22	A			
795	332	7	Visean	306	-16	-19	42.32	8.63	353	Osani Andesite	RC02	A			
799	290.3	2.4	Sakmarian	306	-4	8	42.36	8.81	353	Monte Estremo Rhyolite	RC08	R			
800	292.5	2.1	Sakmarian	306	-5	7	42.67	9.14	353	Asco-Calenzana pyroclastic series	VZ06	R-D			P
801	286.1	2.5	Artinskian	306	-3	12	42.36	8.81	353	Vecchiu Bridge Rhyolite	RC07	R			
802	284.2	4.1	Artinskian	306	-16	-30	42.35	8.63	353	Culombu Rhyolite	RC06	R			
805	339.2	3.1	Visean	306	-16	-30	42.39	8.69	353	Eltru Rhyolite	RC05	R			
806	278.1	2.3	Kungurian	306	-1	18	42.45	9.02	353	Ht. Asco Rhyolite	RC01	R			
812	248	6	Olenekian	453	35	125	45.70	129.20	354	Zhangguangcailing Group	HDL1-2	R			
813	214	3	Norian	453	51	155	45.70	129.20	354	Zhangguangcailing Group	HDL1-2	R			
814	251	4	Olenekian	453	34	124	45.00	129.20	354	Zhangguangcailing Group	HDY16-1	A			
815	211	2	Norian	453	50	156	45.00	129.20	354	Zhangguangcailing Group	HDY16-1	A			
816	218	1	Norian	453	51	167	45.00	129.20	354	Zhangguangcailing Group	HDY21-1	R			
819	375.55	0.1	Frasnian	101	-26	-103	36.50	-83.02	355	Chattanooga Shale	tephra 01				P
820	375.25	0.13	Frasnian	101	-26	-103	36.50	-83.02	355	Chattanooga Shale	tephra 06				P
821	375.14	0.12	Frasnian	101	-20	-99	42.70	-78.93	355	Rhinestreet Shale	tephra 7.67				P
822	311	2	Moscovian	450	43	33	44.00	89.00	356	Qijiagou Group		D	I		P
823	318.8	2.5	Bashkirian	202	-44	-98	-29.00	-71.17	357	Quebrada Chañaral Section	CPV-12-105	R			
824	303.8	2.7	Kasimovian	202	-46	-84	-29.00	-71.17	357	Quebrada Chañaral Section	CPV-12-12	D			
825	291.4	0.8	Sakmarian	202	-29	-71	-29.00	-71.17	357	Quebrada Chañaral Section	CPV-12-127				P
826	310.87	0.55	Moscovian	101	-11	-46	36.41	-84.18	358	Walnut Mountain	RI-89	R			
827	310.71	0.55	Moscovian	101	-11	-46	36.72	-83.82	358	Fire Clay (Dean)	RK-89	R			
828	311.2	0.55	Moscovian	101	-11	45	37.00	-83.40	358	Fire Clay (Hazard #4)	RH-89	R			
829	310.25	0.55	Moscovian	101	-10	-45	37.22	-82.98	358	Fire Clay (Jack Rock)	RB-89	R			
830	311.38	0.55	Moscovian	101	-12	-45	37.02	-82.69	358	Phillips (No. 7)	RFG-89	R			
831	310.27	0.54	Moscovian	101	-11	44	37.63	-82.39	358	Fire Clay	RV-89	R			
832	311.3	0.55	Moscovian	101	-11	-43	38.05	-81.55	358	"Hernsahw"	RS-89	R			
833	342.1	1.3	Visean	315	0	-39	56.00	3.00	359	Garleton Hills Volcanic Formation	MV69	T			
834	342.4	1.1	Visean	315	0	-39	56.00	3.00	359	Garleton Hills Volcanic Formation	MV18	T			
835	380	5	Frasnian	16101	5	-122	57.02	-130.65	360	Undifferentiated Volcanics		R			P
836	344.8	5	Visean	16101	25	-90	57.01	-131.14	360	Undifferentiated Volcanics		A			P
837	319	5	Bashkirian	16101	27	-61	57.01	-131.14	360	Undifferentiated Volcanics		A			P
838	355	5	Tournaisian	16101	21	-103	57.10	-130.82	360	Undifferentiated Volcanics		R			P
839	312	5	Moscovian	16101	32	-67	57.37	-130.75	360	Undifferentiated Volcanics		D			
840	346.6	2.2	Visean	16104	28	-90	61.70	-131.00	361	Wolverine Lake Group					
841	353	7	Tournaisian	16105	30	-94	64.90	-144.90	362	Blackshell Unit	00ADb5	R			
842	372	5	Famennian	16105	20	-115	64.90	-145.40	362	Blackshell Unit	96ADb20	R			
843	360	5	Famennian	16105	27	-106	64.00	-147.70	362	Totatlanika Schist	98ADb78A	R			
844	365	5	Famennian	16105	25	-111	63.90	-147.70	362	Totatlanika Schist	98ADb80	R			
845	358.6	6.2	Tournaisian	16105	27	-103	63.30	-144.20	363	Jarvis Belt	N484563	R-D			
846	364.2	6.6	Famennian	16105	23	-110	63.20	-143.90	363	Jarvis Belt	N484559	D			
847	372	5.8	Famennian	16105	19	-117	63.20	-144.10	363	Jarvis Belt	N484558	R-D			
848	369	4	Famennian	16105	24	-115	63.60	-150.90	363	Spruce Creek Sequence	91BT-181	R			
849	370	5	Famennian	16105	23	-116	63.60	-150.90	363	Spruce Creek Sequence	84DN24	R			
850	369	3	Famennian	18103	23	-108	65.90	-147.80	364	Fairbanks-Chena Assemblage	87ANK081A	R			
851	341.2	4.8	Visean	16104	34	-83	64.20	-141.80	363	Fortymile River Assemblage	98ADb13C				P
852	347.9	1.7	Tournaisian	16104	32	-90	64.50	-140.50	363	Nasina Assemblage	00M103AA	R			
853	359.5	11	Famennian	16104	25	-104	64.60	-141.30	363	Nasina Assemblage	98ADb23A	R			
854	360.9	2.1	Famennian	16104	24	-105	64.30	-140.50	363	Nasina Assemblage	MLB-89-281	R			
855	253.3	1	Changhsingian	16104	44	-58	64.50	-141.00	363	Nasina Assemblage	98ADb19	R			P
856	256.2	1.1	Wuchiapingian	16104	44	-63	64.60	-141.30	363	Nasina Assemblage	98ADb29	R			
857	256.6	0.9	Wuchiapingian	16104	43	-65	64.50	-141.10	363	Nasina Assemblage	96ADb47A	R			
858	260.2	0.6	Capitanian	16104	44	-58	64.50	-141.00	363	Nasina Assemblage	89-MLB-281				P
859	267	2.7	Wordian	16104	39	-76	64.60	-141.10	363	Nasina Assemblage	98ADb25	R			
860	255.1	0.5	Wuchiapingian	16104	44	-61	64.50	-141.00	363	Klondike Schist	99M-20				P
861	256	0.5	Wuchiapingian	16104	44	-63	64.50	-141.00	363	Klondike Schist	MLB-91-108	R			
862	355.6	2.7	Tournaisian	16104	23	-101	60.10	-131.20	365	Dorsey Complex	99RAS-31-1				P
863	341.9	1.1	Visean	16104	27	-85	60.20	-131.30	365	Ram Creek Complex	RCAS-17B	D			
864	336.4	3.6	Visean	16106	22	-73	59.60	-130.50	365	Ram Creek Complex	96JN34-5	D			
865	325.1	3	Serpukhovian	16104	28	-64	59.80	-131.60	366	Big Salmon Complex	MMI97-35-1A	D			
866	281	2	Kungurian	16104	35	-66	59.60	-131.70	365	Butsih Formation	96-DY-58z	A			
867	372	3	Famennian	16105	20	-117	63.90	-147.25	362	Mystic Creek member	97ADb57	R			
868	357	4	Tournaisian	16105	29	-101	63.80	-147.30	362	Totatlanika Schist	DC98-52-54	R			
869	372	5	Famennian	16105	20	-115	64.85	-145.30	362	Nasina Assemblage	96ADb20	R			
870	361.1	1	Famennian	154	-11	-109	54.30	-121.00	222	Exshaw Formation	Red Deer Tuff	R-D			P
871	363.2	2	Famennian	154	7	-111	52.90	-117.50	222	Exshaw Formation	Maligne Canyon Tuff	R-D			P
872	340.4	5.5	Visean	16106	22	-78	59.40	-130.40	252	Upper Dorsey	97TH47	R			
873	277	4	Kungurian	801	-46	136	-16.70	144.60	366	Nychum volcanics		R	I		P
874	301	5	Gzhelian	801	-42	124	-17.60	144.90	366	Boxwood Volcanics		R-D	I		P
875	278	5	Kungurian	801	-46	137	-17.00	144.80	366	Wakara Volcanic Subgroup		R	I		P
876	281	2	Kungurian	801	-45	137	-17.10	144.90	366	Djungan Volcanic Subgroup		R	I		P
877	280	5	Kungurian	801	-45	138	-17.10	144.90	366	Djungan Volcanic Subgroup		R	I		P

878	288	17	Artinskian	801	-44	131	-17.10	144.90	366	Yongala Volcanic Subgroup		R	I	P
879	290	12	Artinskian	801	-44	130	-17.20	144.90	366	Yongala Volcanic Subgroup		R	I	P
880	284	4	Artinskian	801	-45	135	-17.20	144.90	366	Yongala Volcanic Subgroup		R	I	P
881	301	11	Gzhelian	801	-42	132	-17.20	144.50	366	Jamtin Rhyolite		R-D	I	P
882	304	4	Kasimovian	801	-42	124	-17.30	144.80	366	Boonmoo Volcanic Subgroup		R	I	P
883	306	3	Kasimovian	801	-42	125	-17.30	144.80	366	Boonmoo Volcanic Subgroup		R	I	P
884	308	4	Moscovian	801	-41	125	-16.80	144.70	366	Nightflower Dacite		D	I	P
885	299	6	Gzhelian	801	-40	124	-15.80	145.40	366	Obree Point Volcanics		D		
886	289	2	Artinskian	801	-44	130	-17.70	143.90	367	Bulleringa Volcanic Subgroup		R	I	P
887	290	3	Artinskian	801	-45	128	-17.90	143.60	367	Campbell Mountain Cauldron		R	I	P
888	329	9	Serpukhovian	801	-33	132	-17.50	144.00	368	Wirra Volcanics		R	I	P
889	325	5	Serpukhovian	801	-33	133	-17.00	145.00	368	Eveleigh Volcanics		R	I	P
890	283	3	Kungurian	801	-46	134	-18.00	143.80	367	Brodies Gap Rhyolite		R	I	P
891	323	5	Bashkirian	801	-35	132	-18.40	143.75	367	Corkscrew Rhyolite		R	I	P
892	325	5	Serpukhovian	801	-34	132	-18.40	144.00	367	Mosaic Gulley rhyolite		R	I	P
893	329	9	Serpukhovian	801	-34	132	-18.70	143.80	367	Jinker Creek Rhyolite		R	I	P
894	325	7	Serpukhovian	801	-35	132	-18.70	143.80	367	Bousey Rhyolite		R	I	P
895	274	5	Kungurian	801	-46	132	-15.90	142.50	369			R-D	I	P
896	337	6	Visean	801	-34	127	-19.10	146.30	370	Saint Giles Volcanics		R	I	P
897	342	7	Visean	801	-36	126	-194.00	145.20	370	Oweenee Rhyolite		R	I	P
898	351.2	4	Tournaisian	801	-36	145	-22.00	147.10	371	Lone Sister				
899	401	4	Emsian	801	-37	168	-32.00	148.50	371	Mt. Aubry Gold Deposit				
900	356.5	2.9	Tournaisian	801	-31	166	-21.10	147.20	371	Wirralie				
901	350.4	2.8	Tournaisian	801	-36	143	-21.30	147.30	371	Mt. Coolon				
902	332	4	Visean	305	-10	-21	46.00	2.00	372		Fireclay Cl1			P
903	333	2	Visean	305	-11	-19	44.30	2.60	372		Rhyolite Cl6	R		
904	319	5	Bashkirian	302	0	-6	60.10	10.30	373	Dronningvein Tuffaceous Sediment				P
905	274	4	Kungurian	330	19	14	57.00	7.00	374			R		
906	310.7	7.8	Moscovian	315	1	-2	49.60	7.30	375		Tonstein 6	R-D		P
907	310.1	7.6	Moscovian	315	0	-3	49.60	7.30	375		Tonstein 4A	R-D		P
908	309.7	4.4	Moscovian	315	0	-2	49.60	7.30	375		Tonstein 3	R-D		P
909	308	4	Moscovian	315	1	-2	49.60	7.30	375		Tonstein 1	R-D		P
910	302.9	7.4	Sakmarian	315	3	0	49.60	7.30	375		Tonstein 0	R-D		P
911	294.6	4.3	Sakmarian	315	6	5	49.60	7.10	376	Donnersberg Rhyolite		R		P
912	297.8	7.9	Asselian	315	5	2	49.60	7.10	376	Lohmuhle Tuff		R		P
913	295.7	7.7	Asselian	315	6	4	49.60	7.10	376	Nohfeldon Rhyolite		R		
914	298.7	5.3	Asselian	375	5	2	49.60	7.70	376	Hohlbusch Tuff		R		P
915	297	4.5	Asselian	315	6	3	49.80	7.80	376	Kreuznach Rhyolite		R		P
916	293.9	5	Sakmarian	375	7	6	49.60	7.80	376	Veldenz Rhyolite		R	I	P
917	283	2.5	Kungurian	304	-3	8	41.20	-1.00	377	Autunian		A		
920	308.4	0.7	Moscovian	16102	32	-68	57.40	-126.90	378	Asitka Group		R		
921	375	15	Frasnian	16101	10	-120	58.20	-134.10	379	Stikine Terrane		D		
922	367	10	Famennian	16101	14	-116	57.00	-132.90	380	Ruth Assemblage				P
923	307.7	3.1	Moscovian	202	-56	-69	-30.40	-53.10	381	Harare Group				P
924	298.8	1.9	Asselian	202	-56	-60	-30.50	-53.10	381	Rio Bonito Formation				P
925	292	2.5	Sakmarian	304	-5	0	41.10	-1.20	382	Autunian		A		
926	287	12	Artinskian	304	-3	3	41.20	-2.90	383	Atienza		A		
927	304	1.5	Kasimovian	304	-8	-6	42.30	1.50	384	Coll de Vanses Andesite	A611-10	A		
928	300.4	1.4	Gzhelian	304	-7	-5	42.30	1.70	384	Cadi Ignimbrite	A611-12	R	I	P
929	296.2	3.1	Asselian	304	-5	-2	42.40	1.10	384	Estac Ignimbrite	A611-1	R	I	P
930	296.1	4	Asselian	304	-5	-2	42.40	0.50	384	Erill Ignimbrite	A511-8	R	I	P
931	281.5	2.3	Kungurian	304	-2	12	42.30	2.00	384	Castellar de n'Hug Ignimbrite	A611-22	R	I	P
932	315	2	Moscovian	451	40	59	43.90	88.20	385	Liushugou Formation	TC-23	T	I	P
933	319	3	Bashkirian	933	34	58	43.60	91.00	385	Liushugou Formation	DST-02	T	I	P
934	314.4	3.4	Moscovian	934	38	33	43.90	85.40	386	Arbasay Formation	XJ10-04			P
935	322	4	Bashkirian	455	67	60	46.10	115.90	387	Baoligaomiao Formation	4031	A		
936	320	2	Bashkirian	455	68	59	46.10	115.90	387	Baoligaomiao Formation	1016-2	A		
937	318	4	Bashkirian	455	68	64	46.30	115.90	387	Baoligaomiao Formation	213-5	R		
938	317	2	Bashkirian	455	67	68	45.40	115.60	387	Baoligaomiao Formation	219-6	T		
939	310	2	Moscovian	455	66	86	45.80	115.70	387	Delewula Formation	5335	T		
940	300	2	Gzhelian	455	65	95	45.70	115.80	387	Delewula Formation	211-2	T		P
941	252.49	0.76	Changhsingian	602	13	134	30.80	119.00	388	Dalong Formation	ash 1			P
942	252.2	1.8	Changhsingian	602	13	134	30.80	119.00	388	Yinkeng Formation	ash 5			P
943	251.74	0.77	Induan	602	15	133	30.80	119.00	388	Yinkeng Formation	ash 8			P
944	420.2	2.9	Pridoli				-36.00	149.20	389	Rothlyn Formation	2122509	D		
945	419.6	2.7	Pridoli				-35.40	149.50	389	Captaius Flat Formation	2128517	D		
946	311.2	1.8	Moscovian	801	-52	144	-32.80	151.30	389	Pokolbiu Hills Volcanics	2129181	R	I	P
947	208	4.3	Rhaetian	456	48	111	37.50	91.30	390	Qimautage Volcanics	Set-1	R		
948	222.3	2.3	Norian	456	53	103	37.50	91.30	390	Qimautage Volcanics	Set-2	R		
949	419.2	3	Lochkovian				43.60	125.10	391	Taoshan Rhyolite	LK33-1	R		
950	410	2	Pragian	601	8	64	43.10	125.40	391	Wanyue	IILK02-1	R		P
951	403	3	Emsian	601	11	67	43.10	125.50	391	Wanyue	14YT18-1	R		P
952	208	1	Rhaetian	455	55	161	50.50	131.40	392	Ust_Tyrma Volcanic Complex	C-1132	T-R		
953	226	0.9	Norian	606	-2	90	29.40	91.00	393	Changguo Volcanics	TS4-08	A		
954	237	1.1	Carnian	606	-9	89	29.40	91.00	393	Changguo Volcanics	TS4-09	A		
955	226.6	1.2	Norian	606	-2	90	29.40	91.00	393	Changguo Volcanics	TS4-10	A		
956	226.4	1	Norian	606	-2	90	29.40	91.00	393	Changguo Volcanics	TS4-11	A		
957	392.9	2.7	Eifelian	801	-26	164	-22.40	145.00	394	Unnamed	2130084		I	P
958	305.1	2.6	Kasimovian	801	47	132	-23.70	148.60	394	Unnamed	2130075			P
959	263	3.5	Capitanian	334	12	26	48.90	20.20	395	Gregora Body		R	I	P
960	315	1.8	Moscovian	375	-1	2	51.00	15.80	396	unnamed		R-D	I	P
961	222	2	Norian	178	19	-51	38.10	-118.00	397	Candelaria Formation		R		
964	242.9	2.5	Anisian	283	-55	-45	-42.20	-69.30	398	Taquetren Formation	PO-2a	A		
965	235.8	2	Carnian	2901	-47	-46	-34.90	-68.30	399	Puesto Viejo Group			I	P
969	285.4	6.1	Artinskian	307	-2	16	46.40	11.30	400		STP3	R	I	P
970	303.5	4.4	Gzhelian	308	-8	3	46.70	11.70	400		STP4	R-D	I	P
971	298	1	Asselian	305	4	4	47.60	8.40	401	Wieiach Tuff	1432.26			P
972	295.7	7.7	Asselian	305	5	6	47.60	8.40	401	Wieiach Tuff	1586.52			P
973	367.8	4.4	Famennian	461	30	25	44.10	81.50	402	Dahalajunsha Formation	TS31			P
974	376	3.1	Frasnian	461	30	22	44.10	81.50	402	Dahalajunsha Formation	TS32	A		
975	375.1	3.6	Frasnian	461	30	22	44.10	81.50	402	Dahalajunsha Formation	TS26	A		
976	333.2	9.2	Visean	459	33	28	43.30	81.60	402	Dahalajunsha Formation	TS21	A		
977	359.9	5.1	Famennian	459	30	27	43.40	83.10	402	Dahalajunsha Formation	TS17	D		
978	360.5	3.4	Famennian	461	30	26	44.20	81.60	403	Dahalajunsha Formation	TWE-20	A		
979	316	1.7	Bashkirian	459	35	34	43.60	83.10	404	Dahalajunsha Group	DD-145	D		
980	300.3	0.6	Gzhelian	305	4	2	48.30	8.20	405	Stephanian C tuff	159/71S			P
981	302.9	1.6	Gzhelian	375	3	0	49.40	7.00	405	Upper Stephanian A	COT0/2			P
982	309.5	5	Moscovian	315	2	-4	51.70	7.10	405	Middle Westephalian C	COTH1-1			P
983	310.7	5	Moscovian	315	1	-4	51.70	7.10	405	Upper Westephalian B	COT-Z			P
984	319.5	5	Bashkirian	302	-6	4	49.80	18.30	405	Upper Namurian A	COT479			P

985	324.8	5	Serpukhovian	302	-4	-2	49.80	18.30	405	Upper Namurian A	COT365				P
986	324.6	5	Serpukhovian	302	-4	-2	49.80	18.30	405	Upper Namurian A	COT335				P
987	412.3	2.3	Lochkovian	801	-47	167	-35.40	149.70	406	Toggahnoggra Rhyolite		R-D	I		P
988	413	2.3	Lochkovian	801	-47	150	-35.30	149.70	406	Manar Ignimbrite		D	I		P
989	413.4	2.6	Lochkovian	801	-47	149	-35.50	149.70	406	Kadoona Dacite		D	I		P
990	344	6	Visean	461	34	22	44.50	81.30	407	Dahalajunsha Volcanics	III-20				
991	353	3.5	Tournaisian	461	32	22	44.50	81.30	407	Dahalajunsha Volcanics	III-46				
992	416.7	2.6	Lochkovian				44.20	81.80	408	Jingxi Section	JX10				P
993	386.4	9.3	Givetian	461	32	20	44.20	81.80	408	Jingxi Section	JX9	R			
994	356.2	2	Tournaisian	461	32	24	44.20	81.80	408	Axi Section	AX12	A			
995	263	4	Capitanian	602	-3	132	26.70	104.00	409	Xuanwei Formation	JW-1		I		P
996	252.2	1	Changhsingian	601	26	106	31.40	120.30	410	Meishan Section	MS-A-25		I		P
997	251.7	1	Induan	601	26	106	31.40	120.30	410	Meishan Section	MS-A-28		I		P
998	253.5	1.2	Changhsingian	602	12	123	30.90	105.10	410	Shangsi Section	SS-24		I		P
999	249	0.82	Olenekian	601	28	106	31.50	119.20	410	Dongpan section	DPIO-5-13		I		P
1000	377	2	Frasnian	801	-26	-174	-37.20	146.40	411	Toombullup Ignimbrite	Toom-1		I		P
1001	293.7	3.4	Sakmarian	801	-52	141	-28.50	151.50	412	Alum Rock Conglomerate Rhyolite	Z1592	R	I		P
1002	291.3	2.8	Sakmarian	801	-53	143	-28.60	151.50	412	Alum Rock Conglomerate Rhyolite	Z1558	R	I		P
1003	268.9	2	Roadian	801	-63	146	-32.20	151.00	412	Greta Coal Measures	Z1842		I		P
1004	272.2	3.2	Roadian	801	-62	149	-32.90	151.40	412	Branxton Formation	Z2015		I		P
1005	264.1	2.2	Capitanian	801	-65	145	-32.20	150.90	412	Mullbring Siltstone	Z1793		I		P
1006	253.4	3.2	Changhsingian	801	-59	138	-24.00	148.30	412	Ingelara Formation	Z1899		I		P
1007	249.6	2.2	Olenekian	801	-59	138	-24.00	148.30	412	Ingelara Formation	Z1716		I		P
1008	250	2.2	Olenekian	801	-60	138	-24.70	148.10	412	Black Allea Shale	Z1980		I		P
1009	257.4	2.8	Wuchiapingian	801	-63	-145	-28.30	151.80	412	Rhyolitic Range Beds	Z1557		I		P
1010	255.5	3	Wuchiapingian	801	-63	146	-28.40	166.20	412	Condamine beds	Z1546	R	I		P
1011	222	2	Norian	178	19	-51	38.20	-118.10	397	Candelaria Formation		R	I		P
1022	248	3	Olenekian	202	-35	-39	-23.70	-68.10	413	Peine, Cas Formations			I		P
1023	310	4	Moscovian	302	5	5	49.70	20.70	241	Chelmiec		R-D			
1024	294	3	Sakmarian	453	61	118	45.70	127.50	414	J2t Formation	HB1-1	R			
1025	293	2	Sakmarian	453	60	118	45.20	127.20	414	C2t Formation	HB14-1	A			
1026	293	2	Sakmarian	453	61	118	45.90	127.40	414	J2t Formation	HB17-1	A			
1027	286	2	Artinskian	453	56	124	44.90	129.10	414	P2W Formation	HMD4-1	D			
1028	291	4	Sakmarian	453	59	121	45.50	128.50	414	J2t Formation	HYS1-1	R			
1029	291	3	Sakmarian	453	59	121	45.50	128.50	414	J2t Formation	HYs2-1	R			
1030	314	3	Moscovian	430	70	76	48.50	118.00	415	Budate Group	GW 096	R			P
1031	295	3	Sakmarian	430	65	104	48.50	118.00	415	Budate Group	GW 098	D			
1032	313	6	Moscovian	430	70	79	48.50	118.00	415	Budate Group	GW 097	D			P
1033	312	3	Moscovian	430	70	82	48.50	118.00	415	Budate Group	GW 089	D-R			P
1034	356	5	Tournaisian	430	65	48	48.50	118.00	415	Budate Group	Xi9-1	A			P
1035	349	5	Tournaisian	430	63	43	48.50	118.00	415	Budate Group	Xi9-2	A			P
1036	315	4	Moscovian	430	71	72	48.50	118.00	415	Budate Group	GW 028	A			
1037	298	4	Asselian	430	67	101	48.50	118.00	415	Budate Group	GW 030	A			
1038	271	8	Roadian	601	37	94	42.30	111.00	416	Xilimiao Group	CGA 25	R			
1039	276	10	Kungurian	601	37	92	42.30	111.00	416	Xilimiao Group	CGA 26	R			
1040	305	3	Kasimovian	466	31	34	40.70	69.70	417	Akcha Suite	406301				
1041	301	4	Gzhelian	466	25	33	40.90	70.10	417	Nadak Suite	414802	A			
1042	341.7	2.7	Visean	451	35	43	41.80	91.50	418	Aquishan Formation		R			
1043	363.2	5.7	Famennian	1043	39	34	43.80	87.10	419	Dahalajunshan Formation		A			
1044	296	4	Asselian	601	10	56	39.90	116.00	420	Hongmiaoling Formation	T3S-1				P
1045	310.9	0.8	Moscovian	101	-11	-45	37.40	-83.30	421						P
1046	272	3	Roadian	304	4	12	42.60	-0.50	422		5588	R			
1047	332	4	Visean	305	-10	-21	46.00	2.10	372	Stephanian Formation	CI1				P
1048	334	4	Visean	375	-1	-17	50.50	16.60	423	Bardo Unit Paprotruia beds					P
1049	336.22	0.06	Visean	315	-5	-26	50.30	4.90	424	Livian	W1				P
1050	335.59	0.19	Visean	315	-5	-25	50.30	4.90	424	Warnantian	W8				P
1051	332.5	0.07	Visean	315	-5	-21	50.30	4.90	424	Warnantian	W13				P
1052	328.84	0.16	Serpukhovian	302	-1	-8	49.70	18.30	425	Ostrava Formation	Ludmila				P
1053	328.01	0.08	Serpukhovian	302	-1	4	49.70	18.30	425	Ostrava Formation	Karel				P
1054	324.54	0.46	Serpukhovian	315	-8	-14	52.90	-2.00	426	Arnsbergian	B6				P
1055	317.63	0.39	Bashkirian	315	-8	-4	51.30	4.80	426	Langsettian	T75				P
1056	313.78	0.38	Moscovian	315	-3	-3	51.70	6.90	426	Duckmantian	Z1				P
1057	374	2	Frasnian	61601	-53	129	33.80	84.80	427	Riwanchaka	12RW-1	R			
1058	356	3	Tournaisian	616	-52	92	34.40	85.10	427	Laxiongco	12ND-1	R			
1059	353	3	Tournaisian	616	-51	81	34.40	85.10	427	Laxiongco	12ND-5	R			
1060	372	2	Famennian	1060	-53	132	33.80	84.80	427	Riwanchaka	12RW-6	R			
1061	374.3	1.6	Frasnian	304	-6	-53	37.80	-8.70	428	Volcanic Siliceous Complex	CE1	R-D			
1062	371.1	1.2	Famennian	304	-6	-55	37.70	-8.70	428	Volcanic Siliceous Complex	CE2	R-D			
1063	371.6	1	Famennian	304	-6	-55	37.70	-8.70	428	Volcanic Siliceous Complex	CE3	R-D			
1064	369.5	0.85	Famennian	304	-7	-56	37.70	-8.70	428	Volcanic Siliceous Complex	CE4	R-D			
1065	361.8	4	Famennian	304	-13	-57	38.00	-8.50	428	Volcanic Siliceous Complex	AZI4	R-D			
1066	356.5	1.3	Tournaisian	304	-15	-55	37.90	-8.20	428	Volcanic Siliceous Complex	SJ1	R-D			
1067	356.6	2.1	Tournaisian	304	-15	-55	37.90	-8.20	428	Volcanic Siliceous Complex	SJ2	R-D			
1068	364	1.7	Famennian	304	-12	-56	37.90	-8.20	428	Volcanic Siliceous Complex	FEV1	R-D			
1069	354.6	1.7	Tournaisian	304	-15	-54	37.90	-8.20	428	Volcanic Siliceous Complex	FEV2	R-D			
1070	355.4	2.1	Tournaisian	304	-15	-55	37.80	-7.90	428	Volcanic Siliceous Complex	CO5	R-D			
1071	357.2	2	Tournaisian	304	-15	-55	37.80	-7.90	428	Volcanic Siliceous Complex	IP4	R-D			
1072	365.8	2.1	Famennian	304	11	-56	37.70	-7.70	428	Volcanic Siliceous Complex	SB55	R-D			
1073	356.9	5	Tournaisian	304	-15	-55	37.70	-7.70	428	Volcanic Siliceous Complex	SB8-89.7	R-D			
1074	353.9	1.1	Tournaisian	304	-15	-54	37.70	-7.50	428	Volcanic Siliceous Complex	CH601	R-D			
1075	349	4.9	Tournaisian	721	-22	-22	34.70	-7.50	428	Volcanic Siliceous Complex	CH602	R-D			
1076	360.5	0.8	Famennian	315	0	-57	51.40	7.50	429	Hangenberg Limestone	79	R-D			P
1077	360.2	0.7	Famennian	315	0	-57	51.40	7.50	429	Hangenberg Limestone	70	R-D			P
1078	303	7	Gzhelian	304	-5	-10	43.40	-5.40	430	Niao		A			
1083	315	5	Moscovian	16101	29	-64	56.60	-129.60	431	Hazelton Group	91-120	A			
1084	412.6	3.5	Lochkovian	401	46	12	47.80	88.50	432	Kangbutiebao Formation	ABG 178	R			
1085	408.7	5.3	Pragian	401	46	11	47.80	88.50	432	Kangbutiebao Formation	ABG 53	R			
1086	406.7	4.3	Emsian	401	46	11	47.80	88.30	432	Kangbutiebao Formation	TM 51	R			
1087	393.1	3.4	Eifelian	580	27	36	40.90	87.60	433	Saerming Formation		A	I		P
1088	368.8	3.1	Famennian	401	44	20	44.70	96.30	434	Dundunshan Group	09DDS45-1	R			
1089	316	4	Bashkirian	461	34	32	44.70	81.40	435	Dabate	096XJ04	D			
1090	384.4	2.3	Givetian	108	-23	-93	42.90	-69.20	436	Cashes Ledge Igneous Suite	342-1-1				P
1091	383.9	1.6	Givetian	108	-23	93	42.90	-69.20	436	Cashes Ledge Igneous Suite	342-2-5				P
1092	389.3	4.9	Eifelian	101	-27	-103	39.30	-80.10	437	Marcellus shale	ARM-1				P
1093	389.7	3.9	Eifelian	101	-28	-103	39.30	-80.10	437	Marcellus shale	ARM-2				P
1094	390	1.2	Eifelian	101	-28	-103	39.30	-80.10	437	Marcellus shale	ARM-4				P
1095	386.1	6.3	Givetian	101	-27	-103	39.30	-80.10	437	Onondaga Limestone	ARM-7				P
1096	407.7	0.7	Pragian	375	-13	-3	49.80	11.90	438	Hunsrock Slate	Hans-Platte				P
1097	392.2	1.5	Eifelian	315	0	-73	50.10	6.50	438		Hercules I				P
1100	247.32	0.08	Olenekian	602	16	121	25.80	107.10	439	Guandao Section	PGD Tuff-2				P

1102	215.7	2.3	Norian	601	44	127	33.70	109.40	440	Tianshui Rhyolite		R			
1103	229	2	Carnian	604	31	107	14.70	106.00	441			R			
1107	245.67	0.4	Anisian	2901	-50	-43	-38.00	-67.80	442	Choiyoi Group	YK-328	R	I		P
1108	245.95	0.17	Anisian	2901	-50	-43	-38.00	-67.80	442	Choiyoi Group	YK-329	R	I		P
1109	245.95	0.1	Anisian	2901	-50	-43	-38.00	-67.90	442	Choiyoi Group	YK-330	R	I		P
1110	245.9	0.13	Anisian	2901	-50	-43	-38.00	-67.70	442	Choiyoi Group	YK-331	R	I		P
1111	246	0.22	Anisian	2901	-50	-43	-38.00	-67.70	442	Choiyoi Group	YK-332	R	I		P
1112	210.94	1.02	Norian	2901	-41	-38	-38.00	-67.90	442	Choiyoi Group	YK-445	R	I		P
1113	261.29	0.5	Capitanian	2901	-49	-44	-37.00	-67.30	442	Choiyoi Group	YK-440	R	I		P
1114	260.85	0.42	Capitanian	2901	-49	-44	-37.00	-67.30	442	Choiyoi Group	YK-441	R	I		P
1115	261.05	0.22	Capitanian	201	-19	-35	-7.00	-67.30	442	Choiyoi Group	YK-442	R	I		P
1116	261.08	0.12	Capitanian	2901	-49	-44	-37.00	-67.30	442	Choiyoi Group	YK-443	R	I		P
1117	263.51	0.31	Capitanian	801	-68	145	-34.40	150.90	4	Brougton Formation	PCF16				P
1118	254.86	0.3	Wuchiapingian	801	-69	144	-34.20	150.90	4	Huntley Claystone	PCW266				P
1119	254.1	0.32	Changhsingian	801	-69	143	-34.40	150.50	4	Farmborough Claystone	PCF23				P
1120	253.59	0.3	Changhsingian	801	-69	143	-34.40	150.50	4	Farmborough Claystone	PCF24				P
1121	252.6	0.3	Changhsingian	801	-69	144	-34.20	151.00	4	Bulli Coal	SB27				P
1122	248.23	0.32	Olenekian	801	-70	144	-34.30	150.90	4	Garrie Formation	Bulli 5				P
1123	255.26	0.31	Wuchiapingian	801	-68	145	-33.00	151.50	4	Nobbys Tuff	GA2031204				P
1124	253.25	0.3	Changhsingian	801	-68	145	-33.10	151.40	4	Awaba Tuff	GA2031203				P
1125	252.85	0.32	Changhsingian	801	-68	145	-33.10	151.60	4	Great Northern Coal	Myuna 2				P
1126	252.7	0.3	Changhsingian	801	-68	145	-33.10	151.60	4	Mannering Park Tuff	GA2055445				P
1127	252.78	0.3	Changhsingian	801	68	145	-33.10	151.60	4	Cowper Tuff	GA2166418				P
1128	271.6	0.33	Roadian	801	-62	148	-33.00	151.60	4	Rowan Formation	GA2031207				P
1129	257.43	0.31	Wuchiapingian	801	-67	143	-32.30	151.50	4	Fairford Formation	GA2005149				P
1130	257.04	0.31	Wuchiapingian	801	-67	143	-32.30	150.70	4	Fairford Formation	PCF18				P
1131	253.55	0.3	Changhsingian	801	67	144	-32.30	150.90	4	Upper Pilot A	M4				P
1132	253.38	0.31	Changhsingian	801	-67	143	-32.30	150.70	4	Fassifern Lower Seam	M3				P
1133	256.01	0.3	Wuchiapingian	801	-61	143	-26.20	150.70	4	Tinowan Formation	GA2122736				P
1134	254.34	0.31	Wuchiapingian	801	-61	140	-26.20	149.20	4	Black Alley Shale	GA2122738				P
1135	254.1	0.3	Wuchiapingian	801	-61	140	-26.20	149.20	4	Kaloola Member Bandanna Forma	GA2122742				P
1136	253.81	0.3	Changhsingian	801	-61	140	-26.20	149.20	4	Kaloola Member Bandanna Forma	GA2122744				P
1137	253.59	0.32	Changhsingian	801	-61	140	-26.20	149.20	4	Kaloola Member Bandanna Forma	GA2122747				P
1138	253.32	0.3	Changhsingian	801	-61	140	-26.20	149.20	4	Kaloola Member Bandanna Forma	GA2122748				P
1139	252.54	0.31	Changhsingian	801	-61	140	-26.20	149.20	4	Kaloola Member Bandanna Forma	GA2122750				P
1140	317.3	2.8	Bashkirian	801	-49	142	-32.00	145.00	95	Kewell Creek Volcanics	284-2				
1141	324.8	2.9	Serpukhovian	801	-45	144	-31.90	145.00	95	Unnamed Ignimbrite M4	488-16C		I		P
1142	346.1	1.7	Visean	801	-46	143	-31.90	145.00	95	Curra Keith Tongue	542-1				
1143	296	3	Asselian	315	11	6	52.90	14.70	130	Tuchen		R			
1144	285.6	2.6	Artinskian	344	5	17	44.30	7.90	134	Ligurian Alps	Case Lisetto Metarhyo	R			
1145	258.5	2.8	Wuchiapingian	344	16	28	44.30	7.90	134	Ligurian Alps	Lithozone D	R			
1146	275.4	1.3	Kungurian	453	51	116	44.20	117.60	443		HT06-1	R			
1147	277.7	1.2	Kungurian	453	53	115	44.20	117.60	443		HTM03-1	R			
1148	274.1	2.8	Kungurian	453	51	116	44.20	117.70	443		JG21-43-18	R			
1149	263	2.4	Capitanian	2901	-48	-46	-34.90	-68.40	444	Upper Choiyoi Group	PV01-d		I		P
1150	269	3.2	Roadian	2901	-47	-45	-34.70	-68.60	444	Puesto Viejo Group	PV03d		I		P
1151	260.8	3.2	Capitanian	2901	-47	-45	-34.80	-68.50	444	Puesto Viejo Group	PV06d		I		P
1166	247.49	0.29	Olenekian	602	16	120	25.50	106.90	445	Guaundao Section	PGD Tuff-1				P
1167	247.08	0.31	Anisian	602	16	120	25.50	106.90	445	Guaundao Section	PGD Tuff-3				P
1154	246.5	0.11	Anisian	602	17	120	25.50	106.90	445	Guaundao Section	GDGB Tuff-110				P
1155	252.38	0.22	Changhsingian	202	-40	-40	-29.20	-67.80	446	Talampaya Formation					P
1156	316	0.4	Bashkirian	201	-34	-76	-11.60	-68.10	447	Copacabana Formation	MAN 882.4-883.2				P
1171	354	1.3	Tournaisian	461	33	24	44.00	82.50	448	Dahalajunshan Formation		D			
1158	347.5	1.5	Tournaisian	304	-16	-49	37.80	-6.70	449	Zufre	AD-9023				
1159	353	2	Tournaisian	304	-15	-53	37.60	-7.70	449	Zufre	AD-9027	R			
1160	308	3	Moscovian	305	-2	0	46.20	7.10	234	SD flow	CN 125	D			
1161	295	4	Sakmarian	305	3	6	46.20	7.10	234	SD tuff	CN 118				P
1162	307	2	Kasimovian	305	-1	0	46.20	7.10	234	MB rhyolite	FB 947	R			
1163	287.3	2	Artinskian	580	51	60	40.80	83.30	450	Halahatang Trachydacite	HA2-5379	T-D			
1164	260.2	3.1	Capitanian	344	16	28	44.30	8.10	451	Lisetto Metarhyolite	BARBA-1	R			
1165	328.34	0.55	Serpukhovian	315	-5	-20	53.90	-1.50	452	Bentonite B6	BLL 1976				P
1166	314.37	0.53	Moscovian	315	-4	-8	52.90	-1.20	452	Sub-High Main tonstein	Elt 28155				P
1167	262.5	0.21	Capitanian	43202	73	-50	62.00	150.10	453	Atkan Formation	12VD105				P
1168	269.8	0.08	Roadian	43202	70	-44	62.00	150.10	453	Atkan Formation	12VD108a	R			
1169	303	5	Gzhelian	463	40	26	49.00	76.50	454		Akcopah		I		P
1170	299	6	Gzhelian	463	41	28	49.00	76.50	454		Kopazahtac		I		P
1171	212.8	4.2	Norian	16101	45	-49	56.80	-130.90	455	Stuhini Group	92JL0270	R			
1172	355.1	3.7	Tournaisian	16101	21	-103	57.20	-130.80	455	Stikine Assemblage	91-203	D			
1173	380.5	5	Frasnian	16101	5	-122	56.90	-130.90	455	Stikine Assemblage	91-238				P
1174	311.7	2	Moscovian	16101	32	-67	57.20	-131.00	455	Stikine Assemblage	92JL0266	R			
1175	279.8	3	Kungurian	580	51	69	40.60	84.10	456		579	D			
1176	273.7	3.2	Kungurian	580	54	71	40.90	83.80	456		599	D			
1177	281	3	Kungurian	580	51	67	40.70	83.70	456		5102	D			
1178	276.6	2.7	Kungurian	580	53	71	40.70	84.30	456		5114	D			
1179	292	2	Sakmarian	375	10	8	51.50	12.00	140	Halle Formation	1044	R			
1181	297	3	Asselian	315	9	4	51.60	11.80	140	Wettin Subformation	Wettin	R			
1182	292	3	Sakmarian	375	10	8	51.50	12.00	140	Halle Formation	Ha 2/7	R			
1183	293	3	Sakmarian	315	10	8	51.60	12.00	140	Giebicheustein laccolith unit	Steinmiuhlen	R			
1184	302.6	2.8	Gzhelian	375	7	2	50.70	13.30	258	Olbernhan Formation	BOB-1	R			P
1185	298.3	9.1	Asselian	375	8	4	51.00	12.70	258	Kohren Formation	NSVC-1	R			P
1186	290.2	4.1	Sakmarian	375	11	11	51.10	12.90	258	Wurzen Formation	NSVC-3	R			
1187	286	5	Artinskian	430	62	80	47.00	95.70	457	Teel Formation	U 1127-5	R			
1188	330	3	Serpukhovian	451	36	54	43.80	91.30	458	Dashitou Volcanics	ET4QJ22	R			
1189	292	2	Sakmarian	455	62	109	46.30	120.40	459	Dashizhai Formation	DS-005	R			P
1190	284	3	Artinskian	455	58	115	46.30	120.40	459	Dashizhai Formation	DS-019	R			
1191	290	2	Artinskian	455	61	110	46.30	120.40	459	Dashizhai Formation	DS 042	R			
1192	283	3	Kungurian	455	57	116	46.20	120.40	459	Dashizhai Formation	DS 070	R			P
1193	295	4	Sakmarian	455	63	107	46.20	120.40	459	Dashizhai Formation	DS 079	R			
1194	336.5	2.5	Visean	459	34	26	43.70	82.50	212	Baogutu Formation	07TS166				P
1195	342.6	4.3	Visean	459	34	23	43.70	82.50	212	Baogutu Formation	07TS167				P
1196	328.4	3.7	Serpukhovian	459	33	30	43.70	82.50	212	Baogutu Formation	07TS169				P
1197	298.23	0.31	Asselian	202	-57	-60	-31.50	-53.70	93	Candiota A Lower Rio Bonito Form	CT1				P
1198	297.58	1.4	Asselian	202	-57	-60	-31.50	-53.70	93	Candiota C Lower Rio Bonito Form	CT3				P
1199	297.77	0.59	Asselian	202	-57	-60	-31.40	-53.80	93	Hulha Negra Candiota of the Lower	HNC01				P
1200	286.44	0.91	Artinskian	202	-54	-43	-30.30	-51.70	93	Faxinal Upper Rio Bonito Formatio	FAX				P
1201	296.97	0.72	Asselian	202	-56	-55	-30.50	-52.20	93	Quiteria	QUI				P
1202	262	2.3	Capitanian	101	14	-45	35.40	-117.80	230	unnamed volcanic	And D	A			
1203	281	8	Kungurian	178	9	-50	35.40	-118.00	230	unnamed volcanic	And A	A			
1204	321.3	3.2	Bashkirian	801	-41	146	-30.03	150.34	115	Ermelo					P
1208	256	4	Wuchiapingian	801	-68	145	-33.00	151.50	94	Awaba Tuff					P

1211	259.7	2.2	Capitanian	801	-68	146	-32.90	151.80	94	Awaba Tuff					P
1214	324.1	2.1	Serpukhovian	451	33	54	41.80	91.30	460	Bailingshan Fe deposit	BL-004	D			P
1215	314.36	0.38	Moscovian	374	-3	1	50.00	13.60	461	Radnice Member	#3				P
1216	297.16	0.38	Asselian	374	9	6	50.40	14.30	461	Line Formation	#25a				P
1217	298.97	0.36	Gzhelian	374	8	4	50.30	14.00	461	Line Formation	#24				P
1218	301.5	0.37	Gzhelian	374	7	3	50.20	14.20	461	Slany Formation	#16				P
1219	302.47	0.36	Gzhelian	374	6	3	50.40	13.90	461	Slany Formation	#17a				P
1220	307.05	0.39	Moscovian	374	5	2	50.20	14.10	461	Nyrany Member	#11				P
1221	312.38	0.37	Moscovian	374	1	1	50.20	14.00	461	Radnice Member	#9				P
1222	313.22	0.37	Moscovian	374	-1	1	50.10	13.70	461	Radnice Member	#8				P
1223	313.2	0.37	Moscovian	374	0	1	50.30	13.90	461	Upper Radnice Formation	#6				P
1224	313.41	0.37	Moscovian	374	0	1	50.40	13.90	461	Radnice Member	#2			I	P
1225	313.83	0.23	Moscovian	374	-1	1	50.20	14.10	461	Radnice Member	#4				P
1226	303.73	0.38	Kasimovian	374	5	2	49.80	13.30	461	Tynec Formation	#14				P
1227	305.99	0.36	Kasimovian	374	4	2	49.80	13.30	461	Nyrany Member	#13				P
1228	308	0.36	Moscovian	374	3	1	49.70	13.30	461	Nyrany member	#12				P
1229	302	3	Gzhelian	701	-64	-61	-25.95	18.00	10	Ganigobis Shale Member					
1230	299.5	3.1	Gzhelian	701	-64	-58	-25.95	18.00	10	Ganigobis Shale Member					
1231	297.1	1.8	Asselian	701	-64	-56	-24.65	17.90	10	Hardap Shale Member					
1232	290.9	1.7	Sakmarian	701	-62	-46	-26.10	18.20	10	boundary of Dwyka Group and Ecca Group					
1233	288.5	1.6	Artinskian	701	-62	-43	-26.10	18.20	10	boundary of Dwyka Group and Ecca Group					
1234	279.1	1.5	Kungurian	701	-61	-38	-28.50	17.70	10	Uhabis River Tuff					
1235	246.2	4	Anisian	60401	20	109	23.04	102.00	172	Luchan-Pinghe magmatism	K09-83	R			
1236	246	6	Anisian	60401	20	110	23.04	102.00	172	Luchan-Pinghe magmatism	K09-87	R			
1237	361.1	5.2	Famennian	801	-40	140	-24.30	145.00	173	Mt Alma Formation	RH1178	D		I	P
1238	238.4	1.9	Ladinian	64701	0	113	1.30	104.10	214	Pengerang Volcanics	pink rhyolite	R			
1239	358.9	0.1	Tournaisian	101	6	-107	50.75	-115.00	217	Exshaw Formation					P
1240	250.4	0.5	Olenekian	602	16	134	31.00	120.00	102	Chinglung Formation	MDB96-33				P
1241	251.6	0.1	Induan	602	9		23.50	108.50	102	Changsing Formation	H-Matan96-7				P
1242	252.3	0.3	Changhsingian	602	13	135	31.00	120.00	102	Changsing Formation	M296-(-4.3)				P
1243	250.2	0.2	Olenekian	602	16	134	31.00	120.00	102	Chinglung Formation	MD96-293				P
1244	252.4	0.2	Changhsingian	602	6	124	23.00	108.50	102		LP96-2				P
1246	251.4	0.3	Induan	602	15	134	31.00	120.00	102	Changsing Formation	H-Matan96-1				P
1247	251.6	0.1	Induan	602	9	123	23.50	108.50	102	Changsing Formation	H-Matan96-3				P
1249	251.7	0.2	Induan	602	9	123	23.50	108.50	102	Changsing Formation	H-Matan96-6				P
1250	348.9	4.8	Tournaisian	801	-36	143	-22.85	149.43	227	Clive Creek Volcanics	RSC093	R		I	P
1251	313.8	3.2	Moscovian	801	-42	137	-22.87	149.48	227	Broadsound Range Rhyolite	IWSC0323	R		I	P
1252	308.4	3.3	Moscovian	801	-48	137	-22.75	149.45	227	Broadsound Range Rhyolite	IWSC0669			I	P
1253	314.1	5	Moscovian	801	-41	137	-22.22	149.27	227	Whelan Creek Volcanics	LHC927	R		I	P
1254	300.8	4.1	Gzhelian	801	-46	132	-22.89	149.50	227	Tartrus Rhyolite	IWSC0353	R		I	P
1255	295	3.4	Sakmarian	801	-47	134	-22.41	149.26	227	Lotus Creek Rhyolite	RSC074A	R		I	P
1256	293.2	3.4	Sakmarian	801	-46	134	-21.60	148.68	227	Leura Volcanics	BB3399	D		I	P
1257	291.2	4.2	Sakmarian	801	-48	137	-22.51	149.28	227	Leura Volcanics	IWSC0897			I	P
1258	292	3.7	Sakmarian	801	-47	136	-22.16	149.10	227	Leura Volcanics	LHC878	R			
1259	292.8	3	Sakmarian	801	-47	136	-21.99	149.43	227	Carmila Beds	BB3050A	R-D		I	P
1260	284.7	4.4	Artinskian	801	-48	140	-21.09	148.31	227	Lizzie Creek Volcanic Group	RSC011	D		I	P
1261	351	4.9	Tournaisian	801	-34	148	-22.39	149.81	227	Charon Point Rhyolite Member	IWSC1278	R		I	P
1262	356.8	3.8	Tournaisian	801	-35	168	-24.76	145.09	227	Rockhampton Group	MHROYCB			I	P
1263	300.6	2.7	Gzhelian	801	-40	140	-24.22	144.66	227	Youlambie Conglomerate	MHRO970C	R		I	P
1264	303.6	3.7	Gzhelian	801	-48	127	-24.23	144.62	227	Youlambie Conglomerate	MHRO971(1)	R		I	P
1265	300	3.8	Gzhelian	801	-49	126	-24.23	144.62	227	Youlambie Conglomerate	MHRO971(2)	R		I	P
1266	303.1	3.4	Gzhelian	801	-48	127	-24.23	144.62	227	Youlambie Conglomerate	MHRO971(3)	R		I	P
1267	294.3	3.6	Sakmarian	801	-47	136	-22.47	149.84	227	Glenprairie Beds	IWSC1304	R		I	P
1268	418.9	2.5	Lochkovian				-32.00	146.50	462	Babainda Volcanics	2309502				
1269	416.5	2.4	Lochkovian				-34.20	146.80	463	Gurragong Volcanics	2003619				
1270	418.7	1.8	Lochkovian				-34.50	147.10	463	Walleroobie Volcanics	2110016	R			
1271	418.1	3	Lochkovian				-31.60	145.90	463	Peak Rhyolite	2003960	R			
1272	323.2	3.2	Bashkirian	801	-42	150	-32.50	151.50	141	Johnsons Creek Conglomerate	Z1590				
1273	321.9	4	Bashkirian	801	-42	150	-32.50	151.50	141	Johnsons Creek Conglomerate	Z1556				
1274	330.6	4.6	Serpukhovian	801	-41	150	-32.50	151.50	141	Yagon Siltstone	Z1046				
1275	290.6	1.8	Sakmarian	375	11	11	50.90	12.90	464	Leukersdorf Formation	Zeisigwald Tuff			I	P
1276	308	3	Moscovian	305	-2	0	46.00	7.00	234		CN 125	R			
1277	302.7	0.5	Gzhelian	315	4	-1	49.90	7.20	236	Upper Stephanian Dilsburg	COTO/2				P
1278	309	3.7	Moscovian	374	3	1	49.90	14.00	236	Upper Westphalian Radnice	COT-SH				P
1279	309.5	1.6	Moscovian	315	2	-4	52.10	5.80	236	Middle Westphalian Dorsten (Hage	COTH1-1				P
1280	310.7	1	Moscovian	315	1	-4	52.10	5.80	236	Middle Westphalian Dorsten (Hage	COTH1-4				P
1281	310.7	1.3	Moscovian	315	1	-4	52.10	5.80	236	Uppermost Westphalian B (tonstei	COT-Z				P
1282	319.9	1.6	Bashkirian	302	-7	4	49.70	18.50	236	Upper Namurian A Poruba (tonstei	COT479-1				P
1283	324.8	1.2	Serpukhovian	302	-3	-2	49.70	18.50	236	Upper Namurian A Jaklovec (tonste	COT365-1				P
1284	323.7	1.7	Serpukhovian	302	-4	-1	49.70	18.50	236	Upper Namurian A Jaklovec (tonste	COT335-1				P
1285	293	1.9	Artinskian	308	-4	10	47.00	11.50	471	Morchenscharte	MOER	R			
1286	281.8	2.1	Kungurian	283	-57	-65	-39.80	-69.30	254	Choiyoi Formation				I	P
1287	276.7	1.1	Kungurian	308	0	21	46.40	11.00	255	Nalles Formation		R			P
1288	276.9	2.3	Kungurian	308	0	12	46.60	11.00	255	Gries Formation		R			P
1289	274.6	2.1	Kungurian	308	1	21	46.60	11.00	255	Andriano Formation		R			
1290	277	2	Kungurian	308	0	21	46.60	11.00	255	Ora Formation (base)		R			
1291	274.1	1.4	Kungurian	308	2	21	46.60	11.00	255	Orar Formation (top)		R			
1292	228.6	1.7	Carnian	801	-59	128	-25.00	150.00	465	Agnes Water Volcanics	200701665	R			
1293	363.8	2.2	Famennian	108	-15	-82	45.00	-63.90	277	Carrow Formation		R			P
1294	363.4	1.8	Famennian	108	-15	-82	45.00	-63.90	277	Bailey Rock Rhyolite		R			
1296	230.3	1.5	Carnian	202	-42	-44	-31.30	-69.30	310	Marachemill Formation	RB2	R			
1297	262	4	Capitanian	616	-20	88	33.10	95.70	323	Nayixiong Formation	TB071-3	A			
1298	275.4	0.8	Kungurian	616	-39	81	33.10	95.70	323	Nayixiong Formation	TB065-1	A			P
1299	273.3	2.3	Kungurian	616	-35	82	33.10	95.70	323	Nayixiong Formation	TB066-2	D			
1300	273	0.76	Kungurian	616	-35	82	33.10	95.70	323	Nayixiong Formation	TB0132-1	R			
1301	238.6	0.3	Ladinian	616	0	93	33.10	95.70	323	Nayixiong Formation	TB066-3	D			
1302	288	2	Artinskian	1303	-3	11	45.50	8.40	344	Sesia Valley Volcanics	R6	A			
1303	284.8	3.8	Artinskian	1303	-2	15	45.50	8.30	344	Sesia Valley Volcanics	R9	R			
1304	303.95	0.08	Kasimovian	305	-4	0	43.70	3.10	345	Graissessac Formation	MS-2				P
1305	304.07	0.07	Kasimovian	305	-4	0	43.70	3.10	345	Graissessac Formation	MS-3				P
1306	271.5	3.3	Roadian	601	26	89	31.60	117.80	206	Gufeng Formation	Bed 5b				P
1307	314.3	1.9	Moscovian	450	41	33	45.03	89.12	187	BN Formation	09LSG-6	R			
1308	324.9	2.8	Serpukhovian	801	-41	147	-30.40	150.40	165	Unnamed ignimbrite	X131			I	P
1309	303.7	2.4	Gzhelian	850	-62	145	-41.50	148.00	163	Tamby Creek Formation (404m)	95640016				P
1310	302.4	2.2	Gzhelian	850	-63	144	-41.50	148.00	163	upper Tamby Creek Formation (39	95640015				P
1311	303.2	3.2	Gzhelian	850	-63	144	-41.50	148.00	163	upper Tamby Creek Formation (37	95640014				P
1312	300.3	2.4	Gzhelian	850	-63	142	-41.50	148.00	163	top Tamby Creek Formation (347m	95640013				P
1313	287.1	2.4	Artinskian	850	-66	150	-41.50	148.00	163	Beckers Formation	95640012				P
1314	284.1	2.2	Artinskian	850	-67	152	-41.50	148.00	163	Cranky Corner Sandstone	95640007				P
1315	285.4	2.2	Artinskian	850	-67	151	-41.50	148.00	163	Billy Brook Formation	95640006				P

1316	285.8	3	Artinskian	850	-67	151	-41.50	148.00	163	APP22 Zone	95640003				P
1317	307.8	3.7	Moscovian	801	-52	140	-30.70	150.30	162	Yarrari Pyroclastic	403-1				P
1318	309.6	4.3	Moscovian	801	-51	141	-30.70	150.30	162	Carramundra bed b	429-2	D	I		P
1319	317.2	2.4	Moscovian	801	-45	146	-30.70	150.30	162	Piney range bed a	512-1a	D	I		P
1320	355	3	Tournaisian	108	-12	-74	45.60	-63.50	160	Diamond Brook Formation	C7589	R			
1321	355	2	Tournaisian	108	-65	-12	45.40	-64.90	160	Fountain Lake Group	C7592	R			
1322	345.8	1	Visean	16104	30	-87	62.90	-135.80	159	Little Kalzas Formation	98MC125	R			P
1323	295.3	2.2	Asselian	315	10	6	51.60	12.00	140	Siebigerode Formation	Wieskau	R			
1324	280.2	3.6	Kungurian	308	-2	22	46.70	12.50	466	Col Quaterna	CQ1-2	A			
1325	293	3	Sakmarian	315	12	7	53.20	13.50	130	unnamed volcanics	Tuchen 1/74	R			
1326	288.21	0.34	Artinskian	302	34	28	53.88	56.54	119	Dal'ny Tulkas roadcut section	01DES-403				P
1327	290.81	0.35	Sakmarian	302	33	25	53.88	56.54	119	Dal'ny Tulkas roadcut section	07DTRBed2				P
1328	290.5	0.35	Sakmarian	302	33		53.92	56.93	119	Usolka section	97USO-91.0				P
1329	291.1	0.36	Sakmarian	302	33	25	53.92	56.93	119	Usolka section	97USO-66.2				P
1330	296.69	0.37	Asselian	302	32	20	53.92	56.93	119	Usolka section	01DES-212				P
1331	300.22	0.35	Gzhelian	302	31	17	53.92	56.93	119	Usolka section	97USO-23.3				P
1332	301.29	0.36	Gzhelian	302	30	17	53.92	56.93	119	Usolka section	01DES-121				P
1333	301.82	0.36	Gzhelian	302	30	17	53.92	56.93	119	Usolka section	01DES-112				P
1334	303.1	0.36	Gzhelian	302	29	16	53.92	56.93	119	Usolka section	01DES-63				P
1335	303.54	0.39	Gzhelian	303	29	16	53.92	56.93	119	Usolka section	97USO-2.7				P
1336	304.49	0.36	Kasimovian	302	29	16	53.92	56.93	119	Usolka section	97USO-1.2				P
1337	304.82	0.36	Kasimovian	302	28	16	53.92	56.93	119	Usolka section	01DES-42				P
1338	305.49	0.36	Kasimovian	302	28	16	53.92	56.93	119	Usolka section	01DES-31				P
1339	305.95	0.37	Kasimovian	302	28	16	53.92	56.93	119	Usolka section	08USO-7.09				P
1340	308	0.37	Moscovian	302	27	15	53.92	56.93	119	Usolka section	06USO-2.0				P
1341	305.51	0.37	Kasimovian	302	28	16	53.88	56.54	119	Dal'ny Tulkas roadcut section	01DES-371				P
1342	305.96	0.36	Kasimovian	302	28	15	53.88	56.54	119	Dal'ny Tulkas roadcut section	01DES-363				P
1343	307.66	0.37	Moscovian	302	27	15	53.88	56.54	119	Dal'ny Tulkas roadcut section	01DES-362				P
1344	318.63	0.4	Bashkirian	390	20	13	56.42	61.81	119	Kljuch section	Bed 9				P
1345	319.09	0.38	Bashkirian	390	19	13	56.42	61.81	119	Kljuch section	Bed 2				P
1346	333.87	0.39	Visean	302	22	-4	52.59	58.92	119	Verkhnyaya Kardailovka section	02VD-0				P
1347	266	0.4	Wordian	801	-65	147	-32.90	151.51	113	Thornton Claystone	TC-1				P
1348	310.6	4	Moscovian	801	-50	141	-30.09	150.37	115	Eulowrie Pyroclastics	Eulowrie				P
1349	320.2	1.7	Bashkirian	101	-12	-63	30.10	-103.00	467	Tesnus Formation	Unnamed tuff				P
1350	321.5	3.1	Bashkirian	101	-12	-65	30.10	-103.00	467	Tesnus Formation	Unnamed tuff				P
1351	321.9	1.7	Bashkirian	101	-12	-66	30.10	-103.00	467	Tesnus Formation	Unnamed tuff				P
1353	240.6	3.8	Ladinian	60301	-5	102	18.50	99.60	468	Doi Ton igneous belt	TG-17G	R			
1354	240	3.5	Ladinian	60301	-4	102	18.00	99.90	468	unnamed volcanics	TG-19	A			
1355	280	4	Kungurian	451	48	83	41.10	95.90	469	Liuyuan Volcanic Belt	LY-88	D			
1356	277	4	Kungurian	451	47	83	41.10	95.80	469	Liuyuan Volcanic Belt	LY-95	R			
1357	256	1.5	Wuchiapingian	801	-66	145	-30.70	151.40	470	Uralla volcanics	BB-10-WVG-05	R	I		P
1358	255.8	1.5	Wuchiapingian	801	-66	144	-30.90	151.00	470	Attunga Creek volcanics	BB-10-WVG-07	D			
1359	256.3	1.5	Wuchiapingian	801	-65	144	-30.50	151.30	470	Kurrajong Park volcanics	BB-10-WVG-08	D	I		P
1360	340.5	2	Visean	801	-43	139	-32.80	166.10	470	Nerong volcanics	PB-12-PTS-01	R-D	I		P
1361	293	1.9	Sakmarian	308	-4	10	47.10	11.90	471	unnamed metarhyolite	MO1	R			
1362	309.8	1.5	Moscovian	308	-11	1	47.00	11.70	472	unnamed metarhyolite		R-D			
1363	280.5	2.6	Kungurian	308	-1	22	47.00	11.70	472	Pfitsch Formation					

Abbreviations for Volcanic Compositions

R	rhyolite
D	dacite
A	andesite
T	trachyte